Correlation between the cerebralization, astroglial architecture and blood-brain barrier composition in Chondrichthyes

Ph.D. thesis

Csilla Ari

Semmelweis University
Neurobiology School of Doctoral Studies

Supervisor: Dr. Mihály Kálmán, Ph.D.

Reviewers: Dr. Anna Kiss, Ph.D.
Dr. Klára Matesz, DSc
Committee of Final Examination:
Chairman: Dr. Béla Vígh, DSc
Members: Dr.Tibor Wenger, DSc
Dr. Tamás Röszer, Ph.D.

Budapest, 2008

Table of content

1. List of Abbreviations:

1	sulcus limitans lateralis
2	sulcus telencephalicus ventrolateralis
3	sulcus limitans medialis
3V	third ventricle
4	sulcus telencephalicus ventralis
4V	fourth ventricle
af	fusion of alar plates
AQP4	aquaporin4
AQP9	aquaporin9
asb	area superficialis basalis
Aur	auricula cerebelli
BS	brain stem
ca	commissura anterior
Cbl	Cerebellum
CC	canalis centralis
CO	chiasma opticum
cp	commissura posterior
CrCb	crista cerebellaris
DAB	3,3'-diaminobenzidine-hydroclorid
DG	dystroglycan
DGC	dystroglycan complex (dystroglycan and associated proteins)
E, e	ependymal perikarya
ECS	intrusion of the extracerebral space
EM	eminentia mediana
flm	fasciculus longitudinalis medialis
fr	fossa rhomboidea
G	gray matter
GFAP	glia fibrillary acidic protein
gl	granular layer
HE	haematoxyline eosine
Is	isthmus
Lih	lobus inferior hypothalami
lob vlm	lobus vestibulolateralis, pars medialis
lobX	lobus nervi vagi
M, m	meningeal surface
me	meningocyte
ml	molecular layer
ms	medulla spinalis
N	nucleus N
Ndors	nucleus dorsalis areae octavolateralis
NdV	nucleus descendens nervi trigemini
nll	nervus lineae lateralis anterior
Nimed	nucleus intermedius
Nsma	nucleus septi medialis, pars anterior
Nsmp	nucleus septi medialis, pars posterior
nV	nervus trigeminus
nVIII	8th cranial nerve
NVIII	nucleus of 8th cranial nerve

PBS phosphate buffered-saline
Pla pallium laterale, pars anterior
Plp pallium laterale, pars posterior
P8-12 pallial areas
R reticular glial composite
rdV roots to the nucleus descendens nervi trigemini
RI recessus inferior
sgr stratum granulare
siv sulcus intermedioventralis
slH sulcus limitans of His
sm stria medullaris
smol stratum moleculare
spcb tractus spinocerebellaris
SP5-11 subpallial areas
T telencephalon
tect tectum opticum
Tegl nucleus tegmentalis lateralis
Ti telencephalon impar
tolfl tractus olfactorius lateralis
tomsc tractus olfactorius medialis septi cruciatus
tpal tractus pallii
tub olf tuberculum olfactorium
V, v ventricular surface
VC cerebellar ventricle
Ve vessel
Vimp ventriculus impar
VL ventriculus lateralis
Vm meningeal vessel
VT ventriculus tecti
W white matter
WM bundles of myelinated neural fibers
W9 peripheral white matter

2. Introduction

Representing a separate radiation of vertebrates (Carroll, 1988; Butler and Hodos, 2005), Chondrichthyes underwent an independent brain evolution. They display a wide range of cerebralization (Jerison, 1973), differences in the glial architecture and in the composition of the blood-brain barrier (Bundgaard and Cserr, 1981, 1991).

Chondrichthyes have not been studied widely in neuroanatomy, despite that they represent a successful lineage in evolution in terms of evolutionary success, adaptational capacity and behavioral repertoire.

The glial pattern of some groups of Chondrichthyes, such as order Myliobatiformes or subclass Holocephali have not been studied either. Some brain areas, such as rhombencephalon were also neglected in previous neuroanatomical studies and only few immunohistological techniques were applied in order to describe the glial pattern of cartilaginous fishes.

2.1. Cartilaginous fish systematics

Since cartilaginous fishes (Chondrichthyes) are not widely used in neuroanatomical studies, therefore understanding the taxonomical relation between the examined species is needed, for better relevance of the present neuroanatomical work.

The class of **Chondrichthyes** belongs to the Gnathostomata, like the majority of vertebrates. It comprises only about 800 species, whereas bony fishes (Osteichthyes) includes about 25000 species. Several features obviously separate them from the bony fishes, but the most distinctive is their cartilaginous endoskeleton. As distinct from bony fishes, they have internal fertilization with claspers in males, no lungs or gas bladder but instead large, buoyant livers, and a spiral valve intestine, heterocerk tail fins, but they do not have operculum, and insular skullbones, instead a cartilaginous case can be observed, with a usually elongated rostrum.

Cartilaginous fishes (Chondrichthyes) comprise two major divisions (subclasses), the **Elasmobranchii** (sharks, skates and rays) and the **Holocephali** (chimaeras or ratfishes or ghostsharks). These groups are believed to share a common ancestor (Carroll, 1988). Elasmobranchs separated some 400 million years ago from other

vertebrates. However, contemporary elasmobranchs are by no means just living fossils, they display a number of highly derived characteristics.

While Elasmobranchii comprise 11 orders with hundreds of species, the Holocephali were abundant only in the Carboniferous, and they are represented today by only one extant order (Chimaeriformes) with three families (Smeets et al., 1983). Probably for this reason, the chimaeras received less attention in the morphological and histological studies pertaining to chondrichthian brains, than did sharks, skates and rays.

The main traits of the subclass **Elasmobranchii** is that the upper jaw is not attached to the skull, they have placoid scales, serial replacement of teeth, multiple gill slits. External identification characters are: five to seven separate gill openings on each side of the head, with no operculum, the first often modified as a spiracle. Dorsal fins and spines, if present, are rigid and cannot be folded. Few ribs can generally be observed. Their vision, olfaction and lateral line sensation are usually highly developed.

The gill slits of **sharks** are at least partially in lateral position, and the origin of the pectoral fins is behind the gill slits, while in **skates** and **rays** the gill slits are in ventral position, and the pectoral fins are attached directly to the head.

The living elasmobranchs (sharks, skates and rays) comprise four major superorders: Squalomorphii, Galeomorphii, Sqatinomorphii, and Batoidea according to Compagno, 1977. The sharks included in the **Squalomorphii** include about 25% of all shark species. The group contains relatively uncommon six- and seven-gilled forms, such as the order of cow sharks, Hexanchiformes, as well as several better-known species from the order Squaliformes, such as spiny dogfish, *Squalus acanthias,* and the order Pristiophoriformes, sawsharks. Squalomorph sharks have large spiracles and fin spines are present. These shark species are of a more ancient type, showing a more conservative development than most of the galeomorph sharks.

The **Galeomorphii** superorder constitutes 75% of the sharks, such as the orders Heterodontiformes, Lamniformes, Orectolobiformes, Carchariniformes. They show more complex and advanced features (Northcutt, 1989) and include most of the well-known sharks (e.g. *Carcharodon, Carcharhinus, Negaprion, Sphyrna, Ginglymostoma, Mustelus, Scyliorhinus*). Sharks in the Galeomorphii have five gill slits. Other characters of galeomorph sharks are the small or absent spiracle, absence of fin spine

and the closed trunk lateral lines. They evolved a variety of more fully streamlined and fusiform bodies. The articulation between the upper jaw and the braincase moved back on the skull. The general result was a body with an even greater strength, and jaws of great strength and flexibility. Finally, most of the galeomorphs are typically pelagic, found as free-swimming species in warm water, with relatively higher prey densities, while squalomorphs tend to be benthic or inhabit colder and deeper waters.

The **Squatinomorphii** contain only a single family with a single genus, the angel shark (*Squatina squatina*), with charecteristic flattened body shape, similar to batoids, but they use their body and tail for swimming similarly to other sharks and resemble the Squalomorphii in cranial and brain structure.

The **Batoidea** includes the Rajiformes (skates), Rhinobatiformes (guitarfishes), Pristiformes (sawfishes), Torpediniformes (electric rays), and Myliobatiformes (e.g., sting-rays: Dasyatidae, eagle-rays: Myliobatidae, and devil-rays: Mobulidae).

Skates: Disc quadrangular to rhomboidal. Tail very slender, with lateral folds, usually 2 reduced dorsal fins and a reduced caudal fin. Electric organs weak, developed from caudal muscles. Oviparous. Skates feed on other benthic organisms.

Guitarfishes: Body form intermediate between that of a shark and a skate. Also called shovelnose sharks. No spine in tail. Ovoviviparous. They feed on bottom organisms.

Sawfishes: Snout consists of a long flat blade with teeth on each side (teeth of equal size and embedded in deep sockets); barbels absent; body somewhat sharklike, although the head is depressed; two distinct dorsal fins and a caudal fin. Viviparous.

Electric rays: Disc truncated or emarginated anteriorly; jaws extremely slender; no labial cartilages; rostrum absent or reduced.

Stingrays: Side of head continuous with the anterior margin of pectoral fin. Dorsal fin totally absent or indistinct, when present. Disc about 1.2 times as broad as it is long. No caudal fin. Tail long and whip-like. Most species with at least 1 long venomous spine on tail. Ovoviviparous.

Eaglerays, devilrays: Head elevated above disc; eye and spiracles lateral on head; tail much longer than disc; small dorsal fin; pectoral fins reduced or absent opposite the

eyes, but with an anterior subdivision that unites below the tip of the snout. Viviparous. Plankton-filtering manta rays (*Manta birostris* and *Mobulas*) are among the largest fishes, but harmless.

The other subclass, the **Holocephali** differ from elasmobranchs in several ways. The name Holocephali refers to the distinctive autostylic suspension of the jaws of these fishes, in contrast to the hyostylic and amphistylic jaw suspension of elasmobranchs. While the upper jaw of sharks and rays is not attached to the cranium, in holocephalans the upper jaw is completely fused, this is where the name comes from: „holocephali". There are also important differences in skeletal organization and in the structure of the brain. External identification characters are: a single gill flap covers four internal gill openings, and there is no spiracle. The first dorsal fin, with its poison-laden spine, is erectable. All chimaeras lay large eggs with a horny shell and the development of embryos is direct, without a larval stage. Males often have an additional clasping organ on the head, the role of which is still unknown.

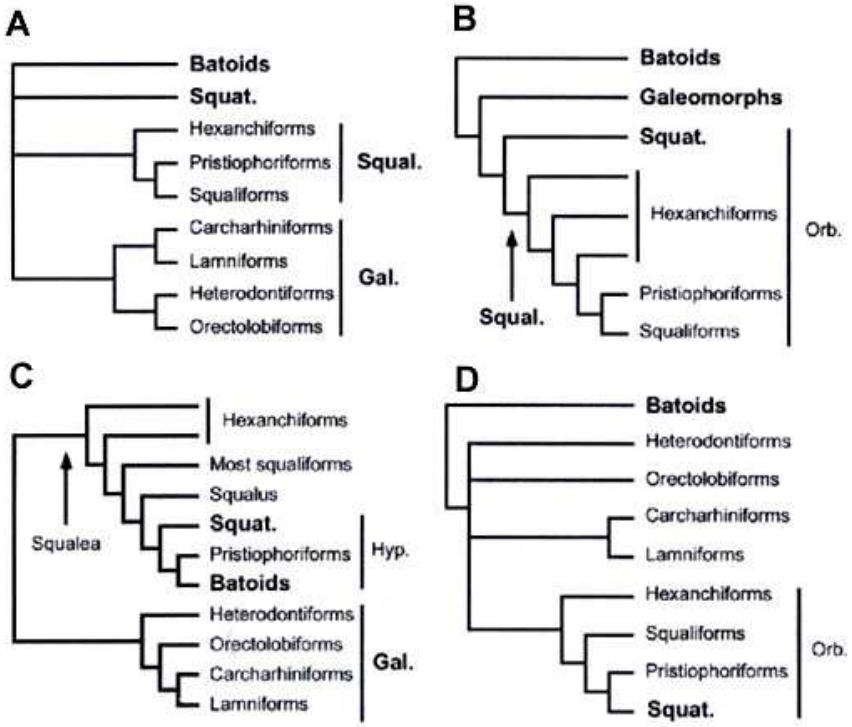

Figure 1. Phylogenetic trees of cartilaginous fishes, according to a) Compagno (1973); b) Maisey (1984); c) Shirai (1992,1996); d) Douady et al. (2003). Squal – Squalomorphii; Gal – Galeomorphii; Orb – Orbitostylic; Hyp – Hypnosqualea. Source: Winchell et al., 2004.

In the last few decades there were a few attempts to reform chondrichthyes phylogeny (fig.1). One of them was made by Maisey (1984), who identified a potential synapomorphy of squalomorphs and squatinomorphs, and united these two superorders as the ’orbitostylic’ sharks. By comparing external, skeletal, and muscular characters in a cladistic analysis, Shirai (1992) revolutionized elasmobranch taxonomy. He showed batoids as derived sharks, grouped with pristiophoriforms and Squatina into ’Hypnosqualea’. With the squalomorphs they formed the supraorder ’Squalea’, the sister group of galeomorphs. The ’Hypnosqualea’ and ’Squalea’ clades became widely accepted (de Carvalho, 1996; McEachran et al., 1996), but problems arise from using morphology to assess elasmobranch phylogeny, so molecular data were used to test phylogenetic hypotheses (Douady et al., 2003; Winchell et al., 2004).

Notably, the status of the phylogenetic placement of Pristiophoriformes is highly controversial. Several authors agree that this order belongs to the Squalomorpha (Compagno, 1973, 1977; Arnason et al., 2001; Douady et al., 2003; Winchell et al, 2004). Others, however, consider it as a sister-group of Batoidea in the frame of the common ’Hypnosqualea’ group (Shirai, 1992, 1996; de Carvalho, 1996; McEachran et al., 1996), although they also accept its close relationship to Squaliformes (thus considering batoids as derivatives of sharks).

The current zootaxonomy books of Hungarian universities also divide the Chondrichthyes class into two subclasses: Holocephali (chimaeras) and Elasmobranchii (sharks and rays) on the basis of Nelson’s (1994) classification. Within the latter subclass Nelson (1994) distinguished the Selachimorpha (sharks) superorder, with the Hexanchiformes, Heterodontiformes, Lamniformes and Squaliformes orders, and the Batidoidimorpha (rays) superorder with the Rajiformes order.

Since no final agreement exists on the classification of chondrichtians yet, in this study I used Compagno’s (1977) classification (fig.2), which had been applied for over 25 years and it is still widely accepted in recent neuroanatomical studies.

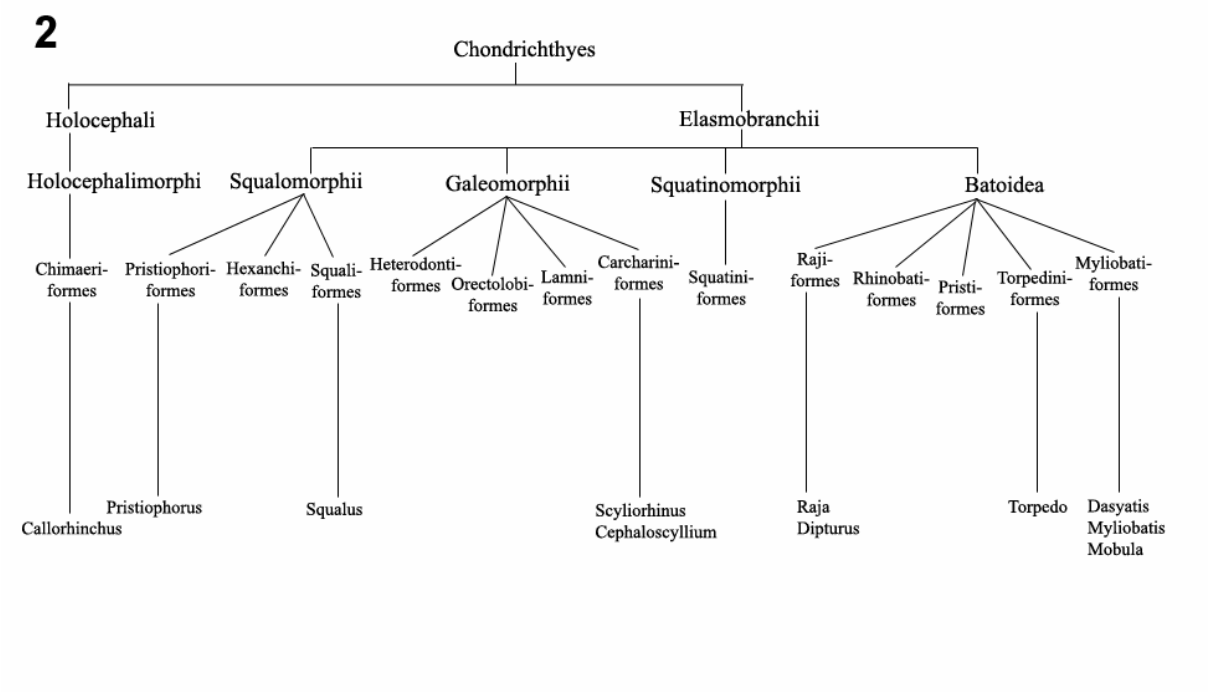

Figure 2. The main groups of Elasmobranchii, according to Compagno et al. (1977), and the representative genera which were used in this study.

2.2. Brain variations

According to some previous studies conducted by Northcutt (1977, 1978, 1985, 2002) the brains of sharks can be somewhat similarly categorized, by the taxonomic scheme proposed by Compagno (1973, 1977), as follows: less advanced squalomorph and squatinomorph and more advanced galeomorph brains. On the basis of his description squalomorph and squatinomorph sharks possess a relatively small telencephalon with relatively large lateral ventricles and thin brain walls. The diencephalon is characterized by prominent periventricular laminae, and the cerebellar corpus is smooth and non-foliated.

The more advanced galeomorph sharks (Heterodontiformes, Orectolobiformes, Lamniformes and Carcharhiniformes) are characterized by a marked hypertrophy of the telencephalon. The pallium, as well as the diencephalon, are sites of extensive cellular migration. The characteristic features of their brain pattern are the optic tectum overlapped by the cerebellum, hypertrophy of the superficial tectal zone, a convoluted

corpus of the cerebellum with hypertrophy leading to asymmetry in many families (Orectolobidae, Lamnidae, Carcharinidae, Sphyrnidae).

According to a more recent study within each of the three major radiations of Gnathostomata -chondrichthians, actinopterygians, and sarcopterygians- two types of organization may be found in the brains of the various species: type I (’laminar’) and type II (’elaborated’) (Butler and Hodos, 2005). In type I brains, the neuronal cell bodies did not or only partially migrated away from the embryonic, periventricular matrix, which is the zone from which neurons develop. Afferent projections to these neurons terminate on the more distal portions of their dendrites near the surface of the brain. The brain ventricles are large, while the brain wall is relatively thin. The term ’laminar’ refers to the periventricular lamina in which the majority of neuronal cell bodies are located.

Cartilaginous fishes with laminar brains include squalomorphs, squatinomorphs and chimaeras. Laminar brains are found in voracious predators, like spiny dogfish, as well as less vigorous swimmers (chimaeras) and benthic species as *Squatina squatina*. Thus, a relatively simple and laminar brain organization does not necessarily preclude an active, predacious lifestyle.

In type II brains extensive migration of neuronal cell bodies away from the periventricular matrix has occurred. Therefore, these brains are generally relatively larger in size and more complex as compared with brains exhibiting laminar organization. Individual nuclei occur, the ventricles are of reduced size, whereas the brain wall has thickened. Among cartilaginous fishes batoids and galeomorph sharks have been classified to have type II brains (Butler and Hodos, 1996). All batoids possess complex telencephalic and diencephalic organization, similar features are attributed to galeomorph sharks. Cellular migration and thickening of the telencephalic wall reduces the lateral ventricles.

Most of galeomorph sharks are active predators, as are spiny dogfishes, they also have modified jaws for deep biting and for successfully attacking larger sized prey. Usually skates and rays have a more sedate lifestyle, foraging on bottom dwelling invertebrates, but also have more complex modes of locomotion. They use undulating movements of the pectoral fins (skates and stingrays) or a flapping motion of the fins similar to the motion of a bird’s wing (manta rays and eagle rays). Rajiformes and

Torpediniformes are benthic, while those in the Rhinobatiformes and Myliobatiformes order are pelagic. The brain nuclei involved in the coordination of motor activities are all relatively enlarged and prominent in galeomorph sharks, skates and rays. Likewise, forebrain areas involved in sensory processing and additional complex behaviors, such as social interactions, courtship, and mating, are all enlarged.

Exceptions to these general trends do occur, when all the characteristic features of a brain pattern do not fit in with a species, e. g. *Scyliorhinus* have galeomorph pattern in general, but their cerebellum is unconvoluted, like that of squalomorph sharks.

The differences in brain organization between type I and type II animals are not as prominent in the spinal cord, lower brain stem and the cranial nerves as in the brain itself. The organization of the spinal cord and cranial nerves is relatively conservative among all vertebrate radiations, and variation in these structures is more related to habitat (aquatic vs. terrestrial vs. aerial) than to the type of organization of the brain itself. However, the types of laminar and elaborated brain organization are clearly different among vertebrates in the midbrain, and, most prominently, in the forebrain (Northcutt, 1978).

The Myliobatiformes and Carcharhiniformes are characterized by the most complex neural development among living elasmobranchs (Northcutt, 1978). At present, all measures of neural complexity fail to distinguish which of these two groups is more advanced. Clearly each has independently reached a complex level of neural organization, presenting a beautiful example of parallel evolution.

2.3. Brain weight/body weight ratios, cerebralization

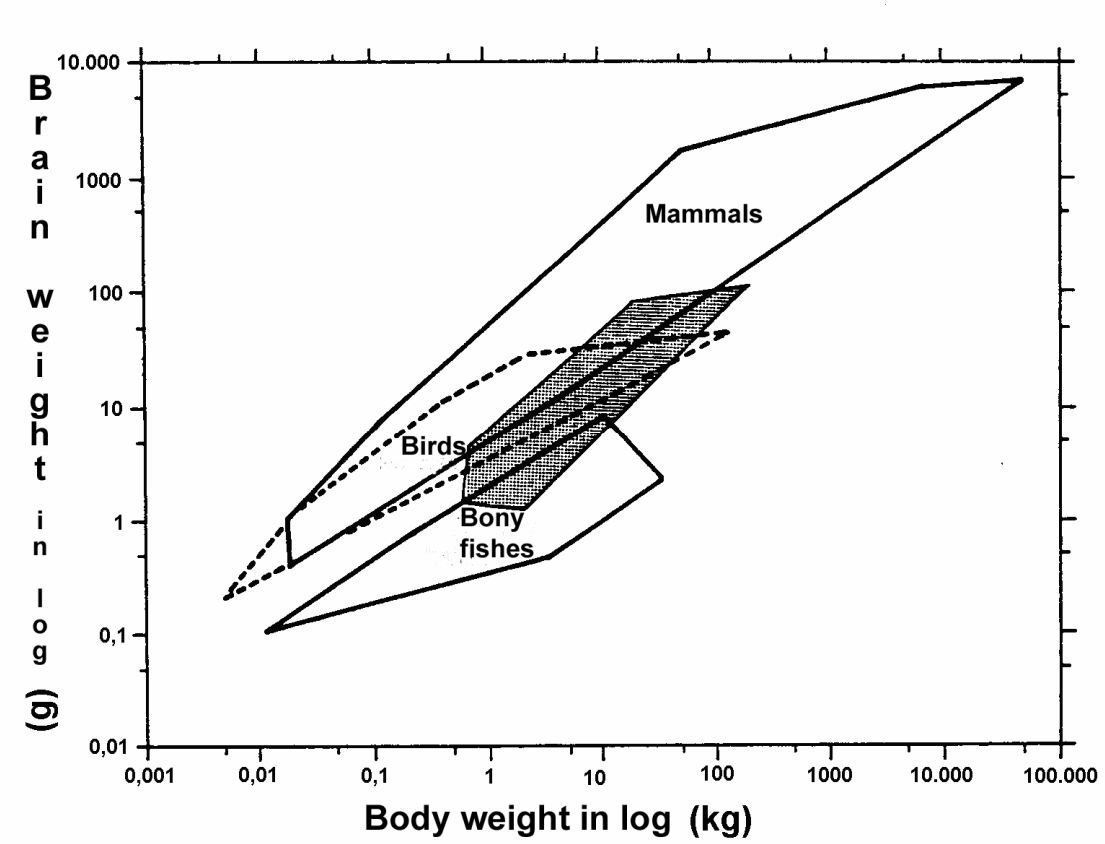

Figure 3. Brain weights and body weights for four vertebrate classes expressed as minimum convex polygons on a double logaritmic scale, after Jerison (1973). The stippled polygon encloses elasmobranch brain-to-body ratios which overlaps polygons for bony fishes, birds and mammals (Northcutt, 1977).

Comparison of cerebralization in chondrichthyan fishes with that of other vertebrate groups has been made by constructing 'minimum convex polygons' to enclose data points in a double logarithmic scale of a brain weight/body weight plot by Jerison (1973). The same method was applied to additional data, by Northcutt (1977, 1978, 1981) and Smeets et al. (1983) (fig.3). According to such analysis, chondrichthians exhibit a wide range of cerebralization. The brain weight/body weight ratios in batoids and galeomorph sharks are two to six times larger than in squalomorph sharks. The former groups overlap with the upper range of teleosts and reptiles as well as the lower range of birds and mammals (Smeets, 1997; Smeets et al., 1983). Within the superorder Batoidea (skates and rays), Rajiformes (skates) have relatively low brain

weight/body weight ratios, whereas Myliobatiformes show the highest brain weight/body weight ratios known for elasmobranchs. This phenomenon has resulted mainly from an intense evolution of the telencephalon, which occurred especially in rays. In batoids and galeomorph sharks the cerebellum has also enlarged, and numerous accessory sulci give it a foliated appearance (Nieuwenhuys, 1967; Yopak et al., 2007). Furthermore, telencephalic data on cartilaginous fishes (Northcutt, 1978) show that squalomorph sharks and skates possess telencephalic volumes comparable to those of bony fishes and amphibians, whereas galeomorph sharks and myliobatiform rays display a 5- to 13-fold increase. With respect to size, the telencephalon of *Squalus* constitutes 24% of the total brain weight, in *Scyliorhinus*, *Raja* and holocephalan *Hydrolagus* approximately 30%, whereas in *Carcharhinus* and *Sphyrna* more than 50% of the total brain weight is constituted by the telencephalon (Northcutt, 1978).

The extremely high brain weight/ body weight ratios for elasmobranchs cannot be attributed to the light weight of their cartilaginous skeletons relative to bone. The analysis of *Mustelus canis* indicates (Northcutt, 1978), that the skeleton accounts for 15% of its body weight. This figure is well within the range of skeletal weight percentages reported for other vertebrates (Reynolds and Karlotski, 1977).

2.4. General gross morphology of cartilaginous fish brain

In general, of all brain parts the telencephalon and cerebellum exhibit the greatest variation in size and shape, while the rhombencephalon seems to be the most conservative structure among Chondrichthyes. The general description of cartilaginous fish brain is based on studies of Ariëns Kappers (1906), Northcutt (1978), Smeets et al., (1983), Smeets (1997), Butler and Hodos (2005). Figure 4 shows the brains of representative species of the orders used in this study.

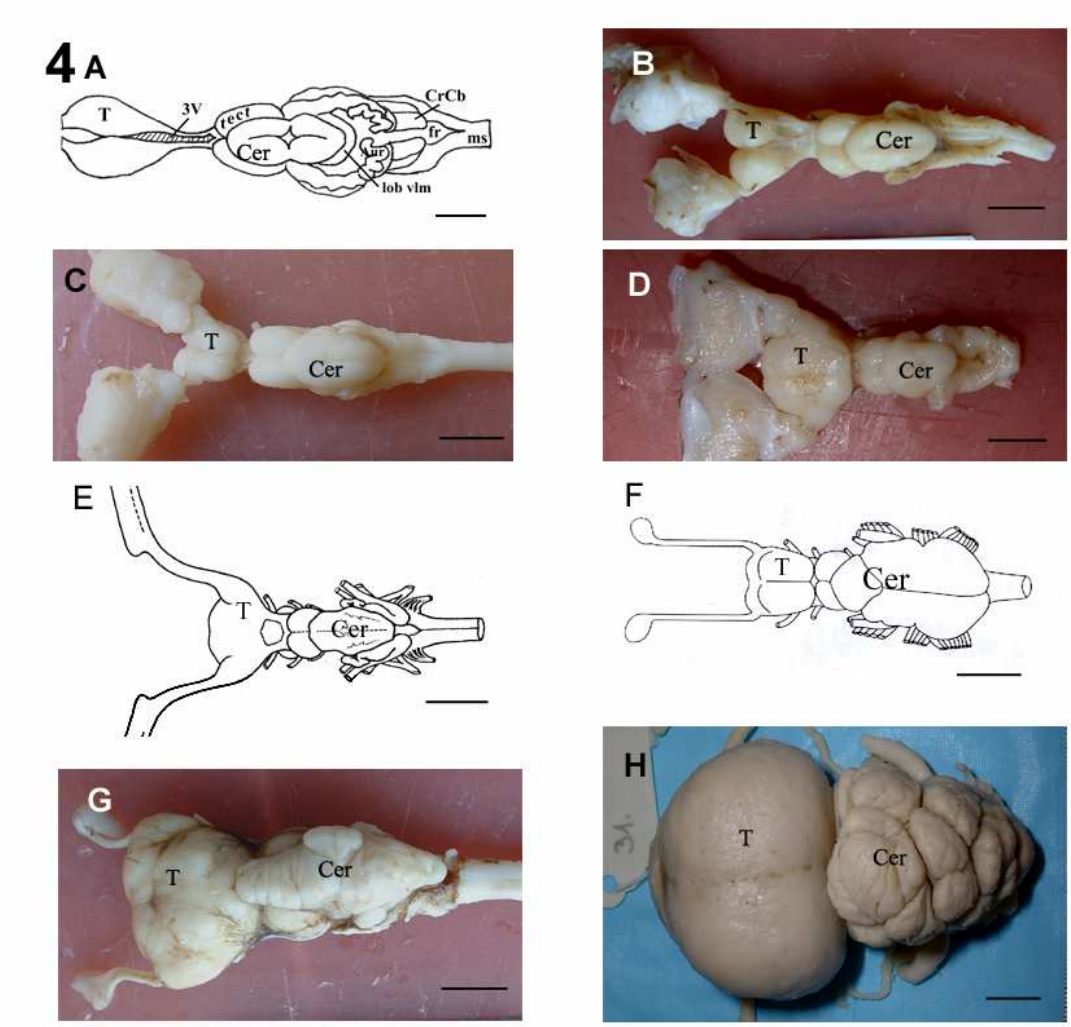

Figure 4. Dorsal view of the brains of representative species from each order used in this study. A – *Callorhinchus* (Chimaeriformes); B – *Squalus* (Squaliformes); C – *Pristiophorus* (Pristiophoriformes); D – *Cephaloscyllium* (Carchariniformes); E - *Raja* (Rajiformes); F – *Torpedo* (Torpediniformes); G – *Myliobatis* (Myliobatiformes); H – *Mobula* (Myliobatiformes); Note the difference in the relative size of the telencephalon and cerebellum between the brains of two rays from the order Myliobatiformes. Scale bars: 0,5; 0,8; 0,7; 0,5; 0,6; 0,7; 0,7; 1,3cm, respectively.

2.4.1. Olfactory bulb

In all cartilaginous fishes the olfactory bulbs are well developed structures, but they vary considerably in shape (Smeets et al., 1983; Nieuwenhuys et al., 1997). In sharks such as *Hexanchus* and *Squalus* the bulbs are ovoid, but in most rays they have a flattened saucer-shaped appearance. Other species like *Scyliorhinus* lie between these extremes. The rostral or rostroventral surface of the bulbs lies near to the olfactory organs, thus the olfactory nerve fibres are short.

2.4.2. Olfactory tract

The olfactory tract is long in batoids and in some sharks, such as *Squalus* and *Ginglymostoma*, but short in *Scyliorhinus*. The pedunculus olfactorius connects to the telencephalon rostrally in Holocephali, in contrast to other cartilaginous fishes, in which it connects laterally (Northcutt, 1977).

2.4.3. Telencephalon

The telencephalon can be divided into telencephalic hemispheres and the telencephalon impar. There are considerable structural differences between the telencephala of different species although evagination is the essential morphogenetic process in this region. The telencephala of the various chondrichtian species also differ remarkably in the degree of fusion between the hemispheric lobes, and the degree of reduction of the telencephalic ventricle.

As in other vertebrates, the telencephalic hemispheres can be divided into pallium and subpallium. The pallium consists of a lateral part, which receives olfactory input from the olfactory bulb, the dorsal pallial complex, and a medial pallium. The dorsal pallium became increasingly complex in some elasmobranch radiations. In *Squalus*, two subdivisions of the dorsal pallium have been recognized: a pars superficialis and a central nucleus (Northcutt 1978; Smeets, 1997). In *Raja*, a skate with a moderately developed telencephalon, the pars superficialis consists of distinct lateral and medial parts (Smeets et al., 1983). A distinct feature of the elasmobranch telencephalon is that the two hemispheres are fused in the midline. Pallial as well as subpallial zones are involved in this fusion. The degree of fusion varies from species to species. In primitive sharks such as *Chlamydoselachus* and *Hexanchus* it is very restricted, *Squalus* occupies

an intermediate position in this respect, but in some rays the medial hemispheric walls are completely united and the whole telencephalon constitutes a solid cell mass with both sides interconnected by the large pallial commissure. The telencephalic floor, or subpallium, consists of several nuclei, however, nothing is known about their connections in elasmobranchs. The subpallium can be divided into a medially situated septal area, the area basalis, and a laterally situated striatal area. It should be noted that there is currently no agreement concerning the homologies of the subpallial areas to other vertebrates, except for the septal nuclei. Some areas labeled as the striatum of elasmobranchs may in fact be homologous to pallial and subpallial parts of the amygdala of other vertebrates (Northcutt, 1989). Therefore, the terminology used here does not imply any homologies to cell groups with the same name in other animals until further data are evaluated.

The telencephalon impar is that portion of the forebrain which is not involved in the lateral evagination of the hemispheric lobes. Following Johnston (1911), its caudal boundary is defined as a plane passing from the velum transversum to the caudal pole of the optic chiasm.

The early development of the telencephalon of batoids closely resembles that of sharks. However, later in development, the two groups diverge with regard to the extent of the ventricular cavities. Whereas in most sharks the lateral ventricles remain wide, in batoids they become gradually reduced to two short, horn-shaped rudiments, or disappear in some cases. Identification of the pallial and subpallial regions in these brains is difficult. According to Northcutt (1981) and Reiner (1991) the formation of the ’central nucleus’ is a pallial hypertrophy parallel with the mammalian cortex development. Massive hemispheres can be found in these species due to the extensive development of pallial cell groups.

In Holocephali specialized hypertrophy of the middorsal telencephalic roof cannot be observed. They have a long telencephalon impar, the length of which can attain the half of the total brain length. A more detailed gross morphological description of holocephalan brain will be presented in the results section, since the brain structure of the species studied here (with the exception of *Hydrolagus*) has not been described before.

2.4.4. Diencephalon

The structure and function of the chondrichthian diencephalon is poorly understood. Unlike other regions of the brain, the diencephalon in cartilaginous fishes has retained essentially the embryonic tube-like shape. Its thickened walls surround a narrow ventricle.

Similarly to other vertebrates, in the diencephalon of chondrichthians three divisions can be recognized: epithalamus, thalamus, and hypothalamus. The epithalamus is formed by the habenular nuclei, the habenular commissure, and a complex series of afferent and efferent pathways (stria medullaris complex) related to the habenular nuclei. Little variation is discernible among the various species. Rostral to the commissure the diencephalon is covered by a membrane-like structure, lamina epithelialis, which continues to the velum transversum, determining the border between the telencephalon and diencephalon. The diencephalon roof becomes thinner caudal from the commissura habenularis to create the epiphysis.

The thalamus of chondrichthians is divided into dorsal and ventral divisions. The thalamus of chimaeras and squalomorph sharks is similar to that of many other anamniotic vertebrates in that it consists of prominent periventricular cell groups and a more lateral sparse- celled neuropil. In contrast, the thalamus of galeomorph sharks and batoids is characterized by a marked thickening of the thalamic wall and cellular migration away from the ventricle.

Little is known about the third division of the diencephalon, the hypothalamus. It consists of a rostral preoptic area, a central or tuberal area including the inferior lobes, and a caudal or posterior hypothalamic area (Northcutt, 1978).

2.4.5. Cerebellum

The cerebellum is part of the rhombencephalon, but I discuss it separetaly due to its great importance.

The cerebella of elasmobranchs is relatively large compared to that of most other vertebrates (Tong and Bullock, 1982; Nieuwenhuys, 1967). The corpus cerebelli varies considerably in external form and size between chondrichtian species, its degree of development seems to be connected more to the lifestyle than to the taxonomical position of the species.

Two parts can be distinguished in the chondrichtian cerebellum: a median, unpaired corpus cerebelli, which forms the roof of the metencephalon, and the bilateral auricles,- vestibulolateral or auricular lobes-, that could be found ventrolaterally from the caudal part of the corpus (Llinás et al., 1969; Nieuwenhuys, 1967). The lateral-line lobe (crista cerebelli) is situated caudally from the cerebellum, and has structural and most likely, also functional connections with the cerebellum.

In its internal organization the chondrichthyan cerebellar corpus is very similar to that of other gnathostomes. Its wall is differentiated into four layers: the innermost granular layer, the fibre zone, the layer of Purkinje cells, and the outer molecular layer. The granule cells are concentrated in two longitudinal ridges, the prominentiae granulares (Nieuwenhuys, 1967), which are situated on both sides of the median plane. In the lateral parts of the corpus cerebelli, where granule cells are absent, only the zone of fibres can be distinguished beneath the Purkinje cells. This zone includes incoming afferent fibres and outgoing Purkinje cell axons. The Purkinje cells form a regular layer, one or two cells thick, which extends throughout the entire wall of the corpus cerebelli, with the exception of the paramedian regions, while the outer molecular layer contains several elements, like parallel fibers.

The auricles have three component regions, the upper and lower leaves and the lower lip, differing in their internal organization and connections.

The cerebellum of present-day cartilaginous fishes is significantly greater and contains much more neurons, than those of bony fishes (except for the hiperfoliated cerebella of knifefishes-Gymnotiformes and elephantfishes- Mormyridae), and more developed than that of the majority of amphibians and reptiles. In general, it can be stated that holocephalians and squalomorph sharks have a nonconvoluted corpus cerebelli, whereas galeomorph sharks usually have a convoluted cerebellar body with hypertrophy that results in asymmetry. Within the group of batoids, the more primitive rajiformes and torpediniformes have a slightly convoluted cerebellum, whereas the more advanced batoids like myliobatiformes possess a complexly convoluted, asymmetrical cerebellum, similar to that of carcharinid and sphyrnid sharks. The species with the highest relative brain weight (manta rays- family Mobulidae and hammerhead sharks- family Sphyrnidae) have also the most differentiated cerebella. Ten to 15 lobes of different size can be recognized, but the size and number varies among individuals.

The biological meaning of these increased values for cerebellar and telencephalic subdivisions is unknown, but there seems to be no linear relationship between these two structures.

While in Amniotes the folium formation involves only the gray matter and the white matter, in cartilaginous fishes (also the electric fishes with hiperfoliated brains from the bony fishes) the ventricular surface is also involved.

Although it is widely held that the cerebellum plays an important role in motor control it still remains unclear how this is achieved in chondrichthians. It is unknown why cartilaginous fishes need such a large cerebellum, the answer might be related to the complex movement of these animals, and the specialization of the lateral-line system. The hypertrophy and development of chondrichtian cerebellum can also be connected to the development of electroreception, probably mainly to the electrolocation.

2.4.6. Mesencephalon

The rostrodorsal border of the mesencephalon is signified by the plane of the commissura posterior. The midbrain consists of dorsal (tectum mesencephali) and ventral (tegmentum mesencephali) regions.

In the majority of cartilaginous fishes the tectum mesencephali is intensely developed and differentiated into bilateral lobes, which surround expansions of the ventricular cavity. The tectum mesencephali is the main centre of termination for retinofugal fibres and, as in other fishes, generally appears to be well developed in those species with large eyes, although it also receives afferent inputs from several non-visual systems. In the chondrichthian tectum several laminae can be distinguished, although still disagreement about the exact number. Most of authors describe six layers in elasmobranchs and five in Holocephali. Among elasmobranchs, squalomorphs probably exhibit the most primitive tectal pattern, characterized by a dense cellular plate in or on the border of the central tectal zone. Both galeomorph sharks and batoids possess tecta with hypertrophied superficial tectal zones of high cell density. Batoids have a very narrow tectal canal.

The midbrain floor, or tegmentum, is a continuation of hindbrain.

2.4.7. Rhombencephalon

In all vertebrates the rhombencephalon harbours the centres of origin and termination of all cranial nerves, except for cranial nerves I,II,III (Butler and Hodos, 2005). In cartilaginous fish the rhombencephalon contains a fairly well developed reticular formation and a number of relay centres and their associated ascending and descending connections.

The name rhombencephalon indicates: surrounding the rhomboid shaped fourth ventricle. The base of the ventricle is derived from the basal plates of the rhombencephalon, while the alar plates give the lateral part. The border between the basal and alar plates is indicated by the sulcus limitans His. Rostrolaterally the fourth ventricle becomes wider and forms the recessus lateralis on both sides, that are surrounded by auriculae cerebelli. The fourth ventricle is covered by a strongly vascularized tela choroidea. In a caudolateral direction, the auricles continue in the dorsal part of the lateral walls of the rhombencephalon (crista cerebelli).

The nuclei of the rhombencephalon are general somatic motor nuclei, branchiomotor nuclei, visceral motor nuclei, nuclei of reticular formation, visceral sensory nuclei, general somatic sensory nuclei and acousticolateral nuclei.

2.4.8. Spinal cord

The spinal cord of chondrichthian fishes merges rostrally with the rhombencephalon and ends caudally in the tail fin, surrounded by lymphatic tissue. It may be considered as a series of segments, essentially identical in organization, that match the segmental divisions of the body musculature. As in all gnathostomata, the gray matter is arranged as dorsal and ventral horns but the dorsal horns, which are separated by small dorsal funiculi fuse centrally as a mass, just dorsal to the central canal. Almost the entire dorsal horn of these fishes constitutes a substantia gelatinosa. On each side a segment provides a dorsal and ventral root which unite as a segmental spinal nerve that passes to the periphery. Cell bodies and their dendrites are located mainly centrally, in the gray matter. The surrounding white matter contains mostly nerve fibers, but lacks any truly giant axons although large axons are found in the ventral funiculi. The ventral root of the spinal nerves consists predominantly of motor axons.

2.5. General features of the glia

Nonneural cells, termed neuroglia, were recognized as independent elements of the nervous system in 1856 by the pathologist Rudolf Virchow in his search for a 'connective tissue' in the brain (Kettenmann and Ransom, 2005). The notable differences between neurons and glia, that glia do not conduct electrical impulses, as opposed to neurons and lack the polarity of neurons, namely the axons and dendrites. The general description of glia is based on the study of Kettenmann and Ransom (2005).

It is inaccurate to consider glia as ‘glue’ in the nervous system (as the name implies- Greek for ‘glue’), rather it is more of a partner to neurons. Some glia function primarily as the physical support for neurons. Others regulate the internal environment of the brain, especially the fluid surrounding neurons and their synapses, provide support, protection, nutrition (Westergaard et al., 1995) for neurons, form myelin (oligodendroglia), isolate one neuron from another and remove dead neurons (microglia). Glia also have important developmental roles, guiding migration of neurons in early development, and producing molecules that modify the growth of axons and dendrites. Glia are also active participants in synaptic transmission, regulating clearance of neurotransmitter from the synaptic cleft, releasing factors such as ATP which modulate presynaptic function, and even releasing neurotransmitters themselves. Glia also have neurotransmitter and hormone receptors (Hösli and Hösli, 1993; McCarthy et al., 1985) and they participate in a bidirectional communication with neurons.

Glia produce isolating sheath (glia limitans) with their connected glial endfeet around the central nervous system, not only under the meninx but also around blood vessels, to control the passage of molecules, if indirectly (but directly in Elasmobranchii, Stewart and Coomber, 1986; Wolburg and Riseau, 1995). Glia also help maintain the ionic balance of the CNS, eliminate toxic metabolites (ammonium ion), and participate in transmitter metabolism and inactivation (Rosenberg and Aizenmann, 1989).

The classical methods of experiments on glia are heavy metal (gold, silver) impregnation techniques. Some of these detected the intermediary filaments (glia fibrillum, Stensaas and Stensaas, 1968ab; Roots, 1986; Weigert- and Cajal-methods), others impregnated the whole cell (Golgi -, Hortega- methods).

2.5.1. Types of glia

No final agreement exists on the classification and nomenclature of glial types as yet. On the basis of previous studies (Schmechel and Rakic', 1979; Rakic', 1981, 1995; Mugnaini, 1986; Privat and Rataboul, 1986; Privat et al., 1995; Reichenbach and Robinson, 1995; Collins, 1999) the following information can be stated on vertebrate glia: The three main glial types in the central nervous system are: astroglia, oligodendroglia, and microglia. Some consider the ependyma as the fourth type, while others (Mugnaini, 1986) classify it as astroglia, on the basis of their histogenetic and evolutionary relations. Association between these glial types and the glia of the peripheral nervous system is not clear either, most probably all subtypes of peripheral glia are closely related to oligodendroglia.

1) Astroglia:

This type gives the major contingent of glia and is responsible for most of the glial functions. It comprises subtypes which are phylogenetically and histogenetically related, they are able to express GFAP, and do not form (compact) myelin.

The electronmicroscopic structure of astroglia: poor in organelles, containing plenty of glycogen, intermediary filaments and loose chromatin structure. The astrocytes are connected by 'gap junctions', which probably connect the cytoplasm of all astrocytes in the brain and assist the passing of small molecules (Mugnaini, 1986; Ransom, 1995). Data exist on other connections, such as puncta adherentia and focal contacts (Abd-el-Basset et al., 1990; Tawil et al., 1993; Arregui et al., 1994; Padmanabhan et al., 1999). On the surface of astrocytes N-CAM (neuron-cell adhesion molecule), N-cadherins, and integrins can be found (Jones, 1996; Redies et al., 2000; Yoon et al., 2000), the former is responsible for contacting other cells, while the latter for contacting the extracellular matrix.

Two main subtypes can be distinguished, i) true astrocytes which have several processes of similar length, and ii) glial cells which have a long, prominent process (often referred to as 'fiber'). Originally Horstmann (1954) used the term tanycyte for these cells, meaning slim cell.

1a) Astrocytes: The true astrocytes possess star- or spider-shaped cells due to their process system. They are independent from the ventricular surface. There are generally two types of astrocytes, protoplasmic and fibrous.

Protoplasmic astrocytes have short, highly branched processes and are typically found in gray matter.

Fibrous astrocytes have long, thin, less branched processes and are more commonly found in white matter.

According to their position, astrocytes can be distinguished as perivascular, submeningeal, subependymal, perinodal. Astrocytes are thought to be capable of proliferation, phagocytosis and migration (300 μm/day in the optic nerve, Huxlin et al., 1992). The pituicytes of neurohypophysis, the interstitial cells of corpus pineale and probably the folliculo-stellate cells of adenohypophysis (Van Nassauw et al., 1987) are local modifications of astrocytes.

1b) Fiber-like elongated cells (Horstmann's 'tanycytes')

Tanycytes: Originally the term was coined by Horstmann (1954) as a synonym for radial glia, and similar thin, elongated glial elements. Recently it refers to glial cells located at the ventricular surface with long process to the brain substance, and responsible for special transport processes, regardless of whether they reach the pial surface or not (Mugnaini, 1986; Abbott, 1995).

Radial glia: Connect the corresponding points of meningeal and ventricular surface with nearly parallel fibers, the cell bodies can lie in the ependyma layer or outside of it. Definitive glial form in most vertebrates but transitory in birds and mammals. In the developing nervous system, radial glia function as a scaffold upon which newborn neurons migrate. In the mature brain, the cerebellum (Bergmann glia) and retina (Müller glia) retain characteristic radial glial cells.

Radial astrocytes (Sasaki and Mannen, 1981) have extraependymal cell bodies, with a lot of short processes, and one radial process extending to the pial surface. 'Astrocytes' described in fishes, amphibian, and reptiles usually proved to be 'radial astrocytes' rather than 'true astrocytes'.

Ependymoglia may refer to any glia with ependymal (ventricle-lining) cell bodies and shorter or longer processes, oriented radially or not.

Bergmann glia: A strictly parallel process system in the molecular layer of cerebellum, which guides the migration of granule cells during development. According to some authors, Bergmann glia is thought to be a modified protoplasmic astrocyte (Mugnaini, 1986).

Müller glia: In the retina, this radial cell is the principal glial cell, spanning out between the outer and inner limiting layers, with a nucleus in the inner granular layer.

Unipolar astrocyte: independent from the ependyma, the cell body has a long radial or non-radial process (Cameron-Curry et al., 1991).

As it appears from the descriptions, some of these categories overlap. For example ’ependymal’ can refer to the position of the cell body, while the word ’radial’ refers to the way processes are oriented, these two categories don’t necessarily go together, but if so, this cell type is called ’radial ependymoglia’, and so on.

2) Ependyma:

These epithelium-like cells line the cerebral ventricles. They can be cuboidal, flat, or columnar; they form usually a simple layer, but pseudostratified and stratified arrangements may also occur. Mugnaini (1986) classifies the ependyma as a type of astroglia, on the basis of its origin, occasional GFAP content and its cell contacts.

3) Oligodendroglia:

Oligodendrocytes: These cells coat axons in the central nervous system with their cell membrane, producing the so-called myelin sheath.

Satellite cells of the central nervous system: cells with round or oval nucleus and scarce cytoplasm attaching to neurons, possibly also to astrocytes. Most probably, these cells are part of the group oligodendroglia, mostly based on their histochemical markers (for example oligodendroglia transmembrane protein, Szuchet et al., 2001).

NG2 cells: Special cell type containing NG2 chondroitin sulfate proteoglycan. These are also present in adult central nervous system, which fact is considered to be important in the remyelinization in adults, and in glial responses to injury (Dawson et al., 2000).

4) Microglia:

Microglia are specialized macrophages that protect neurons of the central nervous system. They are small cells that are capable of removing waste products by phagocytosis. They are derived from hemopoietic precursors, rather than ectodermal

tissue, but are commonly categorized as glia. These cells comprise approximately 15% of the total cells of the central nervous system. They are found in all regions of the brain and spinal cord. They are mobile within the brain and multiply when the brain is damaged. In the healthy central nervous system, microglial processes constantly monitor all aspects of their environment (neurons, macroglia and blood vessels).

5) Glia of the peripheral nervous system:

Schwann cells: One form is similar in function to oligodendrocytes, forming compact myelin sheath around axons. The other form surrounds axons without forming myelin sheath.

Satellite cells: These small cells surround the surface of neurons and help regulate their chemical environment.

Two cell types show closer relationship to astrocytes, for example in the expression of GFAP:

ONEC (olfactory nerve ensheating cells): these cells cover the fila olfactoria outside and inside of the olfactory bulb (Doucette, 1984).

Enteric glia: these cells are present in nerve plexuses of digestive canal (Jessen and Mirsky, 1983).

2.6. Astroglial markers

2.6.1. Glial fibrillary acidic protein

Glial fibrillary acidic protein (GFAP) is an intermediary filament (of type III., diameter 10 nanometer) protein that is found almost exclusively in astroglia. Intermediate filaments GFAP helps maintain the shape of cells and attach to the cell membrane at the points of cell-cell or cell-extracellular matrix adhesion. Like other intermediate filaments, GFAP is formed by monomers containing three domains. The most conserved is the rod domain, whereas the head and tail have greater interspecific variability of sequence and structure. To form networks, the monomers form dimers, the dimers combine to make tetramers, which are the subunit of the filaments. Like other type III filaments, the GFAP can form hybride polymers, e.g. with vimentin. Vimentin, another type III intermediate filament, substitutes GFAP, or colocalizes with it in immature glial cells, as well as glioma (tumor) cell lines.

The amount of GFAP produced by the cell is regulated by numerous ways, such as cytokines, hormones and neuronal activity. Increased expression of this protein is evident in different situations, commonly referred to as "astrocytic activation". In mature cells, the most studied avenue of change in filament amount is the phosphorylation of GFAP, which results in the disaggregation of the filaments. The level of filamentous GFAP is in stable equilibrum with free point, and currently the functional importance of the alteration in the levels of GFAP is not fully understood.

2.6.2. Glutamine synthetase

Glutamine synthetase plays a major role in ammonia detoxification, interorgan nitrogen flux, acid–base homeostasis, and cell signaling. It is an enzyme that plays an essential role in the metabolism of nitrogen by catalyzing the condensation of glutamate and ammonia to form glutamine:

$$\text{Glutamate} + \text{ATP} + NH_3 \rightarrow \text{Glutamine} + \text{ADP} + \text{phosphate}$$

There seem to be three different classes of glutamine synthetase. Glutamine synthetase has been qualified as a very specific marker of astroglial-type neuroglia in vertebrate neural tissues (Martinez-Hernandez, 1977; Norenberg, 1979, 1983; Linser, 1985; Patel et al., 1985).

2.6.3. S-100 protein

S-100 protein is a type of low molecular weight protein found in vertebrates, characterized by two calcium binding sites of the helix-loop-helix conformation. There are at least 21 different types of S100 proteins. S-100 α and S-100 β are distinguished most often, based on the constructing dimers. The name is derived from the fact that the protein is 100% soluble in ammonium sulfate at neutral pH. S-100 regulates the calcium level of astroglia.

Most S-100 proteins are homodimeric. Although S-100 proteins are structurally similar to calmodulin, they differ in that they are cell-specific, expressed in particular cells at different levels depending on environmental factors. By contrast, calmodulin is a ubiquitous and universal intracellular Ca^{2+} receptor widely expressed in many cells. S-100 connecting to the head domain of GFAP filament helps the decomposition of GFAP

filaments. Therefore, it is a useful marker of astroglia (Ludwin et al., 1976). However, it may occur in other cell types too (Hachem et al., 2005). Notably, in a recent study (Chiba, 2000) S-100 has been detected in sharks (*Scyliorhinus torazame* and *Mustelus manazo*).

2.7. Astroglia in cartilaginous fishes and previous studies on glial markers

Horstmann (1954) reported that there was a principal difference between the elements of the astroglial system in sharks and rays. In skates and rays (*Torpedo marmorata, T. ocellata, Raja radiata,* Horstmann, 1954) the preponderant glial elements are true astrocytes, (non-ependymal stellate-shaped cells), independent from the ependyma, such as in birds and mammals. However, in sharks (*Scyliorhinus canicula, S. stellare,* Horstmann, 1954) the preponderant glial elements are ’tanycytes’ (Horstmann, 1954), i.e. thin and elongated, fiber-like and usually radial cells of ependymal origin, as in reptiles and in the majority of anamniotes. The results of the other classical impregnation and electron microscopic studies are in accordance with those of Horstmann (Roots, 1986). It is suggested that a similar (although independent) glial evolution occurred in Chondrichthyes and Amniotes in correlation with their brain evolution: astrocytes have become the predominant elements relative to ’tanycytes’ (Kálmán and Gould, 2001; Kálmán, 2002).

In the evolution of myelin, sharks were the first to have compact myelin (Kitagawa et al., 1993; Waehneldt, 1990). Before them, others like lampreys and worms had loose glial membranes wrapping around axons (Bullock et al, 1984; Waehneldt et al. 1987).

Immunohistochemistry, first of all the investigation of the astroglial marker GFAP (glial fibrillary acidic protein) provided a new method for studying the glial systems, including that of cartilaginous fishes (Dahl et al., 1973, *Squalus acanthias*; Gould et al., 1995, *S. acanthias*; Wasowicz et al., 1999, *Scyliorhinus canicula* and *Torpedo marmorata*; Kálmán and Gould, 2001, *S. acanthias* and *Raja erinacea)*. These studies were confined to the demonstration of cross-reactivity of chondrichthyan GFAP with mammalian anti-GFAP antibodies *in vitro*, and in some tissue samples. Preliminary experiments also demonstrated that glutamine synthetase and S100 protein can be applied successfully in cartilaginous fishes (Kálmán and Ari, 2001, *Raja erinacea*), and

similar results for S100 protein were reported by Chiba (2000, *Scyliorhinus torazame* and *Mustelus manazo*). The astroglial architecture of certain groups, such as Myliobatiformes and Pristiophoriformes has not been studied either immunhistochemical or classical methods as yet.

2.8. Blood-brain barrier of chondrichthyes

The blood-brain barrier is different in chimaeras and elasmobranchs, therefore their gliovascular connections are especially interesting. While in sharks and rays, the blood brain barrier is formed by perivascular glia, in chimaeras endothelial cells are responsible for this function, as in other vertebrates (Bundgaard, 1982; Bundgaard and Cserr, 1981, 1991, Cserr and Bundgaard, 1984; Abbott, 1995). According to the recent work of Bundgaard and Abbott (2008), the ’glial’ blood-brain barrier seems to be plesiomorphic feature, whereas the ’endothelial’ is apomorphic.

Despite such extensive differences among cartilaginous fishes, it is unknown whether there is a difference in the presence and distribution of the proteins required for the proper function of the blood-brain barrier. However, this question has not been investigated by immunohistochemical methods.

2.9. The dystroglycan complex and its associated proteins; aquaporins

The dystroglycan complex (DGC) is the most important laminin receptor beside integrins. It is required for the stabilization of vascular structure (Tian et al., 1996; Zaccaria et al., 2001), and for the maturation and functional integrity of the blood-brain barrier (Jancsik and Hajós, 1999; Nico et al., 2003, 2004). Linking cells to basement membranes, the complex was originally described in muscle but it also occurs in the brain and other organs (Durbeej et al., 1988). A core component of the DGC, dystroglycan (DG) is encoded by a single gene and cleaved into two proteins: DG-α and DG-β by post-translational processing (Ibraghimov-Beskrovnaya et al., 1992; Zaccaria et al., 2001). DG-α is a highly glycosylated extracellular protein which binds laminin and other basal lamina components, e.g. agrin and perlecan (Ehmsen et al., 2002; Henry and Campbell, 1999; Henry et al., 2001). DG-β is a transmembrane protein that anchors DG-α to the plasma membrane. DGC comprises numerous other components, dystrophin of different isoforms (or utrophin), dystrobrevin α or β, syntrophin α, and

others. (For review see e.g. Chamberlain, 1999; Culligan et al., 2001; Moukhles and Carbonetto, 2001). The dystrophin component connects the cytoskeleton (actually, the actin) to the DG-β.

In mammals, DG has been detected in vessels throughout the brain (Uchino et al., 1996; Yamamoto et al., 1997; Zaccaria et al., 2001). Regarding Chondrichthyes, the components of the DGC are well known in the electric organ of *Torpedo* species (Cartaud et al., 1992; Bowe et al., 1994; Deyst et al., 1995; Sadoulet-Puccio et al., 1996; Balasumbramyan et al., 1998, Rovuela et al., 2001) but there is no data published, whether these proteins are present also in the vessels of cartilaginous fishes, especially in their brain.

The DGC, first of all its syntrophin component, is responsible for the distribution and anchoring of the water-pore channel protein, aquaporin-4 (AQP4, Amiry-Moghaddam et al., 2003a,b, 2004; Nicchia et al., 2004; Warth et al., 2005). Aquaporins (AQP4 and AQP9) belong to a family of ubiquitous cell membrane water channel proteins in animals and plants ("small channel-forming protein superfamily") and play a crucial role in volume homeostasis (Venero et al., 2001; Vajda et al., 2002; Agre et al., 2002; Agre and Kozono, 2003; Amiry-Moghaddam et al., 2003a,b). Currently, the AQP family comprises 11 subtypes, ranging from AQP0 to AQP10 (Hatakeyama et al., 2001; Agre et al., 2002). In the mammalian brain (except for the choroid plexus), the prevalent aquaporin proved to be AQP4 (Hasegawa et al., 1994; Jung et al., 1994; Frigeri et al., 1995), which occurs mainly in astroglial endfeet. Nico et al. (2001) found AQP4 to be a marker of the maturation and integration of the blood-brain barrier. Another cerebral subtype is the AQP9 (Elkjaer et al., 2000), which is common to the cell bodies and processes. Aquaporin 4 proved to be identical with the 'orthogonally arranged particles' (OAP) revealed formerly by freeze-fracture technique in the membrans of astrocyte endfeet (Verbavatz et al., 1997; Rash et al., 1998; Nico et al., 2001; Furman et al., 2003).

Whereas aquaporins 4 and 9 have been intensely studied in mammalian brain, no data are found about brains of Chondrichthyes.

3. Aims

The aims of the present study were:

1) To get a better view on the astroglial architecture of elasmobranchs, the present study supplements the former impregnation based studies and GFAP immunohistochemistry by the immunohistochemical detections of glutamine syntethase and S-100 protein.
2) To extend examination to other representatives and important groups of Chondrichthyes, such as Myliobatiformes (because of their large brain), and Holocephali (because of the different blood-brain barrier), on which no glial study has been done as yet.
3) To study the rhombencephalon in greater detail, which has been hardly covered in previous glial studies.
4) To reveal some characteristic features of the blood-brain barrier of cartilaginous fishes: investigating the presence and distribution of the proteins of dystroglycan complex, such as dystroglycan, dystrobrevin, dystrophin, syntrophin and utrophin, in addition to AQP4 and AQP9.
5) To discern correlation between cerebralization types, glial architecture and the composition of blood-brain barrier.
6) To highlight evolutionary changes of astroglia in chondrichthyes.

In appendix:

7) To discuss the significance of the enlarged brain parts in ecological perspectives.

4. Materials and Methods

4.1. Sample collection

Almost every important chondrichthyan group was represented in our study, as it is demonstrated in figure 1. The species (fig. 5) were identified using the identification keys of Last and Stevens (1994). The gender, body length, body weight and in situ brain morphology have been documented. The original research reported herein was performed under guidelines established by the Council Directive 86/609/EEC, the Hungarian Act of Animal Care and Experimentation (1998, XXVIII) and local regulations for care and use of animals for research. All specimens examined were sexually mature adults as estimated from body size and genital organs, to exclude the possibility of ontogenetic shifts during development. The specimens obtained from fishermen were caught as by-catch, and the post-mortem time prior to fixation was 2 to 3 hours. Where it was possible to examine more than one specimen, no intraspecific variation could be observed. More information on the species used in this study is presented in Tables 1 and 2.

Subclass	Superorder	Order	Family	Species
Holocephali	Holocephalimorphi	Chimaeriformes	Callorhinchidae	*Callorhinchus milii*
Elasmobranchii	Squalomorphii	Squaliformes	Squalidae	*Squalus acanthias*
		Pristiophoriformes	Pristiophoridae	*Pristiophorus cirratus*
	Galeomorphii	Carcharhiniformes	Scyliorhinidae	*Cephaloscyllium laticeps*
			Scyliorhinidae	*Scyliorhinus canicula*
	Batoidea	Rajiformes	Rajidae	*Raja miraletus*
			Rajidae	*Raja clavata*
			Rajidae	*Dipturus whitleyi*
		Torpediniformes	Torpedinidae	*Torpedo marmorata*
		Myliobatiformes	Dasyatidae	*Dasyatis pastinaca*
			Myliobatidae	*Myliobatis australis*
			Mobulidae	*Mobula japanica*

Table 1. The taxonomic position of the species studied (according to Compagno, 1973, 1977; Winchell et al., 2004) are demonstrated. The taxonomy of rays and skates of Australia is currently under revision, therefore, *Dipturus whitleyi* can be also termed currently *Spiniraja whitleyi* (Last P, personal communication).

Figure 5. Photographs of species used in this study. A) *Callorhinchus milii;* B) *Squalus acanthias;* C) *Pristiophorus cirratus;* D) *Cephaloscyllium laticeps;* E) *Scyliorhinus canicula;* F) *Raja miraletus;* G) *Raja clavata;* H) *Dipturus whitleyi*; I) *Torpedo marmorata*; J) *Dasyatis pastinaca*; K) *Myliobatis australis*; L) *Mobula japanica.*


A


B

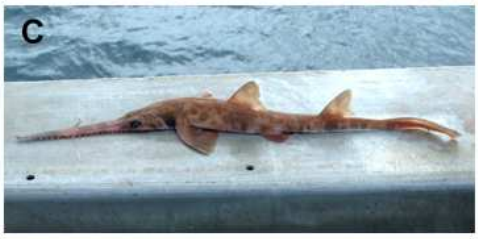
C


D


E

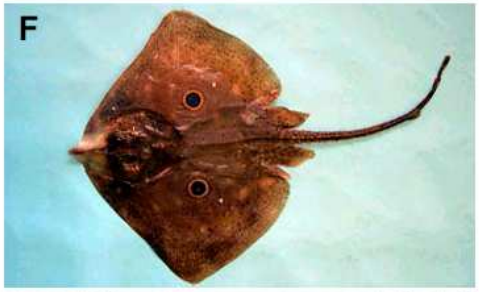
F


G


H


I


J


K


L

Latin name	English name	Date of description, describer	Place of origin	n
Callorhinchus milii	Ghost shark, elephantfish	Bory de Saint-Vincent, 1823	*	2
Squalus acanthias	Piked dogfish	Linnaeus, 1758	*	2
Pristiophorus cirratus	Longnose sawshark	Latham, 1794	*	2
Cephaloscyllium laticeps	Draughtboard shark, Australian swellshark	Duméril, 1853	*	3
Scyliorhinus canicula	Small-spotted catshark	Linnaeus, 1758	*	6
Dipturus whitleyi	Melbourne skate, Wedgenose skate	Iredale, 1938	*	2
Raja miraletus	Brown ray	Linnaeus, 1758	**	3
Raja clavata	Thornback ray	Linnaeus, 1758	**	1
Torpedo marmorata	Spotted torpedo	Risso, 1810	**	1
Dasyatis pastinaca	Common stingray	Linnaeus, 1758	***	2
Myliobatis australis	Southern eagle ray, Australian bullray	Macleay, 1881	*	2
Mobula japanica	Spinetail mobula	Müller és Henle, 1841	#	2

Table 2. The names of the species are indicated, also in English. The date of the description and the name of describer are also presented. The number of specimens used (n) and their origin are shown. * - Commonwealth Scientific and Industrial Research Organisation (CSIRO) Marine Research Laboratories, Hobart, Tasmania, Australia; ** - Institute of Marine Biology, Kotor, Montenegro; *** - Tropicarium, Budapest, Hungary; # - Common expedition of University of California, Scripps Institution of Oceanography, San Diego, Monterey Bay Aquarium, USA, Centro de Investigacion Cientifica y de Educacion Superior de Ensenada (CICESE), Mexico, Oceanario de Lisboa, Portugal.

4.2. Histological processing

4.2.1.Tissue fixation

None of the animals have been perfused. Brains were removed on site and immersion-fixed in 4% paraformaldehide and after 24 hours the fixative was changed and the brains were stored for two more weeks.

Because of their large size, *Mobula japanica* brains have been immersion fixed in AFA fixative (90ml 80% ethanol, 5ml formalin, 5ml glacial acetic acid, Northcutt, 1977, 1978), which penetrates well, and after 24 hours the brains were placed into 70% ethanol for transportation.

4.2.2. Tissue embedding

For embedding the following methods were applied:

- Agarose: Before sectioning the brains were embedded in agarose (5g agar was dissolved in 100ml cold water, stirred and warmed up until it was completely dissolved) After removing the meninges, the brains were placed into blocks of hot agarose, and then cooled in a refrigerator. Because of the large size of *Mobula japanica* brains, it was impossible to use the agarose embedding technique.
- Paraplast: From each species represented by more than one specimen, immunohistochemical reactions were also performed on materials embedded in paraplast (Sigma, Paraplast Plus P3683). A detailed description is given below for Mobula brains but the method was also applicable with slight modifications for the smaller sized brains.

The large-sized *Mobula japanica* brains were dehydrated by storing in 80 % ethanol for 7 days, 90 % ethanol for 7 days, 96 % ethanol for 2 x 7 days, 100 % ethanol for 3 x 1 days, 1 % celloidin methylbenzoate for 1 and 2 days, and xylene for 2 x 1 hours. Before embedding the brain was stored in paraplast: xylene mixtures (1: 2, 1:1 and 2:1), each for half an hour, followed by paraplast for 12 hours, than for 1 day twice. The brains were embedded in paraplast (Sigma, Paraplast Plus P3683).

4.2.3. Sectioning

From the brains embedded in agarose serial coronal sections (60-100 μm thick) were cut with a Vibratome and the sections were floated in phosphate buffer (0.1 M, pH 7.4).

From the brains embedded in paraplast serial coronal sections (10 μm thick) were sectioned by a Reichert microtome and mounted on slides coated with albumin or gelatine.

Where it is mentioned in the text, semithin sections were also prepared, following dehydration in an ascending dilution series of alcohol and propylene oxide, and embedding in epoxy resin (Durcupan), cut by Reichert ultramicrotome, and stained with toluidine blue.

4.3. Immunohistochemistry

Free-floating (Vibratome) sections were pre-treated with 20% normal goat serum for 1.5 hours to suppress the non-specific binding of antibodies. This and the following steps all included a rinse in phosphate buffered saline (PBS, Sigma, 0.01 M, pH 7.4) interposed between the changes of reagents.

Antibody				Manufacturing company	Place of manufacturing
anti-GFAP	1:100	monoclonal	mouse	Novocastra	Newcastle, United Kingdom
anti-GFAP	1:100	polyclonal	rabbit	DAKO	Glostrup, Denmark
anti-glutamine-synthetase	1:100	monoclonal	mouse	Translab	Erembodegem, Belgium
anti S-100	1:100	polyclonal	rabbit	Sigma	Saint Louis, USA
anti-dystroglycan	1:100	monoclonal	mouse	Novocastra	Newcastle-upon-Tyne, England
anti-dystrophin (Dys2)	1:2	monoclonal	mouse	Novocastra	Newcastle-upon-Tyne, England
anti-α dystrobrevin	1:100	polyclonal	goat	Santa Cruz Biotechnology	Santa Cruz, Ca, USA
anti-syntrophin	1:100	polyclonal	rabbit	Sigma	San Louis, Mo, USA
anti-utrophin	1:10	polyclonal	mouse	Novocastra	Newcastle-upon-Tyne, England
anti-aquaporin 4	1:200	polyclonal	rabbit	Sigma	San Louis, Mo, USA
anti-aquaporin 9	1:100	polyclonal	rabbit	Alpha Diagnostic	San Antonio, Tx, USA

Table 3. The characteristic features of primary antibodies applied in this study with dilution rates used.

The primary antibodies used in this study are listed in Table 3. The liophilised immunochemicals were restituted according to the manufacturer's prescriptions**,** and

further diluted to 1:100 in PBS containing 0.5% Triton X-100, and the sections were incubated for 40 hours at 4°C. The markers were examined in each species by using parallel series of sections. Double immunoreactions with anti-dystroglycan and anti-dystrobrevin or anti-syntrophin were also performed.

4.3.1. Visualization

DAB reaction on floating sections:

The immunohistochemical reaction was developed according to the 'ABC'-method. Biotinylated anti-mouse, anti-goat or anti-rabbit immunoglobulin, and avidin-biotinylated horseradish peroxidase (ABC) complex (both with Vectastain kit, Vector Laboratories, Burlingame, USA) were applied subsequently, in a dilution of 1:100, for 1.5 hours, at room temperature. The immunocomplex was visualized by diaminobenzidine (DAB) reaction: i.e. by incubation in a mixture of 0.05 % 3,3'-diaminobenzidine, 0.05 M Tris-HCl buffer (pH 7.4) and 0.01 % H_2O_2 for 10 min, at room temperature. The sections were mounted from PBS, dried in air, and coverslipped with DePeX.

Fluorescent reaction on floating sections:

Fluorescent immunohistochemical reactions were also performed. This technique is insensitive to either endogenous peroxidase activity, or to endogenous biotin (McKay et al., 2004). The incubation with primary antibodies was the same as described above. As fluorescent secondary antibodies, Cy3 dye-conjugated anti-mouse immunoglobulin, or fluorescein-isothiocyanate (FITC)-conjugated anti-rabbit or anti-goat immunoglobulin (products of Jackson ImmunoResearch Lab., Inc., Baltimore, USA) were used, respectively, in a dilution of 1:300 in PBS, for 3 hours, at room temperature. The sections were finally washed in PBS for 1 hour at room temperature and coverslipped in a 1:1 mixture of glycerol and double distilled water. The Cy3 dye emits red light (570nm) when induced by green light (550nm), whereas in the case of FITC the inducing light is blue (495nm) and the emitted light is green (519nm).

DAB reaction on paraplast sections:

The immunhistochemical reactions on sections with paraplast were performed similarly to that on the floating sections, with some modifications (mounted sections, humid chamber, shortened incubation periods).

Some of the sections were counterstained by cresyl violet, according to the Nissl method or with haematoxylin and eosin (HE) for orientation, and mounted in D.P.X.

4.3.2. Immunocontrol

Control reactions were performed by omitting the primary antibody. No structure-bound label was found, if the primary antibody was omitted, using either the immunofluorescent or the peroxidase method. The parallel application of these methods helped to rule out pseudopositivities occurring by either endogenous peroxidase positivity or endogenous biotin (McKay, 2004), as well as spontaneous fluorescence (eg under the effect of formaldehyde). As positive controls, the immunoreactions were performed on rat cortex or chicken cerebellum as well. In some cases, in the peroxidase visualized materials were pretreated 3% H2O2 as well to inhibit the endogenous peroxidase activity.

4.4. Microscopy and charting

The specimens were viewed under an Olympus BX51 microscope, and photomicrographs were taken by an DP50 digital camera, followed by contrast-adjustment using the Adobe 5 Photoshop program.

In case of double labeling, photomicrographs were taken under both green and blue lights, subsequently, from the same areas of alternate sections. The image pairs of different color were digitally united and slightly contrast adjusted using the Adobe5 Photoshop program.

The identification and nomenclature of brain structures are based on the descriptions of Ariëns-Kappers et al. (1906), Northcutt (1978, 1981), Butler and Hodos (2005), Smeets et al. (1983), and Smeets (1997) on the brain of *Hydrolagus collei* (Holocephali), *Squalus acanthias, Scyliorhinus canicula* and *Raja clavata.* The brain of the *Callorhinchus milii* is similar to that of *Hydrolagus collei* as described by Smeets et al. (1983). To demonstrate the macroscopic structure, drawings were made using a microscope slide projector apparatus, which showed the contours of the sections.

5. Results

5.1. Telencephalon: Sharks

In each shark species, used in this study, the telencephalon had relatively thin wall and large ventricles (fig. 6a-e). It consisted of two hemispheres, rostrally separated, but fused caudally, with a common wall. The most caudal part was the telencephalon medium or impar, with one ventricle.

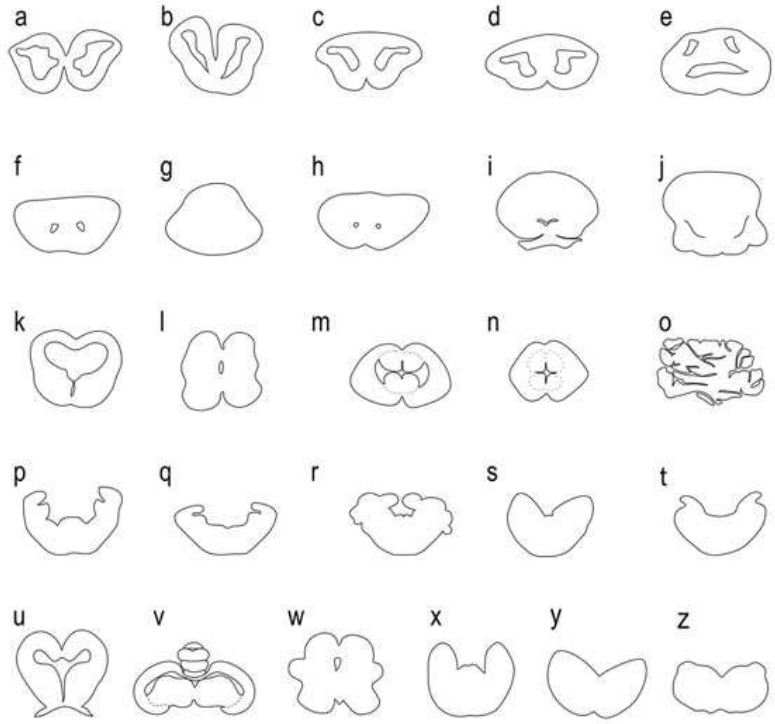

Figure 6. Diagrams of different brain parts in cross sections of the elasmobranch species studied and some Amniotes for comparison. Detailed presentation of the diagrams of each brain was not the goal here, only the visualization of the relation between the contours and ventricles. Brains are not to scale.
Telencephalon, sharks: (a) *Squalus*, (b) *Pristiophorus*, (c) *Scyliorhinus*, (d) *Cephaloscyllium*, each at the level of ventriculi laterales, and (e) *Cephaloscyllium* at the telencephalon impar,
Telencephalon, rays and skates: (f) *Raja*, (g) *Torpedo*, (h) *Myliobatis*, each at the level of ventriculi laterales, (i) *Myliobatis*, at the telencephalon impar, and (j) *Mobula*. Tectum: (k) *Squalus*, and (l) *Dipturus*. Cerebellum: (m) *Pristiophorus*, (n) *Raja*, (o) *Mobula*. Rhombencephalon: (p) *Squalus*, (q) *Cephaloscyllium*, (r) *Raja*, (s) *Myliobatis*, and (t) *Mobula*. Amniotes, tectum: (u) turtle (*Pseudemys scripta elegans)*, (v) chicken (*Gallus domesticus)*, and (w) rat (*Rattus norvegicus)*. Rhombencephalon: (x) turtle (*Pseudemys scripta elegans*), (y) chicken (*Gallus domesticus)*, and (z) rat (*Rattus norvegicus)*.

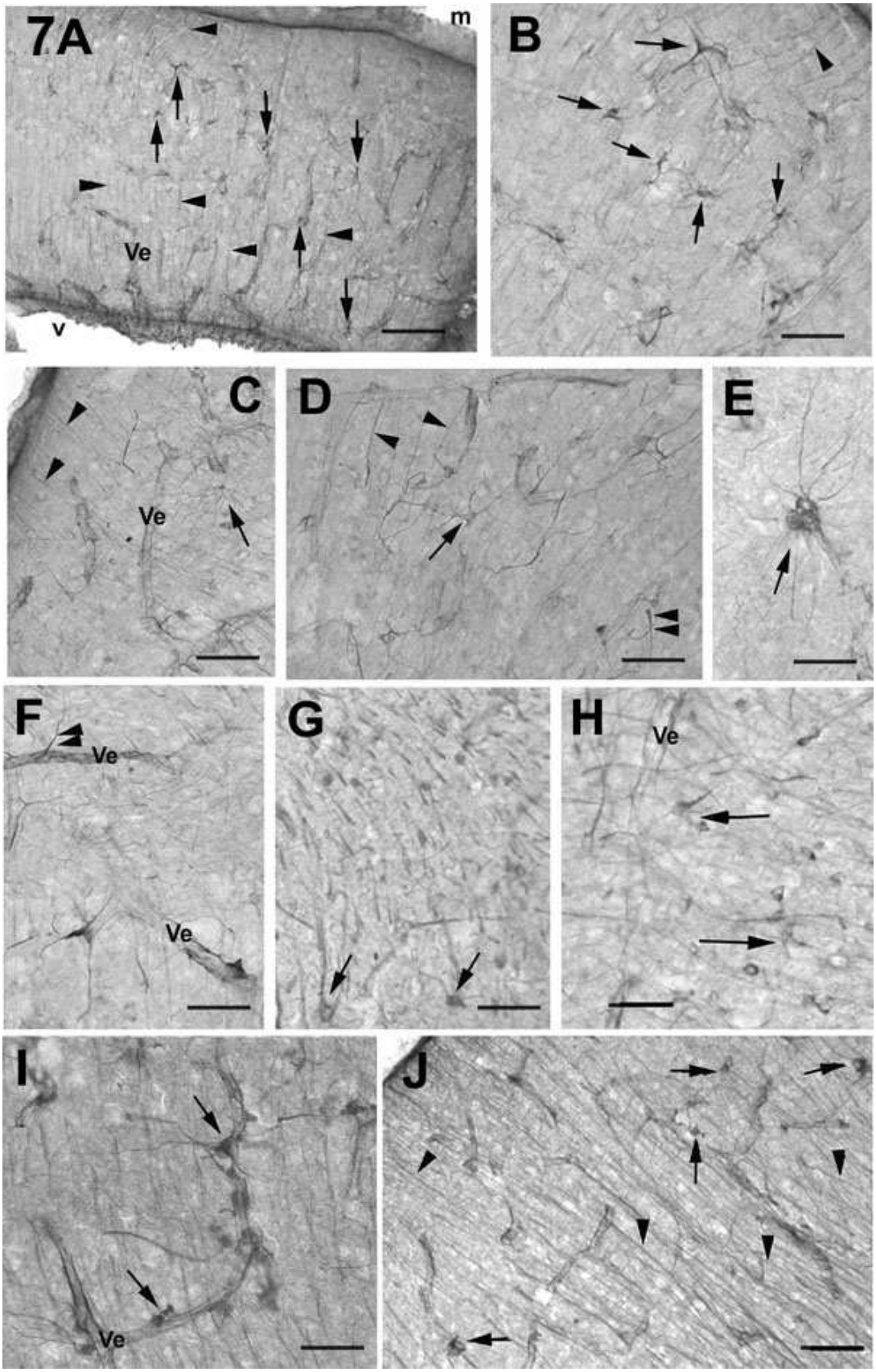
7A
m
Ve
v
B
C
Ve
D
E
F
Ve
Ve
G
H
Ve
I
Ve
J

Figure 7. Shark telencephalon

a) Several astrocyte-like structures are intermingled with the radial glia in the dorsal pallium. *Pristiophorus*, GFAP. Scale bar: 0.2mm.
b) Enlarged part of the previous area. Note the astrocyte-like figures. Scale bar: 0.1mm.
c) Astrocyte-like cell in *Pristiophorus* telencephalon, GFAP. Note the long processes, and the round perikaryon. Scale bar: 0.1mm.
d) Astrocyte-like cell in *Pristiophorus* telencephalon, GFAP. Scale bar: 0.1mm.
e) Round cells attached to a vessel in the telencephalon. Note their long processes in 'vasculofugal' orientation. *Pristiophorus*, GFAP. Scale bar: 0.05mm.
f) Glial end-feet on vessels in the telencephalon. *Pristiophorus*, GFAP. Scale bar: 0.05mm.
g) Astrocyte-like cells in the telencephalon. *Scyliorhinus*, GFAP. Scale bar: 0.1mm.
h) Astrocyte-like cells in the telencephalon. *Cephaloscyllium*, glutamine synthetase. Scale bar: 0.1mm.
i) Round and triangular (i.e. conical) glial perikarya attached to vessels in the telencephalon, and extending processes to the opposite direction. Scale bar: 0.1mm. *Squalus*, glutamine synthetase.
j) Astrocyte-like cells in *Squalus* telencephalon. Glutamine synthetase. Note the round cells of one long process. Scale bar: 0.1mm.

arrows – astrocyte-like and perivascular cells, triangular or round ; arrowhead – radial processes; double arrowhead – glial endfeet; for other abbreviations see List of abbreviations (page 2).

The predominant element was radial ependymoglia (i.e. tanycytes) in every brain area, including the telencephalon. The radial glial processes spanned the distance between the ventricular and meningeal surfaces (fig. 7a). Their ependymal origin was clearly observed, as well as their end-feet lining the pial surface. Where the thickness of the telencephalic wall was uneven, the radial processes remained perpendicular to both the meningeal and the ventricular surfaces. At the fusions of the hemispheres the radial processes did not cross the fusion line. Whereas such local differences were clearly found in any species investigated, no characteristic differences in the tanycyte system were recognizable in the different species, not even between galeomorph and squalomorph sharks. Beside the radial glial system, non-radial, apparently irregular and thin processes also occurred as side-branches of the main radial processes, or as separate, non-ependymal elements.

Non-ependymal cell bodies were found in all of the four shark species studied (fig. 7a-j), either perivascular or apovascular (i.e. non-perivascular) positions.

Immunohistochemical reaction to glutamine synthetase labeled more cells than what was observed using antibodies to GFAP or S-100 protein. Most apovascular cells had polygonal perikarya, with short, or relatively long processes, resembling astrocytes. Typical astrocytes, however, similar to the mammalian and avian ones, were uncommon. Some interspecific differences were observed. Most numerous astrocyte-like cells were found in the *Pristiophorus*, mainly in the dorsal aspect of the telencephalon (fig. 7b-e). In *Scyliorhinus* and *Cephaloscyllium* astrocyte-like cells occurred, mainly in the glutamine synthetase-immunostained materials, but scarcely (fig. 7g,h). Note that these cells were always found intermingled with the radial ependymoglia, but they never predominated in any territory, and never contributed to the glia limitans on the meningeal surface. Perivascular cells had round or triangular (i.e. conical, in three dimensions) cell bodies, which attached to the vessel, and extended a single 'vasculofugal' process into the surrounding brain substance (fig. 7e-f). Endfeet of long processes were also seen on the vessels (fig. 7f). In *Squalus* the non-ependymal cells were also quite numerous, but they, too, could be visualized only by immunostaining against glutamine synthetase but not against GFAP (fig. 7i,j). Most cells were attached to vessels as described above. Especially in the shark telencephalon, the vessels were immunopositive to the astroglial markers, even when the immunofluorescent reaction was applied (fig. 8a,b).

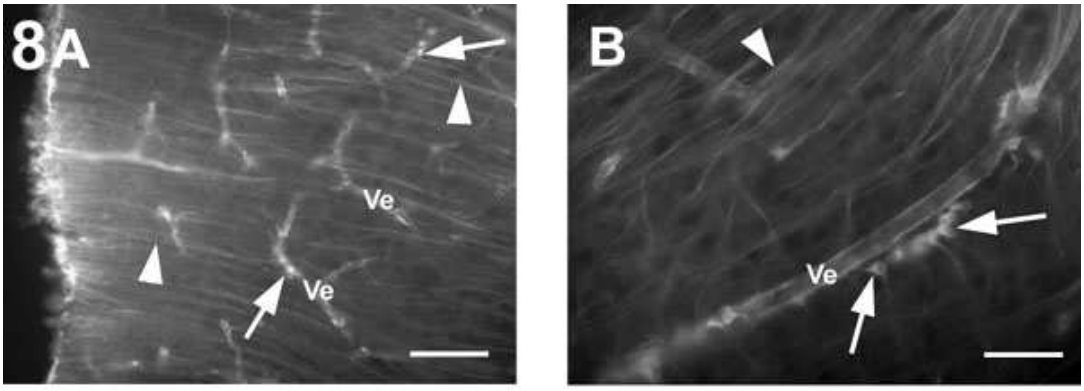

Figure 8. Immunofluorescence histochemistry

a) Note that similar structures (round and triangular glial perikarya attached to vessels, and extending their processes in the opposite direction) are visualized as those observed after the immunoperoxidase reaction. *Squalus* telencephalon, glutamine synthetase. Scale bar: 0.1mm.

b) Higher magnification image demonstrating structures similar to figure 7i. *Squalus* telencephalon, glutamine synthetase. Scale bar: 0.05mm.

Arrows – perivascular cells, triangular or round; arrowheads – radial processes.

5.2. Telencephalon: Skates and Rays

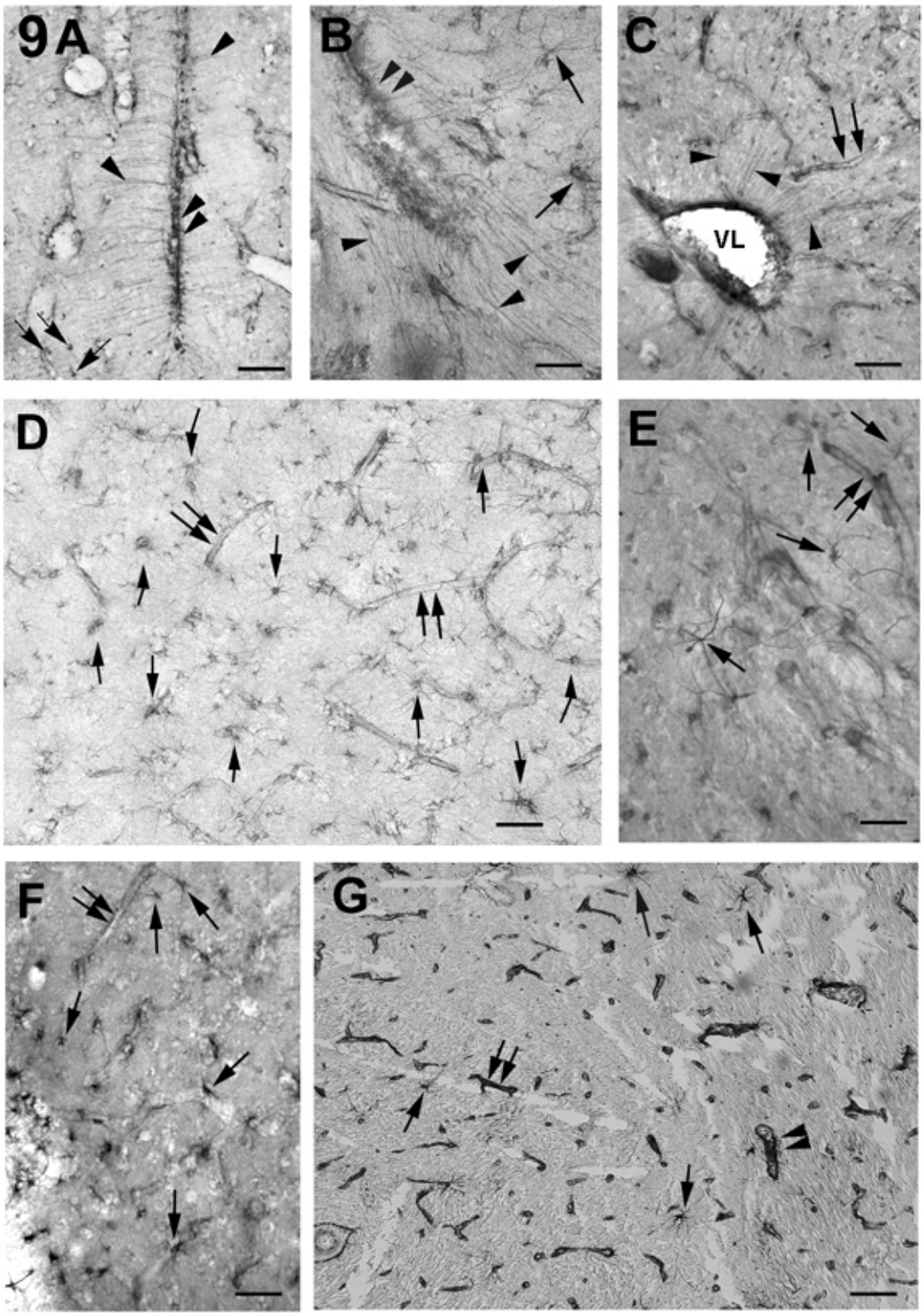

Figure 9. Rays and skates, telencephalon

a) *Raja clavata*, lateral ventricle, glutamine synthetase. Note the radial glial processes, emerging from the ventricular surface.
b) Radial processes around the lateral ventricle of *Raja miraletus*, glutamine synthetase. Astrocytes are also visible in the area.
c) Radial ependymoglial processes around the ventricle of *Dipturus*, GFAP.
d) *Raja miraletus* telencephalon, glutamine synthetase. Both peri- and apovascular astrocytes reacted.
e) Astrocytes in the telencephalon of *Dipturus*, S-100.
f) Astrocytes in the telencephalon of *Torpedo*, glutamine synthetase.
g) Telencephalon of *Mobula*, GFAP with Nissl counterstaining. Typical, but scarce astrocytes. Note the GFAP-immunopositive perivascular glial sheats.

Double arrowheads – compressed ventricle; double arrows – vessels; arrows – astrocytes; arrowheads – radial processes. Scale bars: 0.1mm.

In skates (Rajiformes), the lateral and median telencephalic ventricles have been reduced (fig. 6f). Around them radial ependymoglial processes were observed (fig. 9a-c), which were visualized by all immunohistochemical markers applied in this study. These processes, however, seemed to be thinner and less densely packed than in sharks, and did not span to the meningeal surface. In rays (Torpediniformes and Myliobatiformes) the lateral ventricles were obliterated (fig.6g,h,j), with a rudimentary median ventricle remaining posteriorly (fig.6i). Ependymoglia were not detected around them.

Astrocytes were found in great number in the telencephalon of each species. In skates, following immunohistochemical reaction against GFAP, these were observed only on the vessels and along the meningeal surface, like in our former study (Kálmán and Gould, 2001). When immunohistochemical staining of glutamine synthetase was applied, astrocytes were visualized throughout the telencephalon of skates (fig. 9e) and *Torpedo* (fig. 9f). In *Mobula* not only these markers, but GFAP also showed not only perivascular, but apovascular astrocytes as well (fig. 9g).

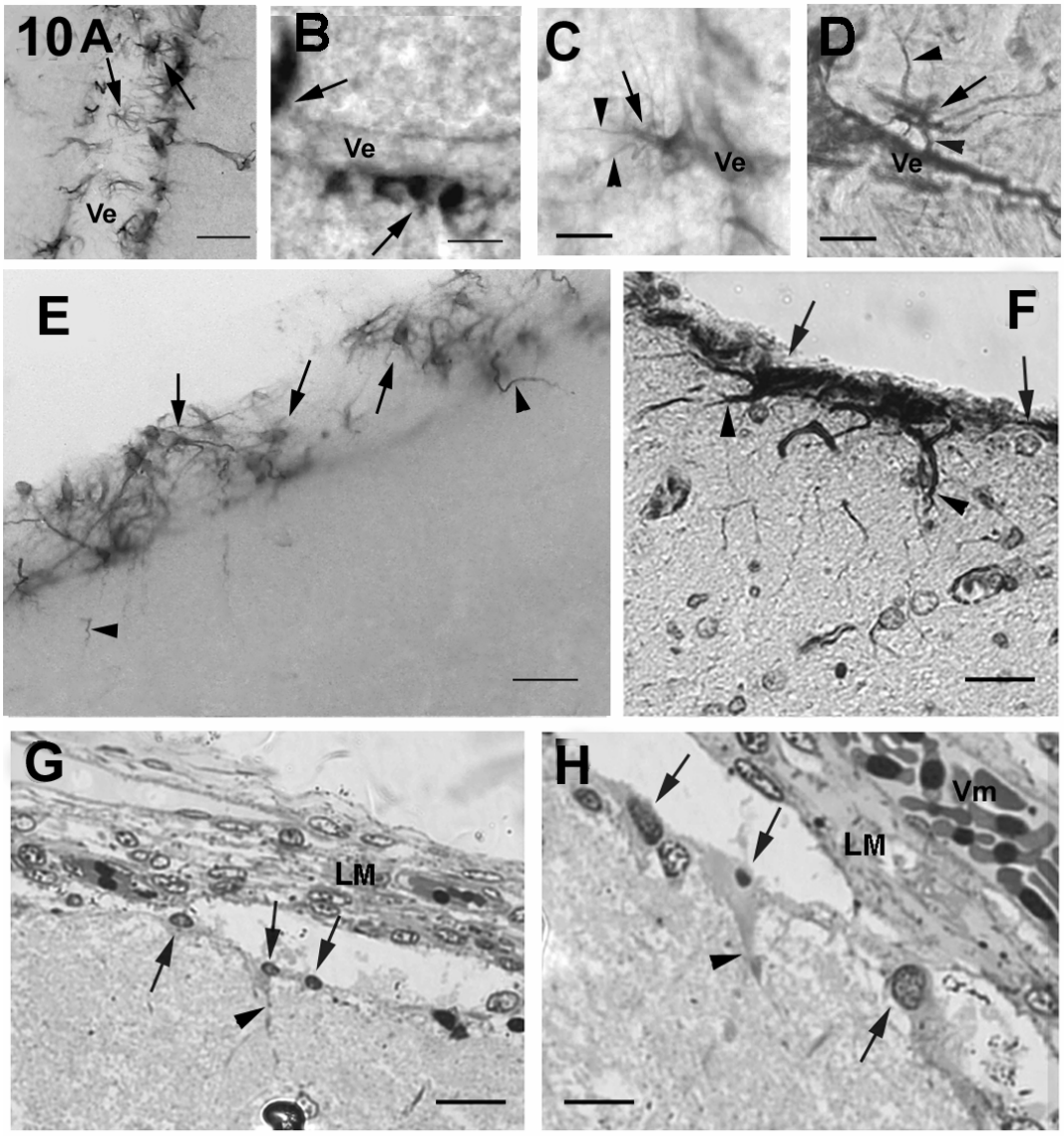

Figure 10. Rays and skates: various forms of perivascular glia and the submeningeal glia (glia limitans)

a) Typical astrocytes, i.e. stellate-shaped cells, spread their processes on the surface of a vessel. *Raja clavata*, telencephalon, GFAP. Scale bar: 0.05mm.

b) Round cells, with short processes, or apparently without processes, attached to a vessel. *Dipturus*, telencephalon, glutamine synthetase. Scale bar: 0.01mm.

c) A cell attached to a vessel, with short, tree-like process system on the opposite side. *Torpedo*, telencephalon, glutamine synthetase. Scale bar: 0.01mm.

d) Astrocyte, sending short processes to a vessel, and into the surrounding brain substance. *Mobula*, telencephalon, GFAP. Scale bar: 0.01mm.

Arrows – perivascular cells; arrowheads – glial processes.

(continued on the next page)

e) The meningeal surface is lined by astrocytes, spreading their processes along it. Note the empty circles corresponding to the positions of nuclei. Small processes perpendicular to the surface are also visible. *Raja clavata*, telencephalon, GFAP. Scale bar: 0.1mm.
f) The surface is covered by a thick, GFAP-immunopositive layer, from which processes submerge into the underlying brain substance. *Mobula*, telencephalon, GFAP with Nissl counterstaining. Scale bar: 0.025mm.
g) and h) Flat cells form a continuous, epithelium-like layer on the brain surface, below the (in part dispatched) leptomeninx (LM). These surface-forming cells extend coarse processes into the brain substance. Note the nucleus containing red blood cells in a meningeal vessel (Vm). *Myliobatis*, telencephalon, semithin section, toluidine blue. Scale bar: 0.025mm and 0.01mm.
Arrows – surface-forming cells; arrowheads – glial processes into the brain substance.

The perivascular glia comprised rather varied elements among batoids, in some cases even within the same species. There were stellate-shaped cells in *Raja* (fig. 10a), which spread their processes onto the surface of the vessels. In other cases, the cell bodies were attached to the vessel, either without processes, with round perikarya in *Dipturus* (fig. 10b), or with outgrowths emerging and branching on the opposite side in *Torpedo* (fig. 10c). Some perivascular glia in *Mobula* were found to contact the vessel only by their processes, a situation commonly found in mammals (fig. 10d). The glia limitans on the meningeal surface was also formed by cell bodies, rather than end-feet of processes, like in sharks. The cells either spread their processes onto the surface in Rajiformes (fig. 10e), or deep into the underlying brain substance in Myliobatiformes (fig. 10f-h). In semithin sections the aforementioned glial cells resembled an epithelial layer (fig. 10g-h).

5.3. Telencephalon: Chimaera

The brain of the *C. milii* (figs. 4a, 11) is similar to that of *Hydrolagus collei* described by Smeets et al. (1983). Most glial structures were revealed by glutamine synthetase immunostaining and the diaminobenzidine reaction. The GFAP and S-100 immunoreactions revealed the same structures as glutamine synthetase but sometimes less intensely. Therefore, the figures represent mainly glutamine synthetase immunostaining, unless otherwise stated. I have included drawings to demonstrate the main areas (left) and schematic glioarchitectonics (right) of the respective sections.

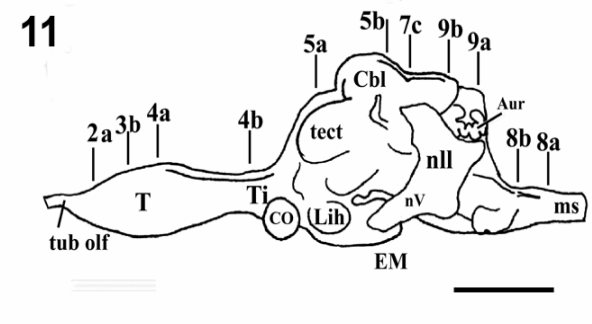

Figure 11. Schematic drawing depicting the lateral aspect of the brain of *Callorhinchus milii*. The perpendicular lines with numbers and letters indicate the positions of the cross-sections in the figures numbered correspondingly. Scale bar: 0.5 cm

The telencephalon of *C. milii* comprises paired evaginated hemispheres joining to the telencephalon medium (impar). The latter structure has a common ventricle and a thin choroid epithelial lamina as its roof. The rostral ends of the hemispheres are round with large ventricles and evenly thick walls. Here, a dense and evenly distributed typical radial glial system was found, with straight and thick radial processes originating from ependymal perikarya, and getting thinner, though still traceable, towards the meningeal surface.

Toward the caudal part of the hemispheres, however, the walls of the ventricles become unevenly thick, and the glial architecture differs (fig. 12a). The aforementioned regular surface-to-surface pattern persisted in only two segments: dorsolaterally, where the wall was thin, corresponding to the pallial area P12, and medially (around the anteromedial septal nucleus, Nsma, see fig. 12a). In the other areas two different patterns were found.

In the ventral segment (apparently in the area of ‘nucleus N’ according to Smeets et al. 1983), there were three zones, distinguished by their glial architecture (fig. 12b). The glial system remained approximately radial only in the zone nearest to the ventricle. Moving away from the ventricle, in the next zone, the processes were seen to cross each other (unusual for ’radial’ glia!). In the outermost (third) zone, the glial processes took an arched course. Several blood vessels were also immunoreactive.

In the lateral and dorsomedial (P9) segments of the wall (fig. 12c), the glial processes could be followed only for a short distance from the ventricular surface. Towards the meningeal surface, higher magnification also revealed individual, almost homogeneous glial processes, forming a dense plexus. Triangular structures with short radial processes were attached to the meningeal surface, which proved to be cell bodies under higher magnification (fig. 12d). In the HE-stained specimen the meningeal surface was lined by cell bodies that differ from meningocytes (fig. 12d, inset).

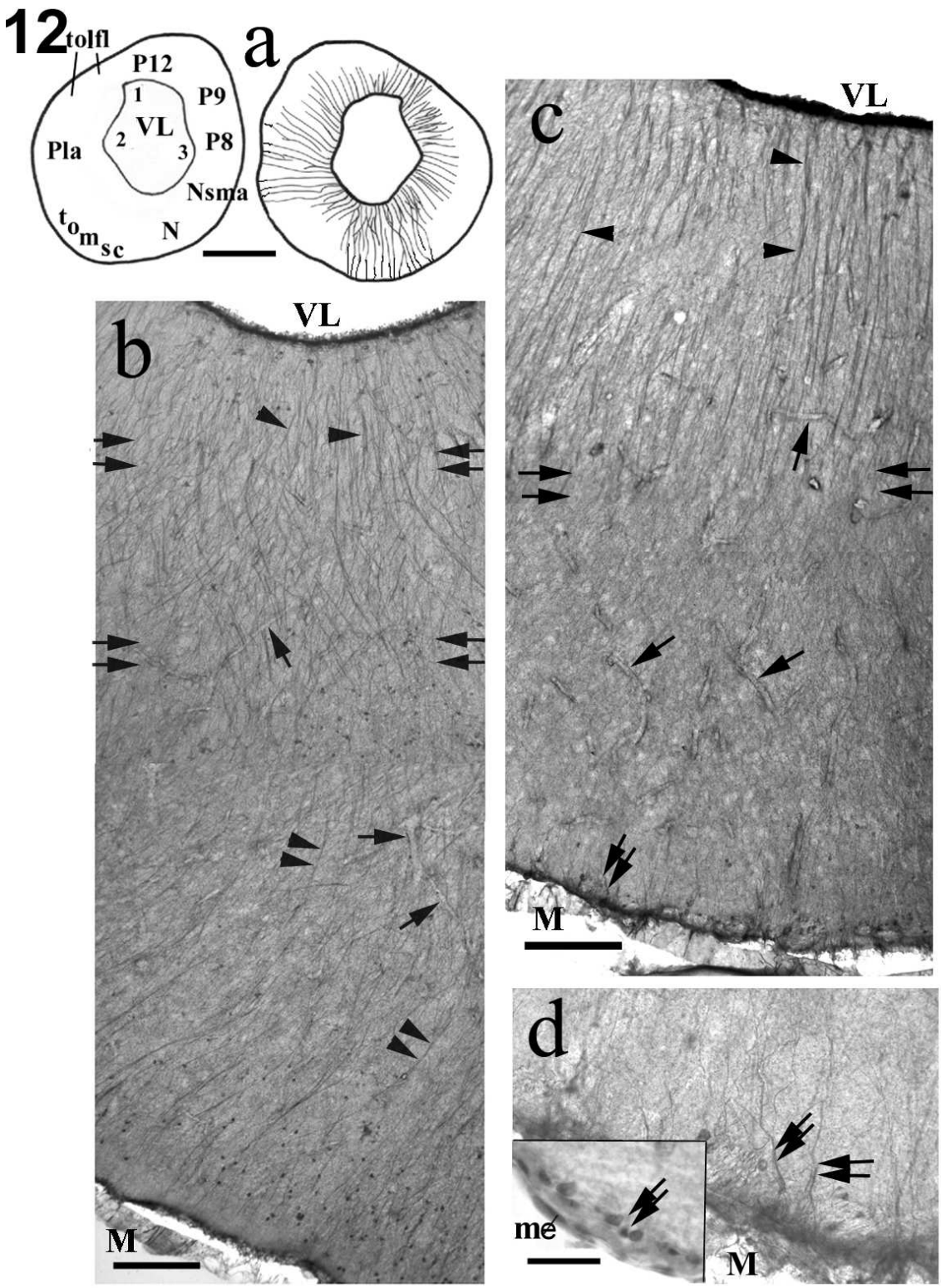
12
tolfl
P12
P9
P8
Pla
VL
1
2
3
Nsma
N
a
b
VL
M
c
VL
M
d
me
M

Figure 12. Chimaera telencephalic hemispheres, rostral part

The macroscopic structure of holocephalan brain is less known (except one species, *Hydrolagus collei*, Smeets et al., 1983), therefore more drawings with more details are included to help the orientation.

a) Schematic drawing depicting the rostral part of the hemispheres, in cross sections. Scale bar: 2.0 mm
b) The segment of the telencephalic wall corresponding to the position of nucleus N. Radial glial processes (arrowheads) originate from the ventricular surface. In the next zone (between the double arrows), the glial processes form a criss-cross pattern. In the third zone, the fibers are slightly curved (double arrowheads). Arrows point to vessels. Scale bar: 0.2 mm
c) The predominant structure of the telencephalic wall: the ependymal processes cannot be traced all the way to the meningeal surface. Radial glial processes (arrowheads) originate from the ventricular surface. In the next zone (the double arrows mark the border) glial processes cannot be recognized at this magnification. Vessels (arrows) are even more numerous, than in the previous zone. Below the meningeal surface tiny perpendicular glial processes are visible (double arrow, also in fig. 2d). Scale bar: 0.2 mm
d) Enlarged area of fig. 2c, from the meningeal surface. Note the cell-like structures (double arrow) attached to the meningeal surface, with short processes. Inset: cells (double arrow) lining the meningeal surface are clearly different from meningocytes (me), HE staining. Scale bar: 0.05 mm

Using immunofluorescence, the results were similar for glutamine synthetase, S-100, GFAP, including the fact that blood vessels were also intensely stained (fig. 13a). Following incubations without primary antibodies no such vessel-like structures were labelled. DAB-positive astrocyte-like structures with short processes among the radial processes, were also seen in the telencephalic wall (fig. 13c), in small and scarce groups but never attached to vessels. They were immunoreactive to glutamine synthetase and S-100 protein but not to GFAP.

In the posterior part of the hemispheres, the subpallial areas SP 10 and SP 11 bulged into the ventricles (fig. 13b). Here the glial processes were thin and hardly visible at the ependymal surface, but they thickened with depth (fig. 13d). They curved at the corners, i.e. at the bottom of the sulcus limitans lateralis and sulcus telencephalicus ventralis. Several vessels were also immunolabeled. Usually, the glial fibers could not be traced below the meningeal surface. Side-branches and non-radial processes were also visible.

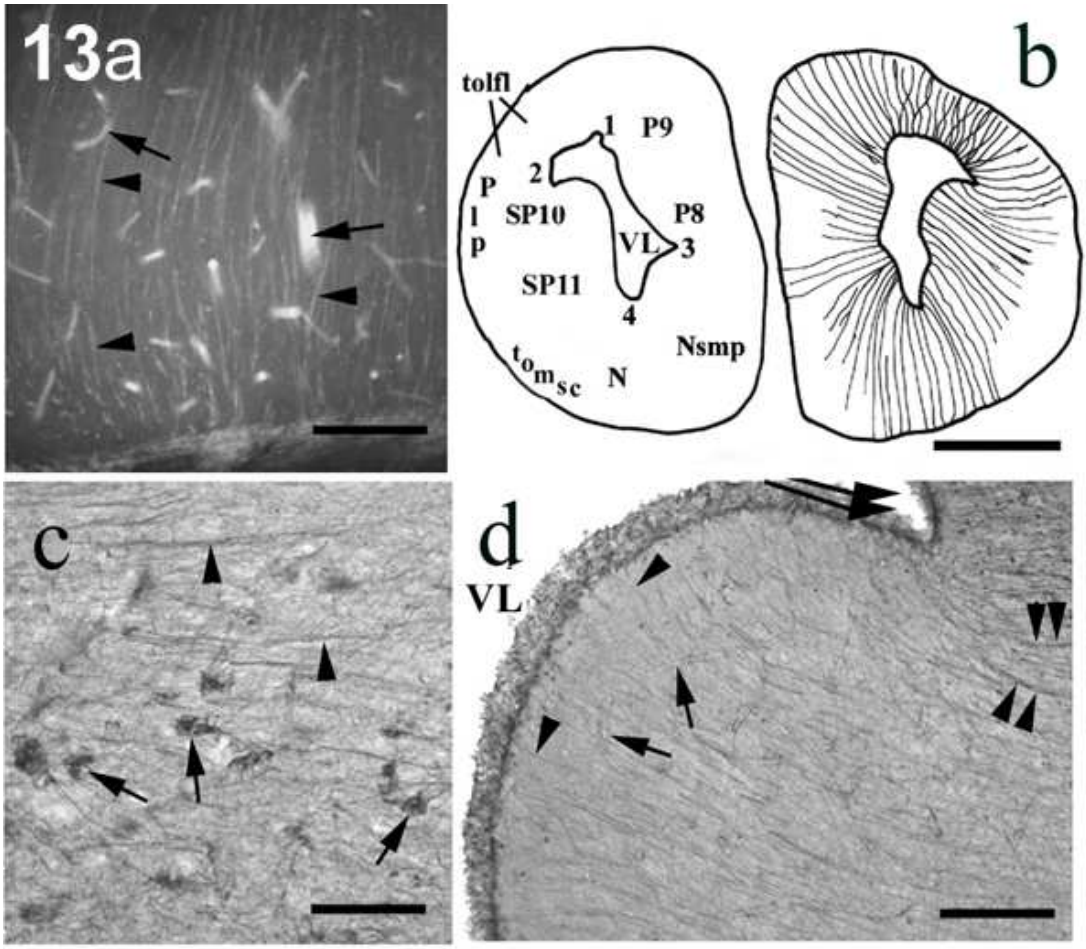

Figure 13. Chimaera telencephalic hemispheres, caudal part

a) Radial glial processes (arrowheads) revealed by immunofluorescent reaction to S-100 protein. Blood vessels are intensely stained (arrows). Scale bar: 0.2 mm
b) Schematic drawing of the caudal part of the hemispheres, in cross sections. Scale bar: 2 mm.
c) Astrocyte-like elements (arrows) with short processes among the radial fibers (arrowheads). For high magnification, see inset. Scale bar: 0.1 mm, for the inset: 0.05 mm
d) Dorsal half of the 'bulky' part (SP 10). The glial processes (arrowheads) are thin and hardly visible at the ependymal surface, but they get thicker with distance. Note their curved shape (double arrowheads), mainly at the sulcus telencephalicus ventrolateralis (double arrows; see also '2' in fig. 13b). Several vessels are also delineated (arrows). Scale bar: 0.2 mm

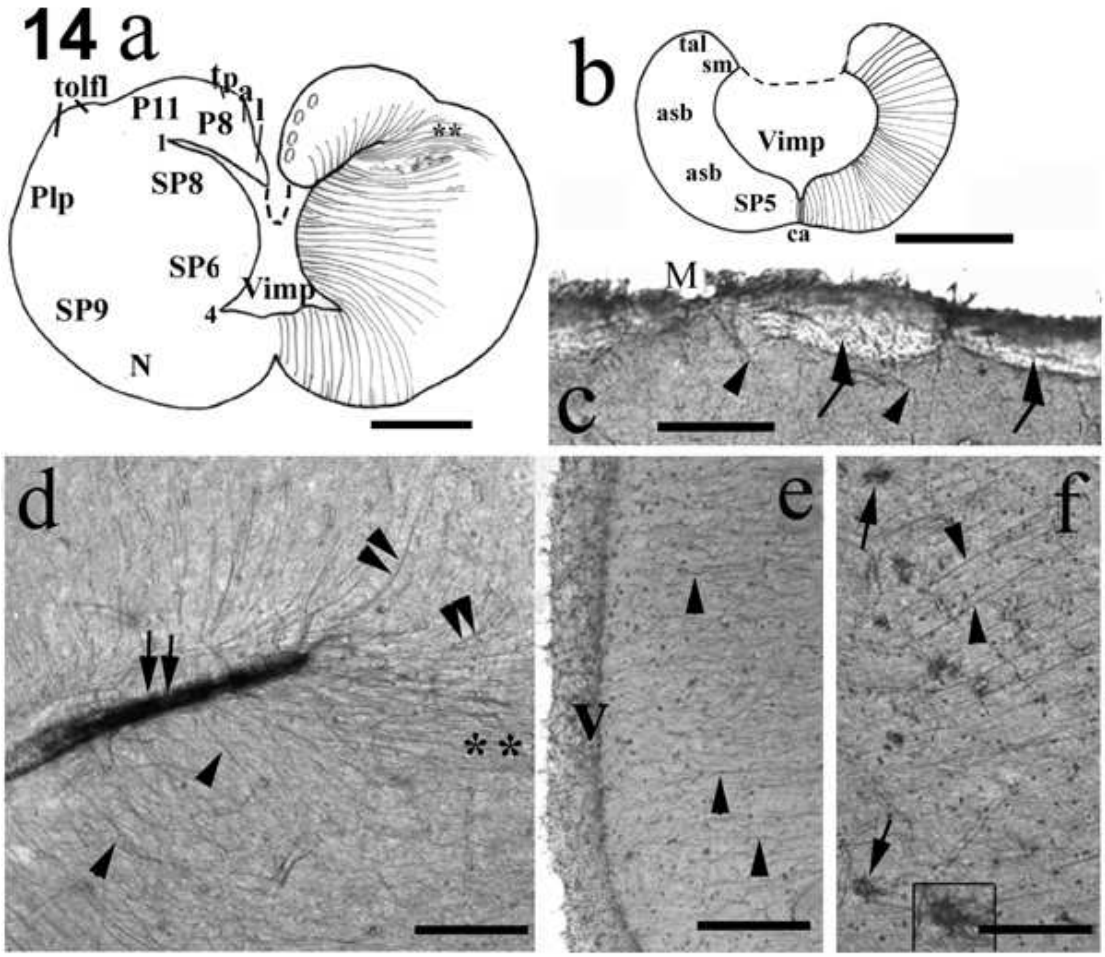

Figure 14. Chimaera telencephalon impar (medium)

a) Schematic drawing of a cross-section through the telencephalon impar (medium). The chorioid epithelial lamina (not preserved in the specimens) is symbolized by the dotted line. Scale bar: 2.0 mm
b) Schematic drawing of a cross section further caudal through the telencephalon impar. Scale bar: 2.0 mm
c) Typical appearance of tightly packed myelinated neural fibers in the tractus pallii (tpal). The fibers appear as light spots (arrows). Note the glial processes (arrowheads) below the meningeal surface. Scale bar: 0.1 mm
d) The deeper part of the sulcus limitans lateralis (double arrow; '1' in fig 14a). The radially orianted processes (arrowheads) appear curved at the corner of sulcus limitans (double arrowheads). A thick fiber bundle courses as an extension of the groove (double asterisk, see also Fig 4a). Scale bar: 0.2 mm
e) The narrow part of telencephalon impar (also shown in fig. 14b). Radial glial fibers (arrowheads) originate from the ventricular surface (V). Scale bar: 0.2 mm
f) Between the radial glial fibers (arrowheads) directed to the meningeal surface (to right), arrows indicate stellate cell-like structures (see enlargement in inset). Scale bar: 0.1 mm (for the inset: 0.05 mm)

The structure of the telencephalon impar is shown in figure 14a and b. The choroid epithelial lamina - the roof of the telencephalon impar- was not preserved in the sections. In the dorsal pallium, lightly stained spots, lacking background DAB staining, marked the positions of the pallial tracts (fig. 14c). Short and coarse glial processes demarcated these tracts. Similar light areas indicated groups of myelinated fibers, since myelin does not contain considerable endogenous peroxidase activity. Otherwise the glial structure was similar to that of the hemispheres, but a denser system of glial processes was observed in places where the wall was thick (i.e., by subpallial areas SP6 and SP8) and ventrally from the sulcus limitans lateralis (‘1’ in fig. 14a). Here the glial processes arising from the bulge became curved (fig. 14d). However, other processes that penetrated the pallial area P8 dorsally, emerged at right angles to the sulcus. Another ‘pony-tail’shaped group of processes coursed as a continuation of the groove and contributed to the separation of pallial area from the subpallium. Limiting the ventral side of the bulge, the radial glia were coarse, their processes curved and converged towards to the sulcus telencephalicus ventralis.

The posterior part of the telencephalon was narrower, with a thinner wall (fig. 14b). Radial processes extended from the ventricular to the meningeal surface (fig. 14e), although the GFAP- immunreactivity was not sufficiently intense to reveal them. The other two markers, however, revealed even astrocyte-like structures, among the radial glia (fig. 14f).

5.4. Diencephalon and Mesencephalon: Sharks, Skates and Rays

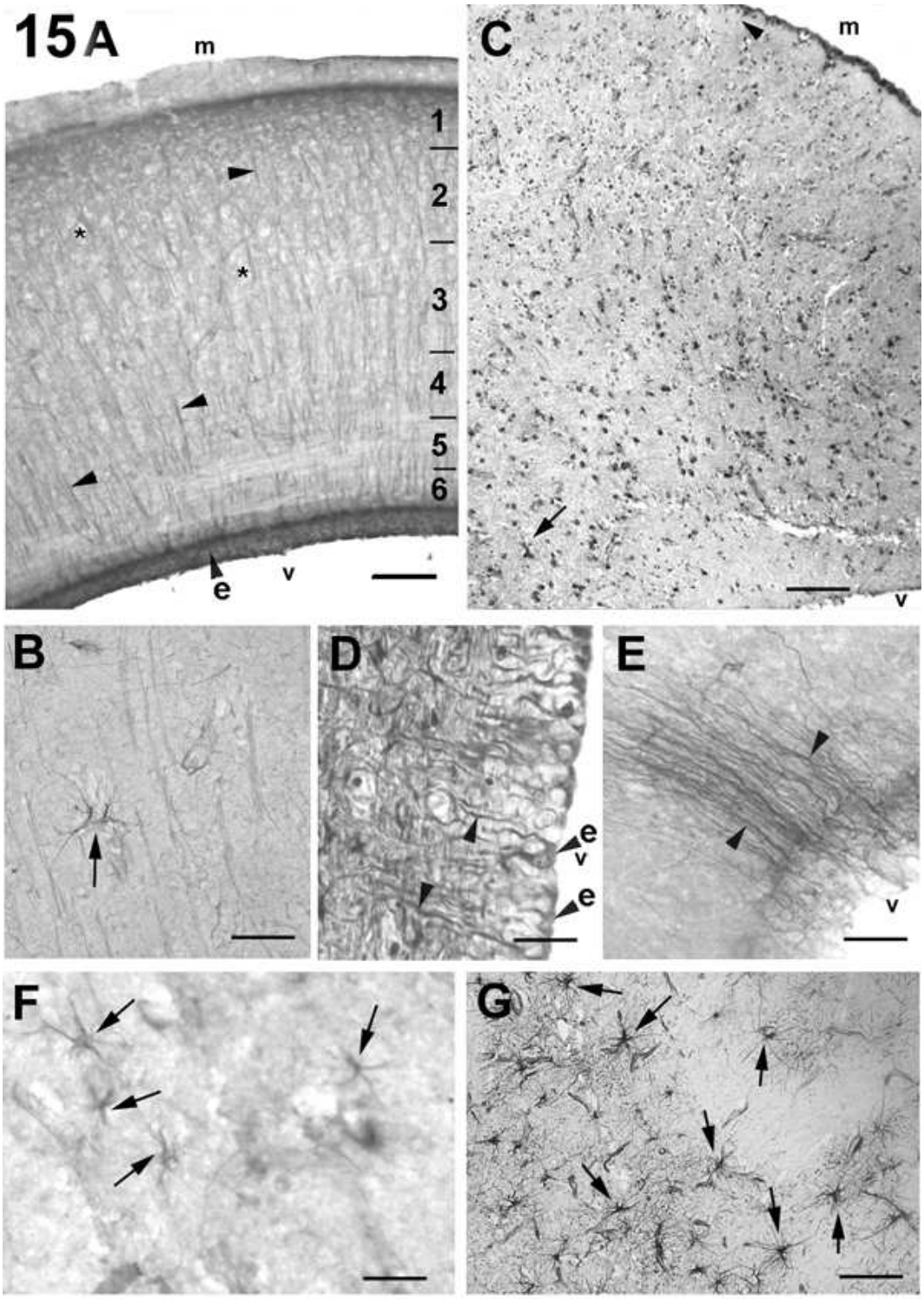

Figure 15. The mesencephalon of sharks, skates and rays

a) The usual astroglial architecture of the shark tectum, formed by radial ependymoglia. *Squalus*, S-100 protein. Despite of the uniformity of radial fibers, the number of the myelinated axon bundles distinguishes a layered pattern (according to Smeets et al., 1983). Note the ependymal origin of processes. Scale bar: 0.15mm.
b) One of the rather scarce tectal astrocytes, from *Cephaloscyllium*, glutamine synthetase. Scale bar: 0.05mm.
c) The tectum of *Raja miraletus*. GFAP, Nissl. No radial glia, but scattered astrocytes are visible between the neurons. The surface is covered by GFAP-containing cells. Scale bar: 0.15mm.
d) In *Mobula* only short glial processes emerge from the ventricular surface, GFAP. Scale bar: 0.02mm.
e) In some segments, radial ependymoglia are found in the narrow tectal ventricle. *Dasyatis*, GFAP. Scale bar: 0.05mm.
f) Astrocytes in the tegmentum. *Torpedo*, GFAP. Scale bar: 0.03mm.
g) Astrocytes in the tegmentum. *Mobula*, GFAP. Scale bar: 0.05mm.

Arrowheads – radial processes; arrowhead with e – ependimal perikarya of radial fibers; double arrowheads – processes below the surface; arrows – astrocytes; asterisks – axon bundles; 1-6 – tectal layers

In sharks, the diencephalic and mesencephalic ventricles were large (fig. 6k). Radial tanycytes were found around them, which formed end-feet on the meningeal surface. Short and dense radial processes delineated the periventricular gray matter, whereas in the white matter the processes were less densely packed. In the tectum, a layered structure was recognizable in some degree due to the invading tracts of myelinated axons, which appeared as faint areas, and due to an uneven density of the side-branches of radial glia (fig. 15a). Astrocyte-like cells were exceptionally rare (fig. 15b), visualized only by the immunostaining to glutamine synthetase. The meningeal surface was lined by end-feet of radial glia, like in the telencephalon.

In skates and *Torpedo*, in the diencephalon both besides astrocytes long radial processes were found, in the Myliobatiformes only short ependymal processes, as well as in the mesencephalon. In skates the mesencephalic ventricle was reduced to a canal (fig. 6l), similar to the cerebral aqueduct in mammals (fig. 6w), and the tectum bulged as solid masses like mammalian colliculi. Both in skates and rays radial ependymoglia proved to be shortened (fig. 15d) and reduced (fig. 15e), whereas astrocytes were the preponderant elements (fig. 15f, g), occurring even among the radial glia in the

tegmentum. The meningeal surface of the tectum was lined by astrocyte-like cellular elements, which extended processes into the brain substance (fig. 15c).

5.5. Diencephalon and Mesencephalon: Chimaera

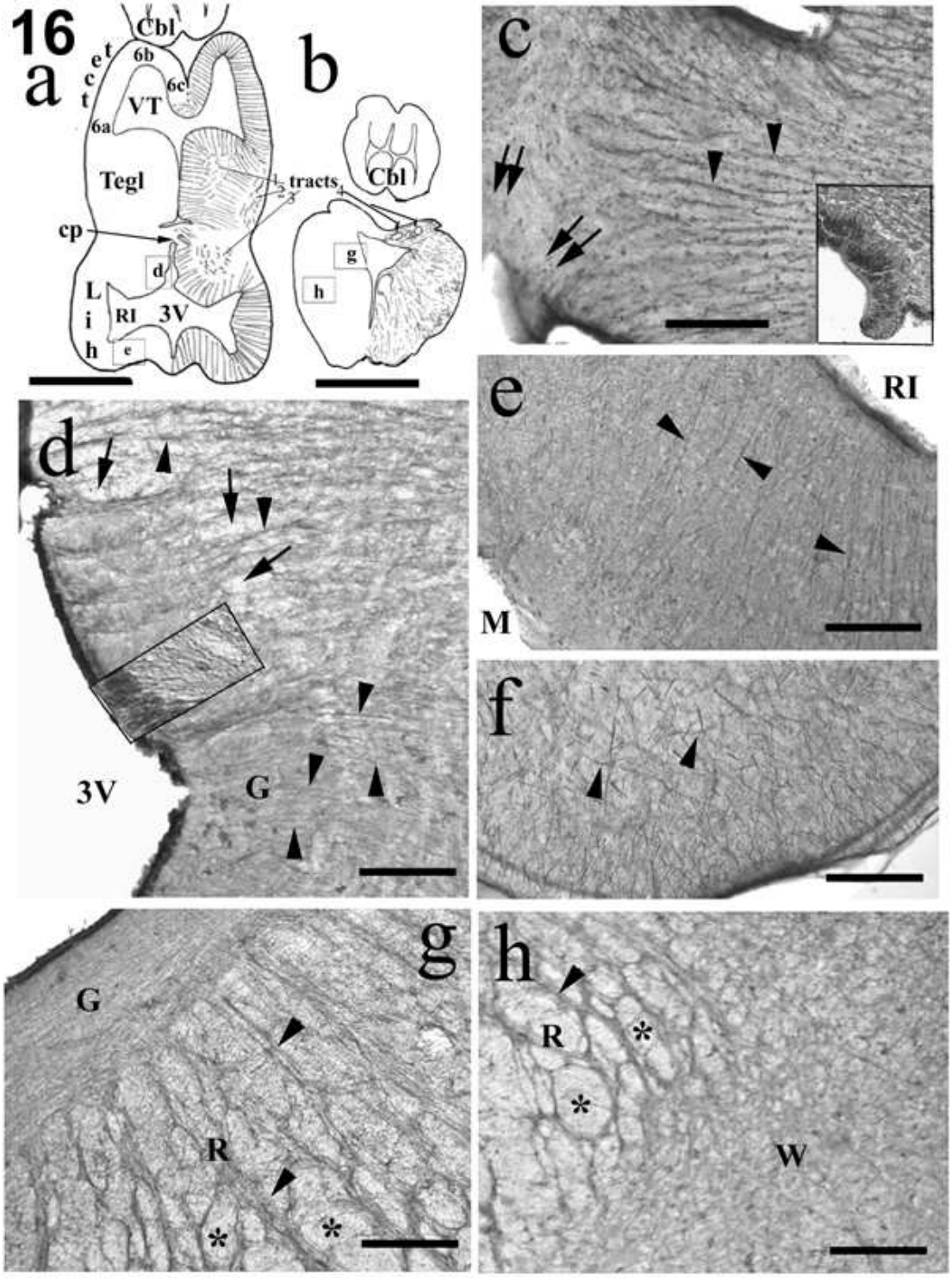

Figure 16. Chimaera mesencephalon with pretectum and isthmus

a) Schematic drawing of a cross section representing the diencephalic/mesencephalic border. The ventral part belongs to the diencephalon, e.g. posterior commissure and inferior recesses are visible. Tracts 1,2,3 – retinotectal, mesencephalic tegmental, and hypothalamic tracts, their glial structure is similar to that seen in fig. 16c. Tracts 4 –tracts of isthmus tectum, their appearance is similar to that seen in fig. 14c. The contralateral rectangles labeled with letters indicate the areas shown in the identically labeled frames. Scale bar: 3 mm.
b) Schematic drawing of the isthmus. The contralateral rectangles labeled with letters indicate the areas shown in the identically labeled frames. Scale bar: 3 mm.
c) Posterior commissure. Note the thick glial bundles (arrowheads) separating the axonal fascicles (light strips). Double arrows point to the subcommissural organ (see also the inset with HE staining). Scale bar: 0.2 mm (also for the inset).
d) Wall of the third ventricle with predominantly radial fibers. A very dense, near-homogenous system of delicate glial processes is visible in the central gray (G) from which longer fibers (arrowheads) emerge. Light spots (arrows) correspond to fascicles of nerve fibers. The inset (HE staining) shows columnar ependymal cells and their basal processes. Scale bar: 0.2 mm (for the inset 0.1 mm)
e) In the narrow wall of the inferior recess (RI) of the hypothalamus, radial glial fibers (arrowheads) are the predominant elements. GFAP, Scale bar: 0.2 mm
f) In the lobus inferior a radial arrangement of glial processes (arrowheads) is not evident. GFAP, Scale bar: 0.2 mm
g) Glial architecture of the isthmus, near the ventricle. Thin ependymal processes form an apparently homogenous layer (central gray, G). Emanating from this layer, glial bundles (arrowheads) form a network (’reticulum’ R) around the nerve fiber tracts (light spots, asterisks). Scale bar: 0.2 mm
h) The network becomes denser and finer, in the white matter (W) toward the periphery. (other marks as in fig. 16g). Scale bar: 0.2 mm

The diencephalon had a thin wall, with a fine and dense meshwork of radial glial processes of ependymal origin. In the optic chiasm and tracts, all the immunolabeling was confined to a few coarse glial septa. The posterior part of the diencephalon - e.g. posterior commissure and inferior recesses- is visible in several sections together with the mesencephalon (see fig. 16a).

The posterior commissure (fig. 16c) displays the pattern of immunoreactivity characteristic for large cerebral tracts: bundles of immunoreactive glial fibers alternating with lightly stained immunonegative strips, i.e. fascicles of myelinated neural fibers. A similar glial pattern characterized also the other large tracts, e.g. the optic tract, the chiasma, and the retinotectal and tegmental tracts. Below the posterior commissure, the subcommissural organ (see also inset in fig. 16c) remained immunonegative.

In the other parts of the diencephalon radial glia was the dominating element. The periventricular gray matter, however, showed a distinct glial pattern (fig. 16d). Here fine basal (i.e. abluminal) processes of ependymal cells formed a dense system that appeared almost confluent in thick vibratome sections; the filamentous structure of the processes (see inset in fig. 16d) was revealed only in thin paraffin sections. This zone, therefore, proved to be intensely immunoreactive. Some radial processes extended further laterally, separated by light strips corresponding to fascicles of myelinated neural fibers. This pattern of the central gray and the flanking white matter continued into the mesencephalic tegmentum and extended even into the isthmus. In those places, where the wall was narrow and sectioned at right angles, the radial glial processes could easily be traced as far as the meningeal surface, e.g. in the recessus and lobus inferior (fig. 16e, f). In the tegmentum of mesencephalon, a large protrusion contained the tegmental nucleus (see fig. 16a). Glial processes were observed to originate from the ventricular surface of the nucleus radially (i.e. perpendicular to the ventricular surface), but they could not be traced deep in the tegmentum.

In the isthmus, fine ependymal processes formed an apparently homogenous periventricular gray layer. The white matter contained bundles of glial processes that emanated from the gray matter toward the meningeal surface, where they formed endfeet (fig. 16g). These bundles formed a loose ’lacework’ in the white matter. Below the meningeal surface this network became denser and finer. This structure was similar to that found in the brain stem (see below). The medial longitudinal fascicle, however, was very light and poor in glial septa. Along the midline a glial bundle appeared. In the tectum of the isthmus light, DAB-negative spots indicated bundles of myelinated neural fibers, similar to those shown in figure 14c. The mesencephalic tectum forms bilateral domes (which appear as arches in cross section), which surround expansions of the spacious ventricular cavity (’tectal ventricle’).

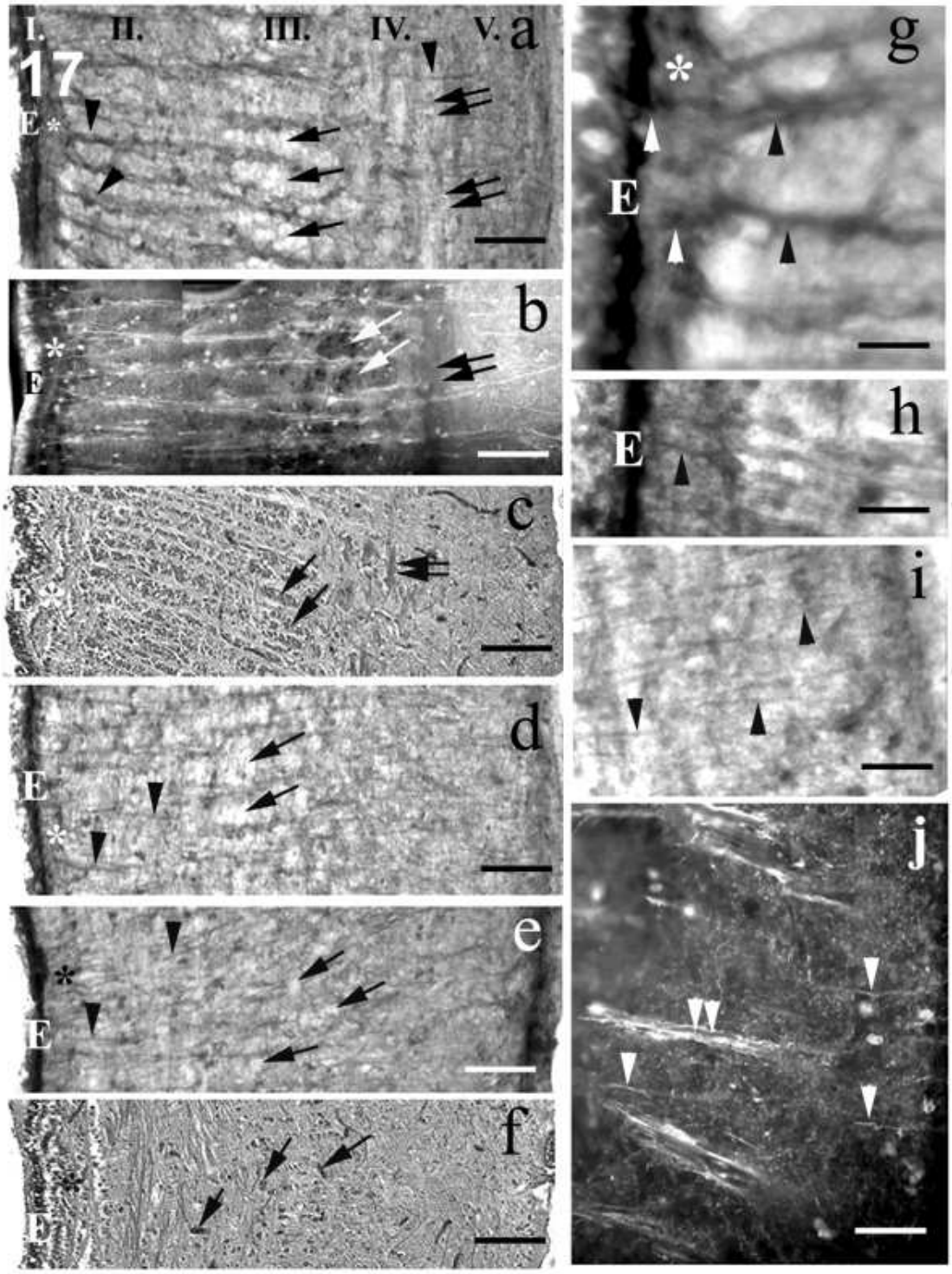

Figure 17. Chimaera optic tectum
For a better comparison, photomicrographs a-f show the entire thickness of the tectum, in the same size and orientation.
Double arrows- transverse fascicles; arrows-fascicles of neural fibers; arrowheads-radial processes; *- subependymal subdivision of layer I.

a) In the inferolateral part of the tectum (17a as indicated in fig.16a), five layers of glial architecture can be distinguished. Scale bar: 0.2 mm.
   I) Ependymal (E), and 'subependymal'(asterisk) subdivisions. See enlarged view in fig. 17g.
   II) The thick radial processes(arrowheads) are separated by lighter areas.
   III) The areas between the radial processes appear 'foamy' (arrows).
   IV) Radial processes (arrowhead) and transverse light strips (double arrows).
   V) An apparently 'homogenous' layer, in which radial processes can be discerned only under high magnification (fig. 17i).

b) The five zones can also be revealed by immunofluorescence (arrows and double arrow point to similar structures as in fig. 17a). The 'subependymal' zone (asterisk) is immunonegative, except for the radial processes. Scale bar: 0.2 mm

c) HE staining confirms that the spots that appear light in fig. 17a, and dark in Fig.17b correspond to fascicles of neural fibers (arrows). The transverse fascicles (double arrow) represent retinotectal fibers. Scale bar: 0.2 mm

d) On the top of the tectal domes (17b as indicated in fig.16a) the light areas of layer III. (arrows) are diminished, whereas the radial processes (arrowheads) seem to get thinner and denser. Scale bar: 0.18 mm

e) In the tectal arch near the midline (17c as indicated in fig.16a) the structure is more uniform and zones cannot be easily distinguished. Scale bar: 0.16 mm

f) HE staining in the tectal arch near the midline. Scale bar: 0.16 mm

g) Enlarged detail of the ventricular surface and the ependymal layer (E). Asterisk marks the same layer as in fig. 17a -f. Arrowheads point to roots of radial processes. Scale bar: 0.03 mm

h) A perikaryon is connected with the ventricular surface by a short process (arrowhead). Scale bar: 0.06 mm

i) Enlarged view of the layer V showing the radial fibers (arrowheads). Scale bar: 0.06 mm

j) Layer V with dense plexus of delicate glial processes as revealed by immunofluorescence. The apparently 'homogenous' background is composed of a dense plexus of delicate glial processes (note the tiny dots throughout the image). Arrowheads - single processes; double arrowheads - bundles of processes. Scale bar: 0.03 mm

The tectum of chimaeras is similar to that found in sharks and the majority of vertebrates, but it differs from the solid tectum of batoids (which resembles the tectum of mammals). The basic pattern corresponded to radial glia. The optic tectum, however, has a layered cytoarchitectonic pattern in all vertebrates, including Chondrichthyes (see Smeets et al., 1983), which raises the question whether modifications of the radial pattern reflect a layered structure. The following segments of the tectal wall were

distinguished: an inferolateral segment (fig. 17a,b,c) ; a segment at the top of the tectal dome (fig. 17d); and a paramedian segment (fig. 17e,f). For their positions see figure 16a. In the inferolateral segment five layers were distinguished:

I) This layer comprised two subdivisions (see enlargment in fig. 17g). One was formed by the ependymal perikarya lining the tectal ventricle (’ependymal’, Ia), where the radial processes originated. The other subdivision (’subependymal’, Ib) contained mainly immunoreactive processes, but a few immunoreactive cells were also found here, connected to the ventricular surface by short basal processes.

II) In this layer, thick radial processes were separated by lighter areas but interconnected by side-branches.

III) In this layer, the interposed areas were very light and took on a ’foamy’ appearance.

IV) In this layer, transverse light strips appeared, crossing the radial pattern.

V) This layer appeared to be rather homogenous, although radial processes and a dense plexus of delicate glial processes could be recognized (fig. 17i).

Regardless of whether the immunoperoxidase (fig. 17a) or immunofluorescence technique (fig. 17b) was applied, the results were similar. The subdivisions of layer I appeared more distinct with the latter method, where the ’ependymal’ layer (Ia) was as intensely immunostained as in the DAB stained sections, but the ’subependymal’ (Ib) layer was immunonegative (i.e. black in this case). HE staining demonstrated that the unlabelled (light in fig. 17a, but black in fig. 17b), ’foamy’ structures correspond to fascicles of neural fibers (fig. 17c). The transversely oriented axonal fascicles were traced back to the optic chiasm in subsequent sections, thus they must have belonged to the retinotectal tract. The neurons were concentrated in the vicinity of the ventricle, corresponding to the ’subependymal’ (Ib) layer.

The layering pattern changed along the arch of the tectum; at its top the light areas were reduced, and the radial glial pattern seemed to be denser (fig. 17d). Therefore, layers II to IV were less distinct. Near the midline the layer III contained relatively few axonal fascicles, making the layers harder to be discerned (fig. 17e,f). In every segment of the tectum the superficial layer was homogenous and radial glial processes were recognizable at high magnification (fig. 17i). Where the bilateral tectal ’arches’ (domes) were fused in the midline, a group of extarordinarily large neurons was seen in HE

stained sections. These cells were regarded as the pseudounipolar neurons of the mesencephalic trigeminal nucleus (see Smeets et al., 1983). No characteristic glial structure was, however, found around these neurons, excepting the glial pattern of the tectal commissure resembling cerebral tracts.

5.6. Cerebellum: Sharks, Skates and Rays

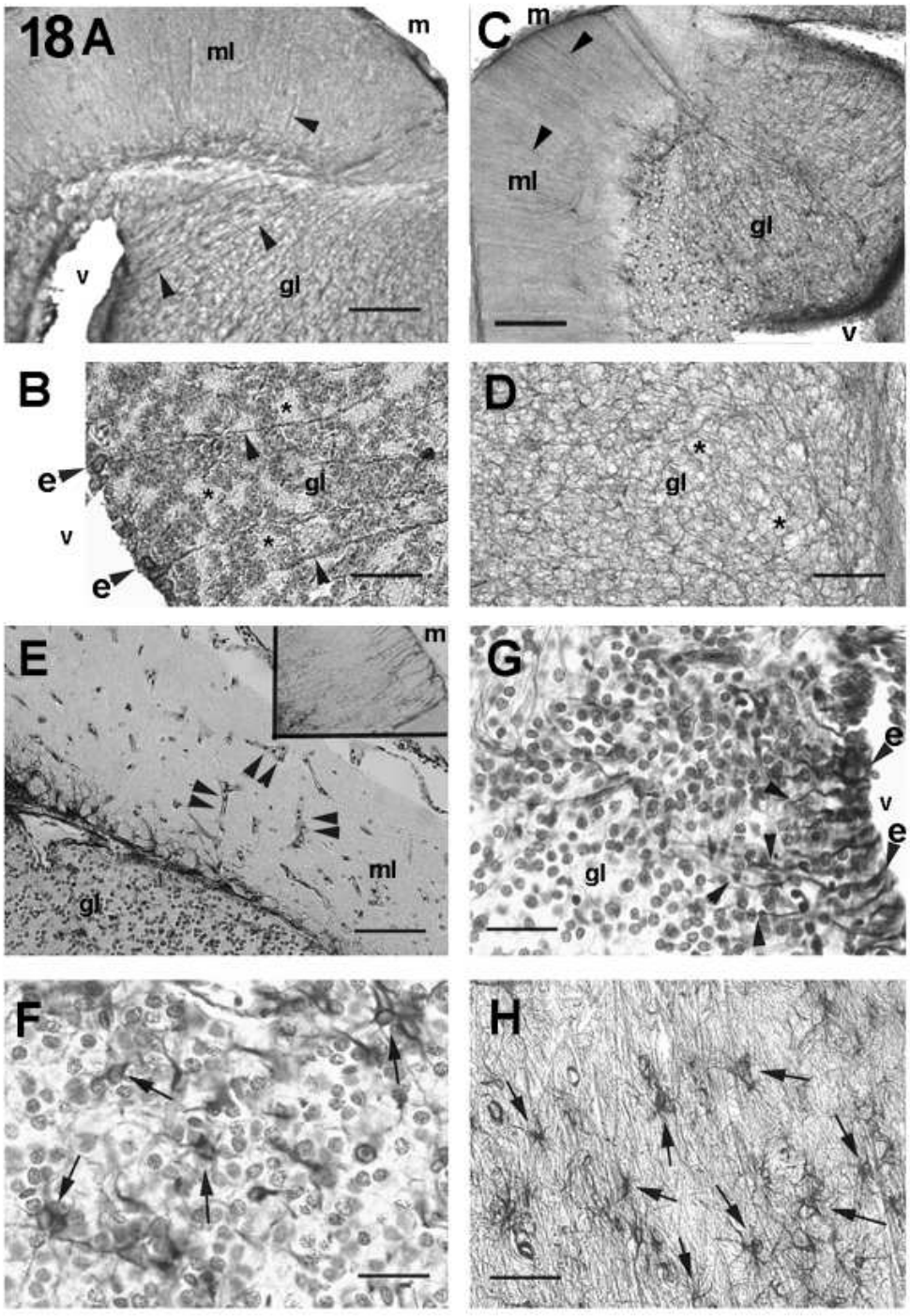

Figure 18. The cerebellum of sharks, skates and rays

a) The astroglial pattern of the shark cerebellum. Note the Bergmann-fibers in the molecular layer, and the elongated fibers from the surface of the granular eminence (equivalent of the granular layer). *Pristiophorus,* glutamine synthetase. Scale bar: 0.2mm.
b) A detail of the granular eminence. The granule cells and the light spots of the cerebellar glomeruli are conspicuous. Between them glial processes, which loosely separate them. Note the well-visible ventricular origin (ependymal perikarya) of glial processes. *Scyliorhinus,* glutamine synthetase with Nissl counterstaining. Scale bar: 0.04mm.
c) A part of the ray cerebellum (i.e. the granular eminence), *Raja miraletus,* glutamine synthetase. Scale bar: 0.2mm.
d) Granular eminence of *Dasyatis*: the glia seems to form rings, as nests for neurons and glomeruli. Glutamine synthetase. Scale bar: 0.1mm.
e) No Bergmann-glia are visualized, and glial system forms nests at the border of the molecular and granular layers (*Mobula*, GFAP with Nissl counterstaining). Scale bar: 0.2mm. Immunohistochemical reaction against GS, however, reveals the Bergmann-glia (inset, Scale bar: 0.1mm).
f) Inside the granular layer, between the cerebellar glomeruli, astrocytes are found in *Mobula,* GFAP with Nissl counterstaining. Scale bar: 0.02mm.
g) The ventricular surface of the granular layer is formed by ependymoglia in the *Mobula* as well, but their processes were relatively short, did not extend into the depth of the layer (GFAP with Nissl counterstaining). Scale bar: 0.02mm.
h) The area of nerve tracts contains GFAP-immunopositive astrocytes in skates and rays, mainly in *Mobula*. Scale bar: 0.04mm.

Arrowheads – ependymoglial processes; arrowheads with e – ependymal perikarya; arrows – astrocytes or their processes; asterisks – cerebellar glomeruli; double arrowheads – vessels

The structure of the cerebellum was similar in each of the sharks studied (fig. 6m, for detailed macroscopic descriptions of the cerebellum of Elasmobranchii, see Nieuwenhuys (1967), Smeets et al. (1983), and Smeets (1997)). Immunostainings revealed, that the main system consisted of radial ependymoglia, which penetrated the molecular layer like Bergmann-fibers. The meningeal surface of cerebellum was lined by their end-feet. The granular layer (here: an elongated granular eminence) was enmeshed by glial processes which formed a reticular pattern with holes for the granule cells and the cerebellar glomeruli (fig. 18a).

In skates (contour: fig.6n) and rays (fig.6 o) the cerebellar astroglial architecture was rather unclear on the basis of GFAP-immunohistochemistry. However, immunoreaction to S-100, and even better to glutamine synthetase, revealed a system similar to that of sharks (fig. 18c, d). In *Mobula,* GFAP-immunopositive glia formed

nests for the Purkinje cells (fig. 18e). The Bergmann-glia, however, were not immunoreactive to GFAP, only to glutamine synthetase (fig. 18e, inset), although the perivascular glia was GFAP-immunopositive in the molecular layer, too. The astroglial network of the granular eminence proved to be composed of astrocytes (fig. 18f) rather than ependymoglia, the latter contributing to it only in the zone adjacent to the ventricle (fig. 18g). The area occupied by nerve tracts also contained numerous GFAP-immunopositive astrocytes in *Mobula* (fig. 18h).

5.7. Cerebellum: Chimaera

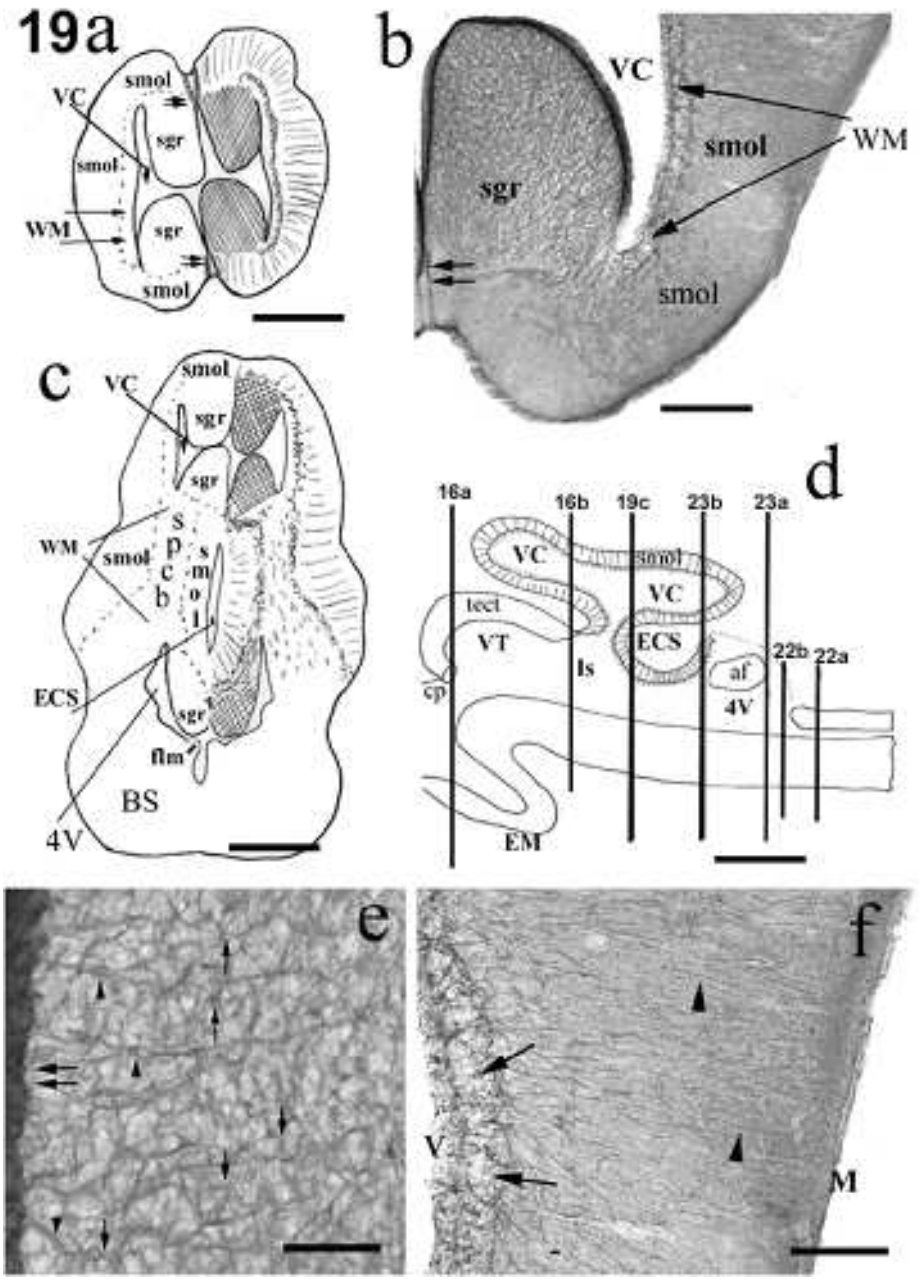

Figure 19. Chimaera cerebellum

a) Schematic drawing of the body of cerebellum, where it is not connected to the brain stem, in cross-section. Scale bar: 2 mm
b) A quarter of the immunostained cerebellum. Note the differences in glial pattern in the different layers (glial septum is indicated by double arrows). Scale bar: 0.4 mm.
c) Schematic drawing of a cross-section at the level of the connection between the cerebellum and brain stem. Scale bar: 2.5 mm
d) Sketch of a midsagittal section of the cerebellum (redrawn after Smeets et al., 1983) (stratum granulare, symbolized by a series of dots). The perpendicular lines represent the position of the cross-sections shown in the figures numbered accordingly. Dashed line-the roof of the ventricle (lamina epithelialis). Scale bar: 5 mm
e) Enlarged detail of the granular eminence. Note the criss-crossing fiber network, the holes (downward arrows) that may represent nests of granular cells and cerebellar glomeruli and the midline glial septum (double arrow). Upward arrows point to astrocyte-like structures. Scale bar: 0.08 mm
f) In the molecular layer radial processes are visible (arrowheads).They resemble Bergmann glia, but are less regularly arranged. The typical glial pattern of neural tracts of the white matter is indicated by arrows. Scale bar: 0.2 mm

An extrusion of the metencephalon, the cerebellum is an oval-shaped sac extending over the medulla and the midbrain. Holocephalans, like squalomorph sharks, have a non-convoluted corpus cerebelli (for details see Nieuwenhuys, 1967; Smeets et al., 1983). The cerebellum encloses a large cerebellar ventricle, which is contiguous with the fourth ventricle. The rostral and caudal ends of the cerebellum, therefore, appear separate in cross-section from the mesencephalon and the rhombencephalon, respectively (figs. 16a,b; 23b). The understanding of basic structure of cerebellum is facilitated by the schematic drawing featuring these ‘separate segments’ (fig. 19a).

The wall of the cerebellar ’sac’ corresponds to the molecular layer (stratum moleculare) plus Purkinje cells and white matter. Inside the ventricle, paired columns termed the granular eminences (eminentia granulares) represent the granular layer (stratum granulare). The granular eminences overlap and contact only the medial parts of the molecular layer. They run parallel to the midline, on both the roof and floor of the ventricle. The glial structures of the molecular and granular layers are easily distinguished (fig. 19b) by all immunostaining we performed.

The drawings in figure 19c and d demonstrate the connection between the cerebellum and the brain stem, as the walls of the cerebellum continue into the walls of the fourth ventricle in transverse and sagittal sections. Finally, the granular eminences

are continuous with the auricules and the cerebellar crest (crista cerebelli) as described below (fig. 23a).

Under higher magnification, a plexus of irregularly coursing glial processes was found in the granular eminence (fig. 19e). Granular cells and cerebellar glomeruli may occur in the spaces of this plexus. The two eminences are separated from each other by a glial septum. Some glial processes perpendicular to this septum were also visible. Blood vessels were delineated by immunolabeling. Spider-shaped, astrocyte-like structures were also visible, but these may have represented crossing side-branches of separate fibers.

The stratum moleculare was populated by radial fibers, which become thinner toward the meningeal surface (fig. 19f). This system of fibers resembles the Bergmann glia, which is common occurrence in the cerebella of vertebrates. Below the ventricular surface the characteristic glial pattern of neural tracts was seen.

5.8. Rhombencephalon, Spinal cord: Sharks, Skates and Rays

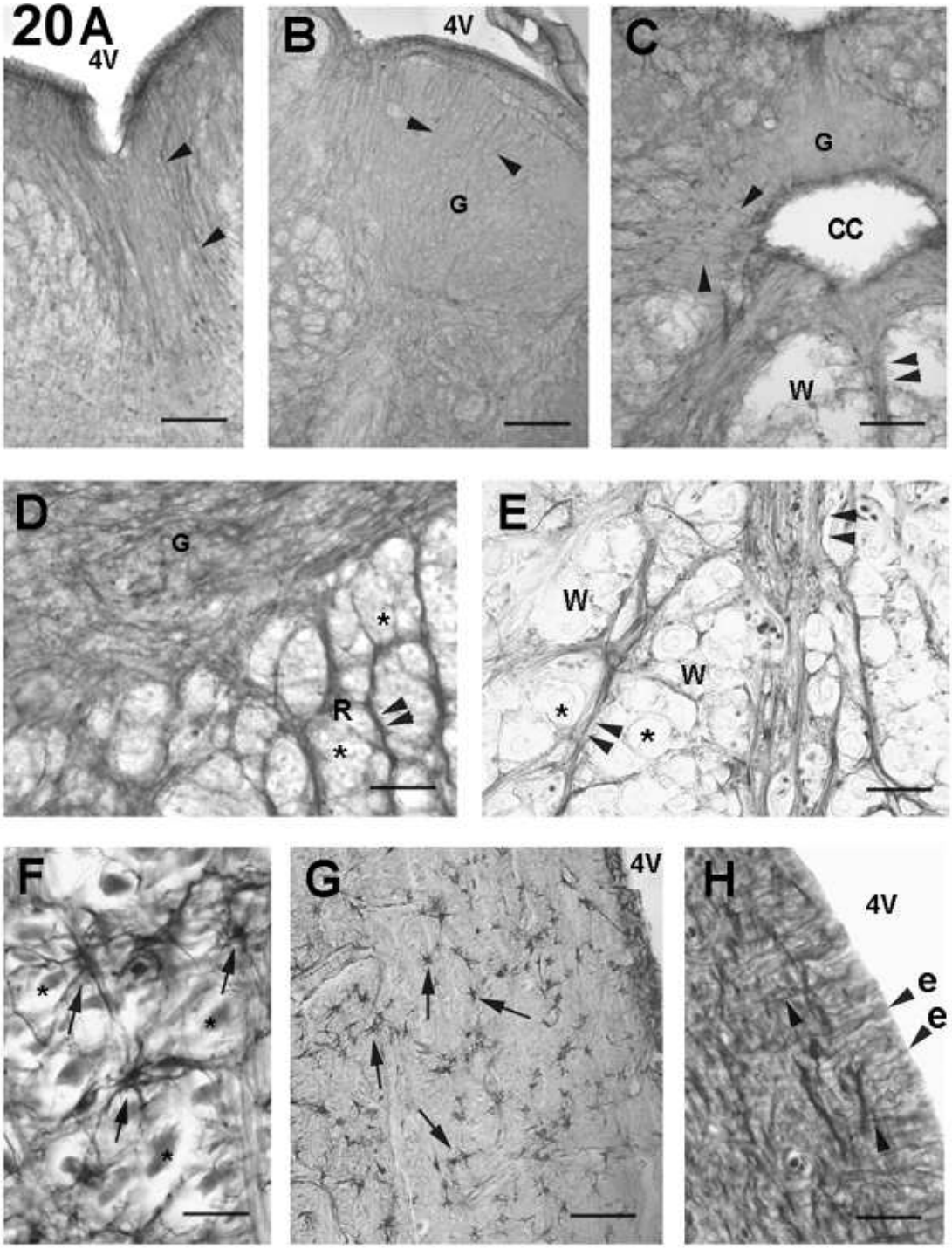

Figure 20. The rhombencephalon of sharks, skates and rays

a) The bottom of the rhomboid fossa, in the midline. From the surface of the 4th ventricle, a dense process system is oriented downward. *Cephaloscyllium*, glutamine synthetase. Scale bar: 0.2mm.
b) The other parts of gray matter (G) are also penetrated by a regular, parallel pattern of glial processes, the lobus nervi vagi, *Cephaloscyllium*, S-100. Scale bar: 0.2mm.
c) The gray matter around the central canal contains fine radial glial processes. As the gray matter extends apart from the central gray, the fine glial processes loose their radial course, and form rough thick plexuses. Note the glial septum in the midline. *Pristiophorus*, glutamine synthetase. Scale bar: 0.2mm.
d) A distant part of the gray matter. The astroglia is formed by thin processes so densely that no radial pattern can be traced. Note the 'reticular' (lattice-like) pattern (R) of glial fiber bundles around light axon fascicles. *Squalus*, GFAP. Scale bar: 0.1mm.
e) Boundles of fine glial processes of ependymal origin form septa between the brain tracts. (Note the faint contours of myelinated axons). The system of septa originate from the thickest septum of midline. *Myliobatis*, glutamine synthetase. Scale bar: 0.1mm.
f) In *Mobula*, there are astrocytes in the septa. Between their processes, the axons are visible, due to the eosin counterstaining of the immunohistochemical reaction to GFAP. Scale bar: 0.01mm.
g) In *Mobula*, astrocytes are also found in the gray matter of the rhombencephalon, below the ventricle, GFAP. Scale bar: 0.05mm.
h) In *Mobula* the ventricle is lined by ependymoglia, with short processes, GFAP. Scale bar: 0.03mm.

Arrowheads – ependymoglial processes; arrowhead with e – ependymal perikaryon; double arrowheads – glial septa; arrows – astrocytes; asterisks – axons.

In these areas the contours of cross sections were rather similar in sharks and batoids (fig. 6p-t). The difference in the astroglial architecture of gray and white matters was obvious. Gray matter formed the areas of the nuclei of cranial nerves, and the cerebellar crest. The astroglia of the gray matter were formed by dense populations of fine processes. Their ependymal origin and radial course were obvious near the ventricular system (fig. 20a-c), but their arrangement became less and less regular with the distance from it (fig. 20d,e). Between the white and gray matters a 'reticular area' took place (fig. 20d, R), where bundles of glial processes formed loops around the groups of axons, forming a lattice-like pattern. Hematoxylin-eosin staining revealed neurons amid these glial bundles, and the area corresponded to the reticular formation.

The white matter appeared really ‘white’, due to the low non-specific activity of peroxidases (e.g. cytochrome oxydase). In the midline the ependymal processes formed a thick glial septum (fig. 20a, c). The axons of the white matter were fasciculated by coarse septa woven from long glial processes. They spread from a midline glial septum like the veins of leaves (fig. 20e). These main types of glial patterns, in the gray matter, white matter, and their reticular combination were similar in sharks and batoids, only the distributions were different. Astrocytes were not observed in sharks, skates, and *Torpedo*. In *Myliobatis* scarce astrocytes were found in the ‘closed’ part of the medulla (i.e. caudal to the rhomboid fossa). In *Mobula*, astrocytes were rather commonly observed in the gray matter (fig. 20f,g), and also occurred in the glial septa of the white matter. The ventricle, was lined by ependymal cells with radial processes, which, did not extend to the meningeal surface (fig. 20h).

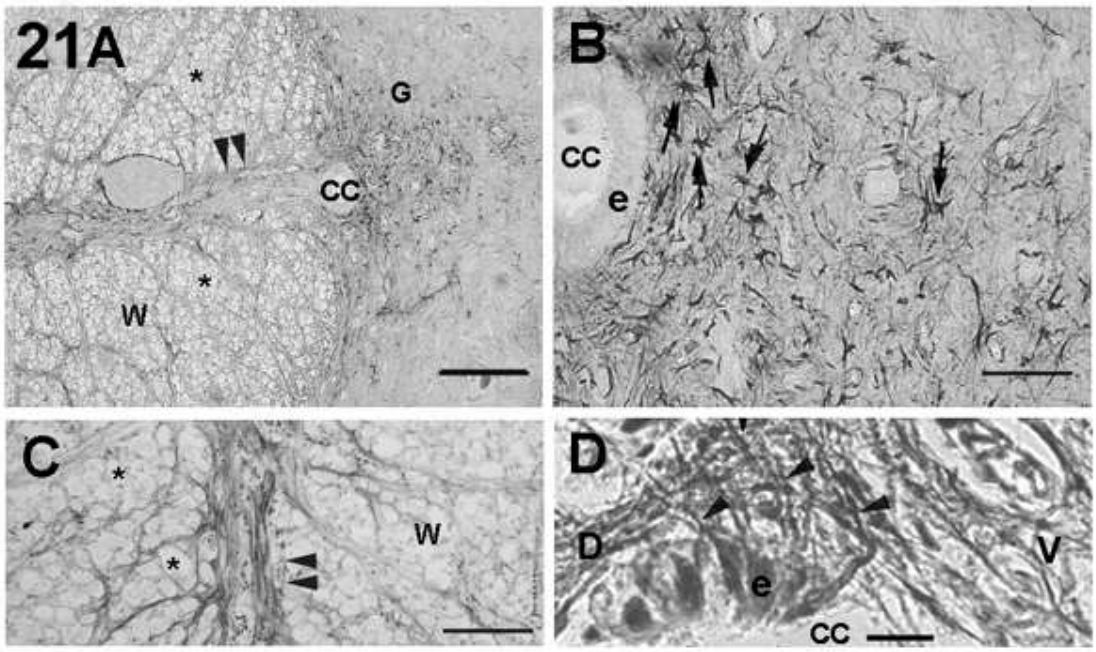

Figure 21. Spinal cord of sharks, skates and rays

a) *Mobula* spinal cord around the central canal (CC). Whereas the gray matter (G) of the spinal cord contains astrocytes (see enlarged also in fig. 21b), on the opposite side of the central canal, the white matter (W) is septated by glia (see a detail also in fig. 21c). GFAP. Scale bar: 0.2mm.
b) Astrocytes in the gray matter of *Mobula* spinal cord, enlarged from figure 21a, GFAP. Scale bar: 0.05mm.
c) White matter with glial septa from *Mobula* spinal cord, GFAP. Scale bar: 0.1mm.

d) Detail of the central canal, on the side of the white matter. Note the long processes, which continue in the glial septa of the white matter. On the side of the gray matter no similar processes are found. *Mobula*, GFAP with HE counterstaining. D – dorsal side; V – ventral side. Scale bar: 0.01mm.
Arrows – astrocytes; arrowheads – ependymoglial processes; e – ependymal perikaryon; double arrowhead – glial septum; asterisks – axons.

In skates and *Torpedo*, as well as in sharks the spinal astroglial architecture was similar to that described in the rhombencephalon: the gray matter contained densely packed, short and fine glial processes, whereas in the white matter bundles of long processes formed a system of glial septa. In the *Mobula* spinal cord the white matter was also enmeshed by a system of glial septa (fig. 21a, c) formed by long ependymal processes (fig. 21d), whereas the gray matter was populated by astrocytes (fig. 21b).

5.9. Rhombencephalon, Spinal cord: Chimaera

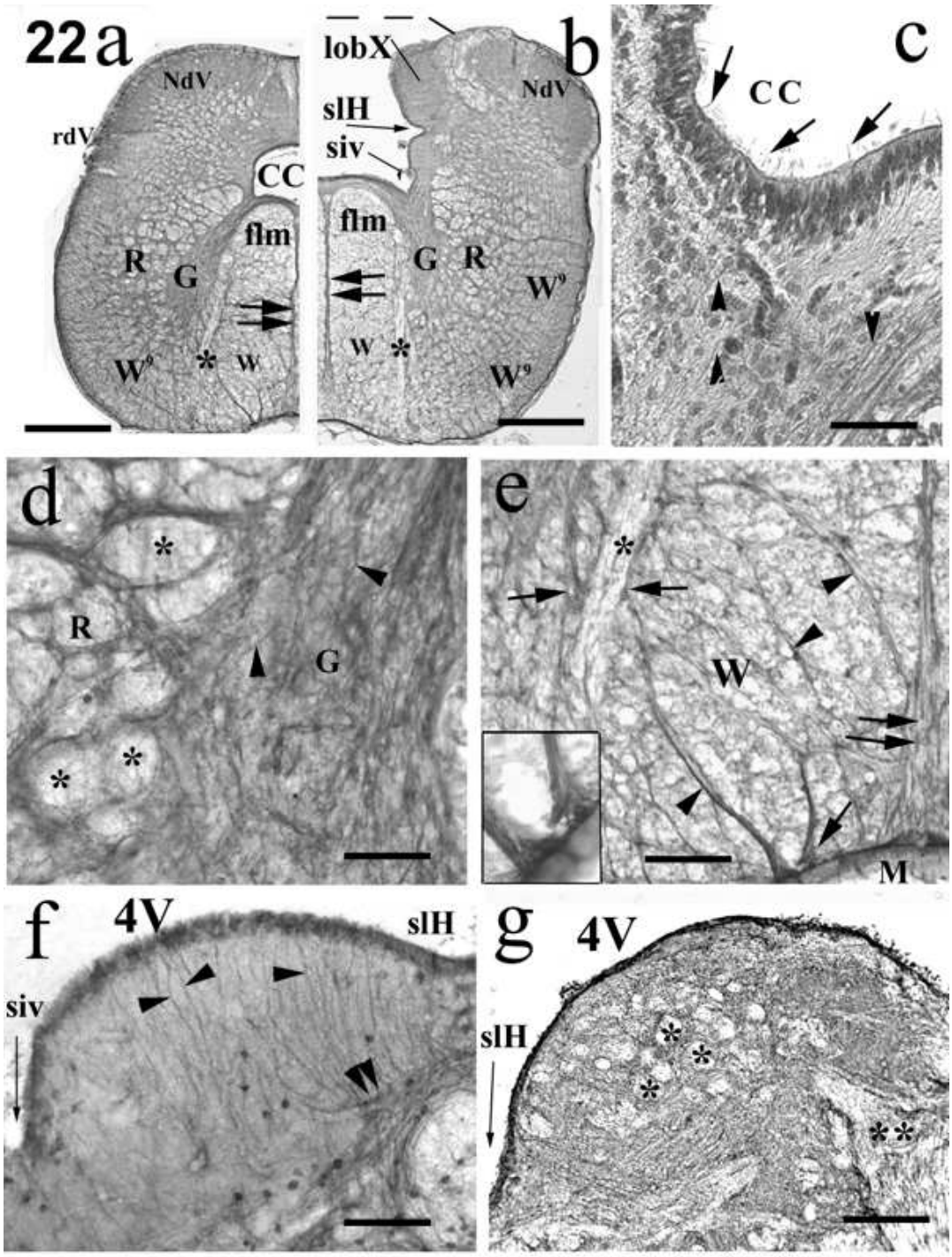

Figure 22. Chimaera rhombencephalon (caudal end)

a) The 'closed' part (i.e. caudal to the obex) of the rhombencephalon. Scale bar: 0.8 mm
b) The 'open' part (i.e. cranial to the obex) of the rhombencephalon. Three main areas can be distinguished: i) the gray matter (G); ii) a reticular glialcomplex (R); iii) and the white matter (W).

The dashed line represents the (missing) roof of the fourth ventricle (the choroid epithelial lamina). The asterisk labels a bundle of motor fibers, whereas a strong glial ’septum’ is visible in the midline (double arrow). Scale bar: 0.8 mm

c) Detail of the zone adjacent to the central canal. HE staining. The lumen is bordered by columnar, ciliated cells (arrows). Their basal (i.e. contraluminal) processes (arrowheads), extending toward the left bottom corner, continue in the fiber system of the gray matter. Scale bar: 0.1 mm

d) Detail of gray matter with a dense and rather irregular plexus of thin processes, in which individual processes (arrowheads) are scarcely recognized, and the reticular area. The light areas (asterisks), i.e. fascicles of myelinated axons are enmeshed with finer glial processes. Scale bar: 0.1 mm

e) Detail of white matter in the ventromedial part of the rhombencephalon. Here the ’foamy’ appearing fascicles of cross-sectioned axons are separated by very thick glial fibers (arrowheads). These processes form glial endfeet (arrows) on the meningeal surface, as well as around a fascicle of axons (asterisk). The midline glial septum (double arrows) fans out toward the meningeal surface. Inset: endfeet attached to the meningeal surface; note their inner fibrillar structure. Scale bar: 0.1 mm (for the inset: 0.05 mm).

f) Eminence between the sulcus limitans of His, and the sulcus intermedioventralis containing loosely arranged parallel glial processes (arrowheads) emerging perpendicularly from the surface of the fourth ventricle. The processes join a glial sheath surrounding a fascicle of myelinated axons (double arrowhead). Scale bar: 0.1 mm

g) Lobus nervi vagi. Fascicles of myelinated axons (asterisks) are embedded into a very dense plexus of glial processes. Double asterisk marks a fascicle of axons oriented to emerge from the brain. Scale bar: 0.2 mm

The description begins at the ’closed’ part of the rhombencephalon (i.e. below the obex, caudal to the fourth ventricle) and continues in a rostral direction, in order to facilitate the description of structural changes. The major structures and an overview of the glial patterns of the ’closed’ part, and the caudal end of the ’open’ part are shown in figure 22a, b. The ’closed’ part of the rhombencephalon resembles the spinal cord, except that it has a wider central canal. The glial patterns of the gray and white matter are conspicuously different. Three main areas can be distinguished by their glial pattern: i) The gray matter (see G in fig. 22a, b) is dark and intensely immunostained; ii) The white matter (see W in fig. 22a, b) is rather light and weakly immunoreactive; iii) Between the gray matter and the white matter there is a reticular glial substance (R in fig. 22a, b).

The processes originated from the ependymal cells lining the central canal (fig. 22c), and extended ventrolaterally. Here the astroglia of the gray matter consisted of a dense mesh of fine glial processes, imparting a ’dark’ appearance (fig. 22d), in contrast to the poor immunoreactivity of the ’white’ matter. The latter contained a loose system of delicate glial processes in the area of the medial longitudinal fascicle, making this structure appear ’foamy’ (fig. 22e). However, the processes became gradually denser in ventral and lateral directions, (fig. 22a, b), forming bundles that separated fascicles of neural fibers in the white matter.

The dark and dense glial structures of the gray matter surrounded the central canal and form wing-like extensions ventrolaterally. A similar dark and intense immunostaining was found in the nucleus descendens nervi trigemini and in the area of the nuclei of the vagus nerve (fig. 22a, b).

In the midline, a strong septum is formed by bundles of glial processes. Unusually strong glial processes extended to and formed endfeet on the intracerebral parts of emerging cranial nerves and also along the meningeal surface (fig. 22e). On the latter, the endfeet matched the cell bodies in size, but no cell bodies were detected with HE staining in this region.

In the ’reticular’ area, between the gray and white matters (R in fig. 22a,b,d), thick bundles of glial processes surrounded relatively small and light GFAP-free spots that likely represented fascicles of myelinated axons.

In the caudal end of the open part, we observed hillocks bulging into the fourth ventricle (fig. 22b) on both sides of the sulcus limitans of His. The medial, smaller hillock (corresponding to the vagal motor nuclei) showed a loose and radial glial pattern, i.e. parallel ependymoglial processes perpendicular to the ventricular surface (fig. 22f). The larger, lateral hillock represented the lobe of the vagus nerve, with a glial system characteristic of the gray matter, but with several light areas indicated the penetrating fascicles of myelinated axons.

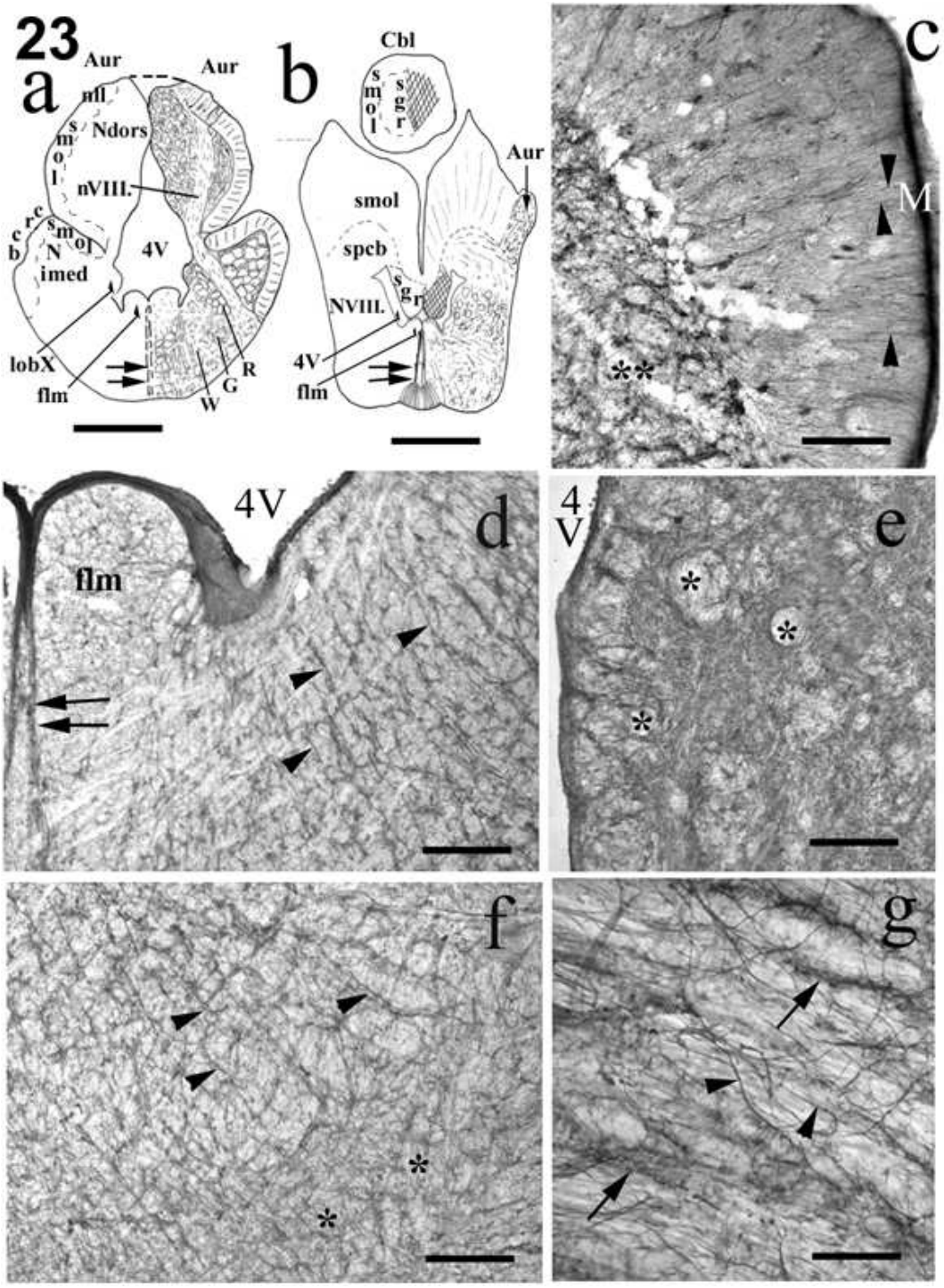

Figure 23. Chimaera rhombencephalon (rostral end)

a) Schematic drawing of a cross section through the rhombencephalon, just caudal to the fusion of the alar plates. Most of the characteristic glial populations (G, R,W) are similar to those seen in fig. 22. Cerebellar glial patterns also appear in the crista cerebelli (crcb) and in the auricle (Aur), see also fig. 23c,e. The dashed line symbolizes the missing roof of the fourth ventricle (choroid epithelial lamina). Scale bar: 3.0 mm

b) Schematic drawing of a cross section through the rhombencephalon at the level of the lobus vestibulolateralis (pars medialis, lob vlm). Note the cerebellar structures (sgr, smol) on the dorsal side of the brain stem and the fan-shaped basal widening of the midline glia (double arrow). In this section the tegmental glial pattern is rather uniform. Scale bar: 3.0 mm.
c) Glial pattern of the crista cerebelli. Very thin glial fibers (arrowheads) run perpendicular to the meningeal surface. The underlying glia (double asterisk) forms a network as in the granular layer. Similar glial patterns are found in the lateral part of the auricle. Scale bar: 0.2 mm
d) The tegmentum of the rostral rhombencephalon. The medial longitudinal fascicle (flm) is light and poor in astroglial structures. Note the double line representing the midline glial septum (double arrows). Loosely packed glial processes (arrowheads) form a discontinuous network. S-100, Scale bar: 0.5 mm
e) Detail of the medial part of the auricle. It contains a very dense glial system, with myelinated axon bundles (asterisks). Scale bar: 0.2 mm
f) The network of glial fibers (arrowheads) becomes denser in basal and basolateral directions (asterisks). This represents the usual glial pattern for the peripheral white matter (W9 in the fig. 22a, b). Scale bar: 0.5 mm
g) Longitudinal section of a nerve tract (emerging part of a cranial nerve (see nll in fig. 23a). Thin glial fibers (arrowheads) are interrupted by a few thick bundles (arrow). GFAP, Scale bar: 0.1 mm

Proceeding rostralward, several structures belonging to the cerebellar system appeared (fig. 23): dorsolaterally the cerebellar crest (crista cerebelli, lobus lineae lateralis anterior); and dorsally the cerebellar auricle (auricula cerebelli). The auricle connects the cerebellar crest (fig. 23a) with the granular eminence (fig. 23b). For the spatial configuration of the auricle see also figure 17b-f; for a further description, see also Nieuwenhuys (1967) and Smeets et al. (1983).

The meningeal surface of the crest and auricle was formed by the molecular layer of cerebellum, as indicated by the glial pattern (fig. 23c). The underlying zone in both areas contained a dense glial system and several light spots revealed the positions of myelinated axon bundles (fig. 23e). On the apical part of the auricle there was an area of emerging lateral line nerves. In these nerves the glial network consisted of thin fibers alternating with a few thick bundles, all oriented along the course of the nerve (fig. 23g).

In the sections represented in figure 23a, the ventromedial part still reveals the glial patterns seen in figure 22: the gray matter, the ’reticular’ glial composition, and the white matter (see G, R, W in fig. 23a, respectively). Here the gray matter contained a

delicate and dense, almost ‘obscure’ fiber system. The latter pattern occurred in the areas of the vagal lobe, nucleus dorsalis in the auricle, nucleus intermedius in the cerebellar crest, and the nuclei of the eighth nerve. The medial longitudinal fascicle contained only a few dispersed GFAP immunopositive glial fiber bundles, generally oriented toward the basal surface. On the basal side of the sections, the glial processes in the white matter were thicker and stronger.

At the level represented by figure 23b, the glial pattern became more homogeneous. The area of the medial longitudinal fascicle was almost devoid of glial bundles. Moving in basal and lateral directions, more and more bundles of glial processes were seen to form a loose ’lacework’ in the white matter (fig. 23d). At the basal and basolateral submeningeal zones, this glial network appeared rather dense (fig. 23f), as in the identical parts of the sections shown in figures 22a,b, and 23a. In the midline, the glial septum bifurcates (fig. 23d), diverges slightly in a ventral direction, and becomes fan-shaped at the basal surface. Dorsally, the typical glial patterns were visible in brain tracts (i.e. spinocerebellar tract) and in the gray matter around the nuclei of the eighth nerve, as well as in parts of the cerebellum.

The results based on all immunohistochemical stainings using GFAP, glutamine synthetase and S-100 protein are summarized in Table 4.

	Telenc.	Dienc.	Mes/ Teg	Mes/ Tec	Cbl/ Mol	Cbl/ Gran	Rh/ Gray	Rh/ Retic	Rh/ White	Sp/ Gray	Sp/ White
Callorhinchus	RR,a	RR	RR	RR	Be	EE,a	EE	EE	EE	EE	EE
Squalus	RR,a*	RR	RR	RR	Be	EE	EE	EE	EE	EE	EE
Pristiophorus	RR,a	RR	RR	RR	Be	EE	EE	EE	EE	EE	EE
Cephaloscyllium	RR,a	RR	RR	RR	Be	EE	EE	EE	EE	EE	EE
Scyliorhinus	RR,a	RR	RR	RR	Be	EE	EE	EE	EE	EE	EE
Raja	r,AA*	r,A	RR	AA*	B*	EE*	EE	EE	EE	EE	EE
Dipturus	r,AA*	r,A	a	a	B*	EE*	EE	EE	EE	EE	EE
Torpedo	AA	r,A	r,A*	a	B*	EE*	EE	EE	EE	EE	EE
Dasyatis	A*	r,A*	a	A	B*	EE*	EE	EE	EE	EE	EE
Myliobatis	AA*	r,A	a	r*,a	B*	EE*	EE,a	EE	EE	EE	EE
Mobula	AA	r,AA	r,AA	AA*	Bn	e,AA	EE,A	EE,A	EE,A	E,A	EE

Table 4. The most characteristic glial features of certain brain areas, based on immunohistochemical stainings against GFAP, glutamine synthetase and S-100 protein.
AA, A, a – astrocytes: abundant, intermediate, or low density, respectively; RR, R – radial ependymoglia (with processes extending to the meningeal surface): high or low density, respectively; r – radial ependyma with only short processes and rare occurrence; EE, E – non-radial ependymoglia with long processes: high or low density, respectively; e – non-radial ependymoglia with short processes; Be – Bergmann-like processes of ependymoglia; Bn – true Bergmann-glia with separate, non-ependymal perikarya; Asterisk – detected in part or in whole by glutamine synthetase immunostaining only. Telenc – telencephalon; Dienc – diencephalon; Mes – mesencephalon; Teg – tegmentum; Tec – tectum; Cbl– cerebellum, Mol – stratum moleculare; Gran – stratum granulare; Rh – rhombencephalon; Gray – gray matter; Retic – stratum reticulare; White – white matter; Sp – spinal cord.

5.10. Immunohistochemical reactions against dystroglycan complex and its associated proteins in cartilaginous fishes

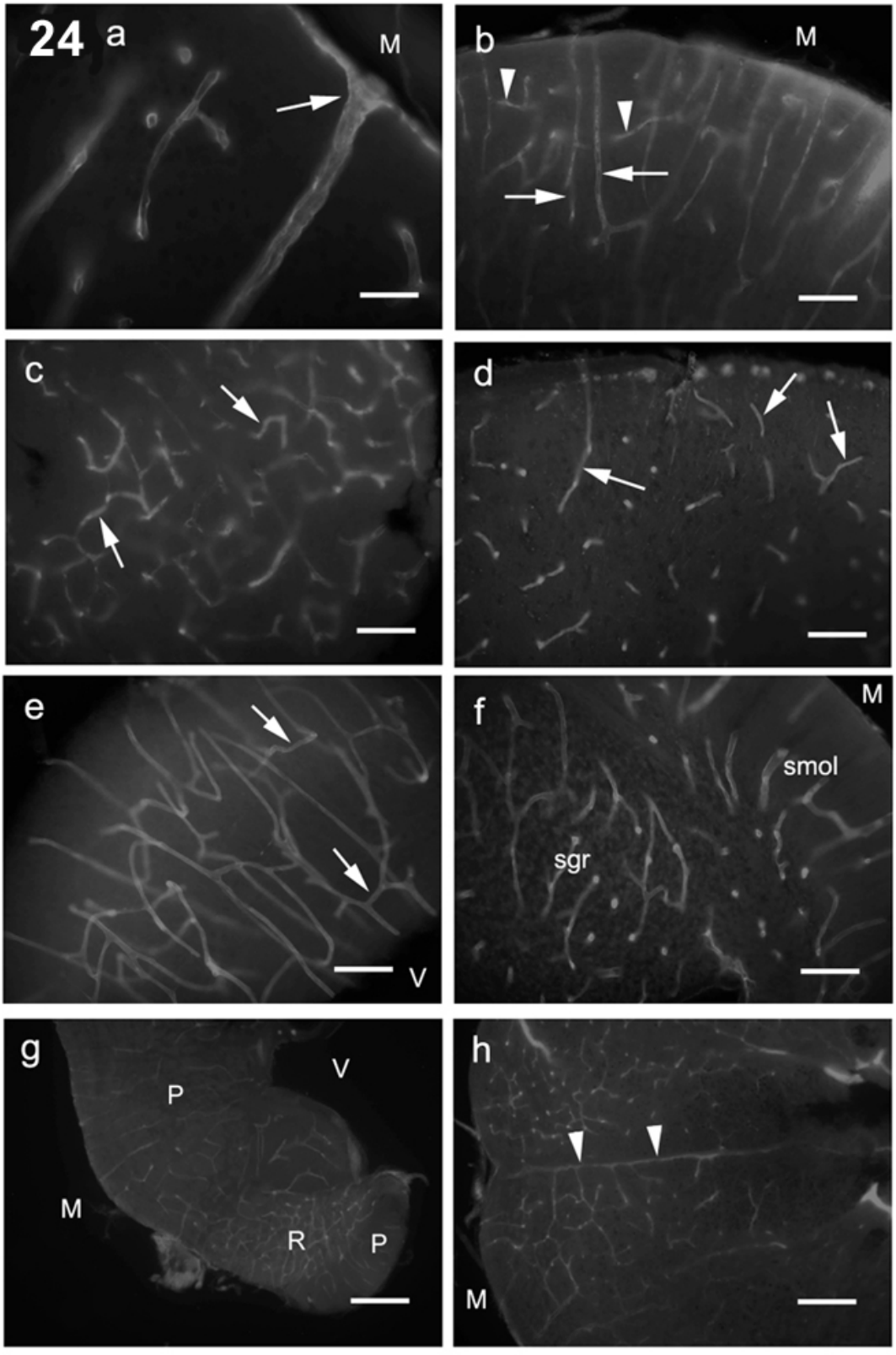

Figure 24. Immunohistochemical staining against DG

a) *Cephaloscyllium*, telencephalon. A large vessel (arrow) entering the brain substance. Note the continuity of DG immunopositivity along the vessel and on the meningeal surface. Scale bar: 30 μm.

b) *Squalus*, telencephalon, pallium. Note that most of the vessels are perpendicular to the brain surface. Arrows point to parallel vessels, arrowheads show other vessels interconnecting them. Scale bar: 120 μm.

c) *Dipturus*, telencephalon. The vessels (arrows) have different orientations, they form a network rather than a system of parallel vessels. Scale bar: 120 μm.

d) *Callorhinchus*, telencephalon, subpallium. An apparently irregular vascular system, with vessels of different orientations (arrows). Scale bar: 120 μm.

e) *Pristiophorus*, tectum. Note that most of the vessels are near-perpendicular to the brain surface. There are two zones, where these vessels are interconnected (arrows), therefore a layered pattern is formed. Scale bar: 120 μm.

f) *Pristiophorus*, cerebellum. Note the different vascular patterns in the stratum granulare (granular eminence), and in the stratum moleculare: network and parallel vessels, respectively. Scale bar: 120 μm.

g) *Pristiophorus*, rhombencephalon. Areas of rich (R) and poor (P) vascularization can be distinguished. Scale bar: 300 μm.

h) *Dipturus*, spinal cord. Note the characteristic basal artery (arrowheads). Scale bar: 300 μm.

The cerebral vascular system was clearly visualized by the immunostaining against DG-β in Chondrichthyes (fig. 24), like in mammals, and the interspecific differences in the vascular system could also be recognized. In *Cephaloscyllium* the DG immunostaining clearly showed the continuity of the vessels within the brain tissue and DG immunopositivity could also be observed along the meningeal surface (fig. 24a). In *Cephaloscyllium*, and also in *Squalus*, which have thin-walled telencephala with large ventricles, the vessels were oriented at a right angle to the surface of the wall, i.e. they ran parallel to the radial glia (fig. 24b). Compared to the shark telencephalon, the skate (*Dipturus*) telencephalon has a thick brain wall, and the vascular network is more complex. The immunopositive vessels had different orientation, they formed a network rather than a system of parallel vessels (fig. 24c). In the telencephalon of *Myliobatis* the vessels were DG immunopositive, mainly in the subpallium, forming a network similar to that found in *Dipturus*. The different brain parts of the species could also be recognized in DG-immunostained sections. In the *Callorhinchus* telencephalon, the

subpallium, a characteristic bulky structure, protrudes into the ventricle (fig. 24d), containing an apparently irregular vascular system with vessels of different orientations. The glia is less organized here than in the pallium, in which the pattern is similar to that seen in figure 24b.

In the tectum of the shark species studied here, most of the vessels were near-perpendicular to the brain surface (fig. 24e, *Pristiophorus*). There were two zones, where these vessels were interconnected. Therefore a layered pattern was formed, similar to that found in other vertebrates. In the tectum of *Myliobatis* the DG immunostained vessels could be observed only in the vicinity of the surface. In the shark cerebellum (fig. 24f, *Pristiophorus*), the vascular patterns were different in the molecular and granular layers: almost parallel and reticular, respectively. In the rhombencephalon of the sharks, skates and rays studied, the dense and loose vascular networks were easy to distinguish (fig. 24g), as well as a strong artery in the midline. In the spinal cord, the ventral artery and the arcuate arteries were recognizable (fig. 24h).

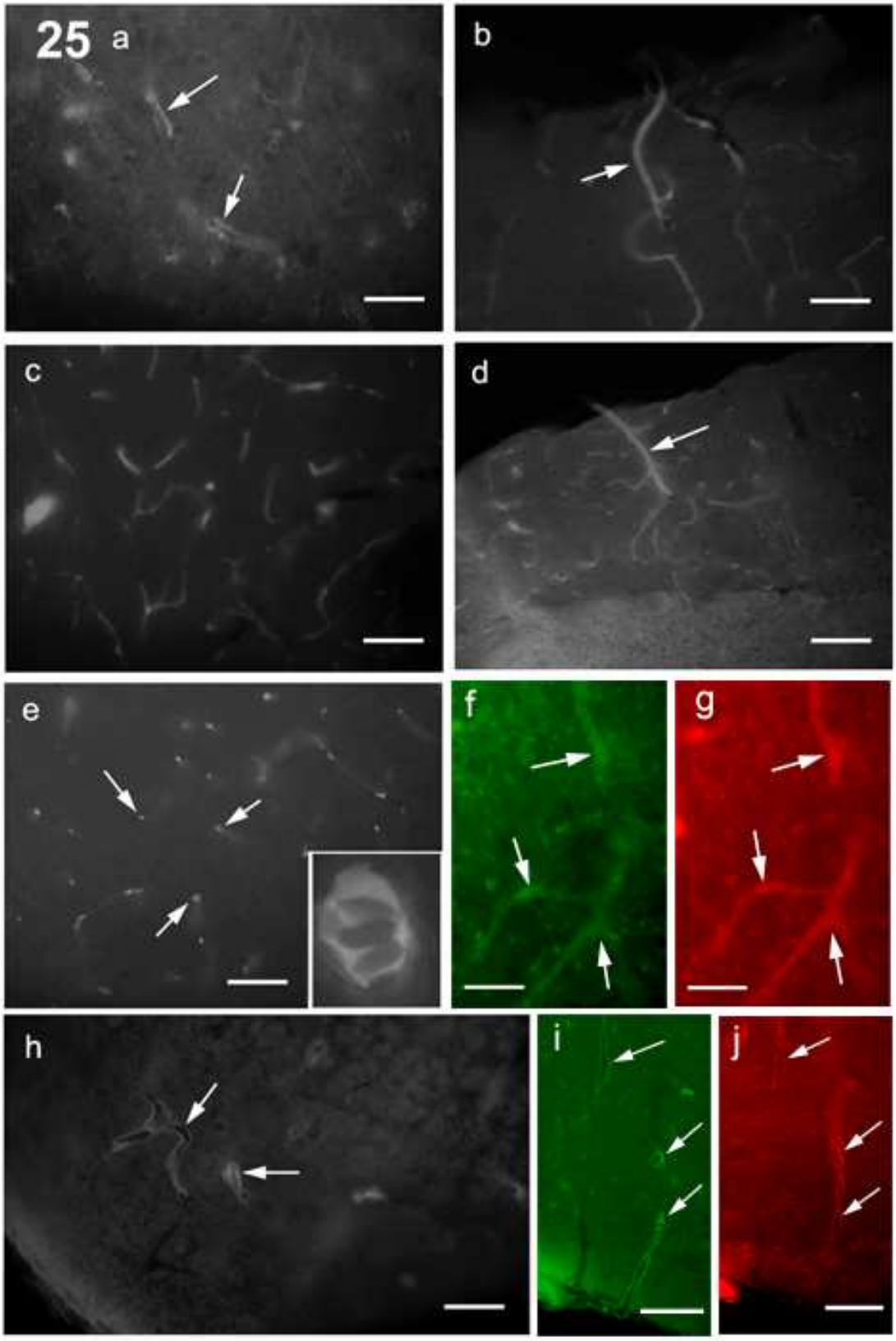
25 a
b
c
d
e
f
g
h
i
j

Figure 25. Immunohistochemical staining against other components of the DGC

a) Dystrophin immunopositive vessels (arrows), *Callorhinchus,* mesencephalic tegmentum. Scale bar: 120 μm.
b) *Dipturus*, telencephalon. Arrow points to a dystrophin-stained penetrating vessel. Scale bar: 120 μm.
c) Utrophin, *Dipturus*, telencephalon, note the vascular network similar to that seen in fig. 24c, although not continuously labelled. Scale bar: 120 μm.
d) Utrophin, *Callorhinchus*, cerebellum. A vessel (arrow) penetrates from the pial surface. Scale bar: 120 μm.
e) Syntrophin, *Cephaloscyllium***,** telencephalon. The cross-sectioned vessels (arrows) run parallel. The inset displays an enlarged image taken at the trifurcation point of a vessel. Scale bar: 200 μm, inset: 10 μm.
f-g) Syntrophin and DG, double-labeling, respectively, *Callorhinchus,* rhombencephalon. Identical vessels (arrows) are presented. Scale bar: 60 μm.
h) Dystrobrevin, *Dipturus*, telencephalon. Note the immunopositivity of the walls of the vessels (arrows). Scale bar: 120 μm.
i-j) Dystrobrevin and DG, double-labeling, *Cephaloscyllium*, rhombencephalon. Identical structures marked by arrows. Scale bar: 120 μm.

Of the proteins which form a complex with the DG and interconnect it with the cytoskeleton and the intracellular signaling system: dystrophin, utrophin, syntrophin, and α-dystrobrevin could be visualized in every species. Only a few characteristic photomicrographs are demonstrated (fig. 25a-e,h) for every substance, and only in one species, but similar labeling was seen in every area of each species. In general, the labeling was weaker than in the case of DG, and it never visualized the whole vascular system. Double-labeling experiments were performed only where antibodies of different origin (i.e. rabbit or goat, versus mouse) were available against the components. These studies demonstrated the co-localization of the syntrophin (fig. 25f-g) and dystrobrevin (fig. 25i-j) with DG.

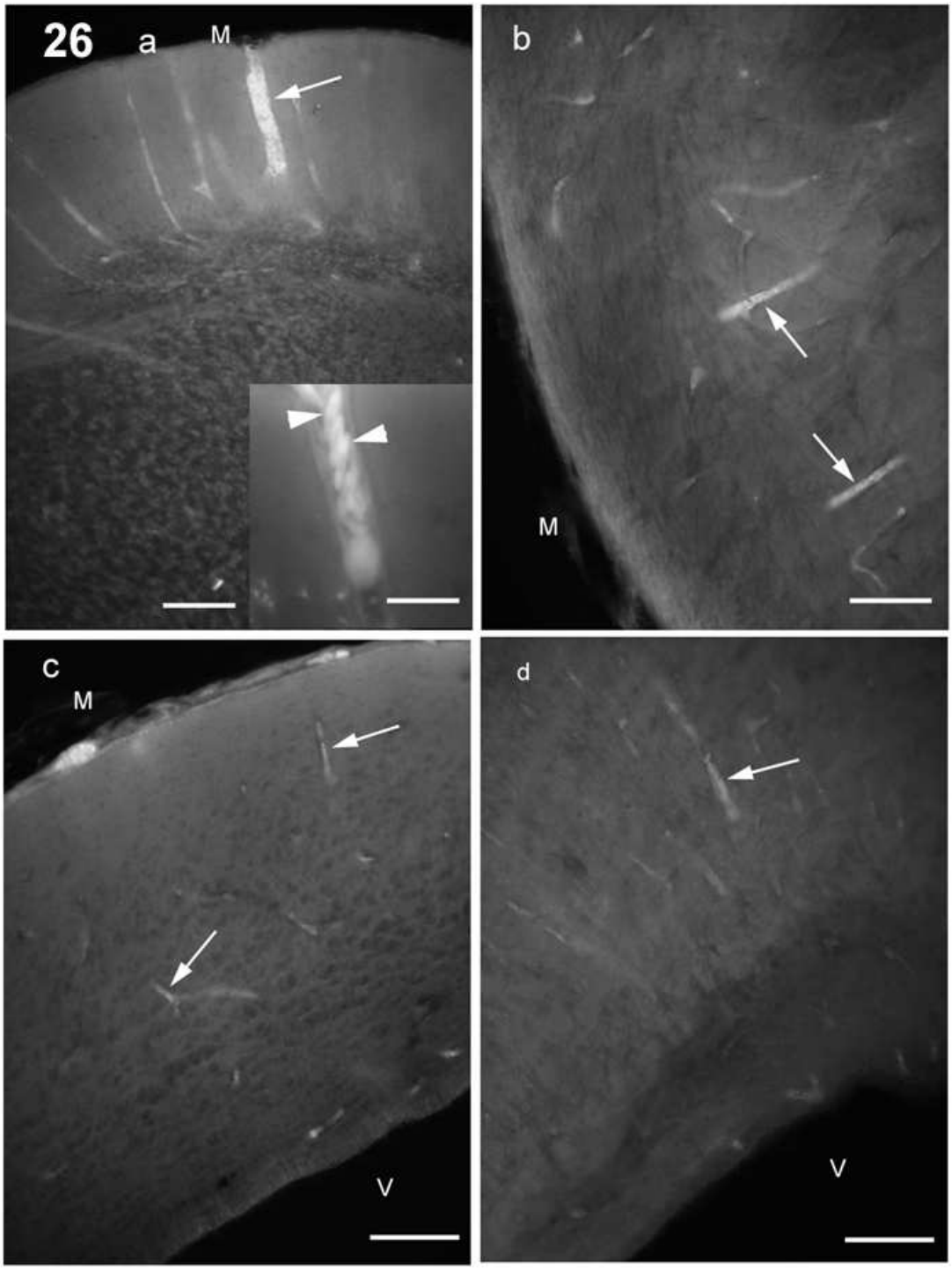

Figure 26. Immunohistochemical staining against aquaporin

a) Cerebellum of *Pristiophorus.* The fluorescence in the vessels (arrow) is confined to red blood cells (arrowheads) rather than the wall of the vessels (see inset). Scale: 50 µm, inset: 10µm.

b-d) Only a very limited immunoreactivity can be observed in every brain area of each species. Mainly red blood cells display fluorescence (arrows): e.g. in the mesencephalon of *Dipturus* (b), in the telencephalon of *Cephaloscyllium* (c), and in the telencephalon of *Pristiophorus* (d). Scale bars: 50 um.

Immunolabeling against AQP4 or AQP9 was not convincing. Although the autofluorescence of red blood cells (fig. 26a) clearly revealed the course of the vessels (fig. 26), specific immunoreaction was not detected either in their walls or glial processes, as it would have been expected in the cases of AQP 4 or AQP 9, respectively.

6. Discussion

6.1. Astroglia of Elasmobranchii

6.1.1. Previous studies on the astroglial structure of sharks

Former studies on the astroglial structure of sharks have been performed mainly on galeomorph sharks, applying impregnation techniques (dogfish *Scyliorhinus canicula*: Horstmann, 1954; Smeets and Nieuwenhuys, 1976; nurse shark, *Ginglymostoma cirratum:*, Long et al., 1968; Schroeder and Ebbesson, 1975; lemon shark, *Negaprion brevirostris:* Klatzo, 1967; tiger shark, *Galeocerdo cuvieri*, and hammerhead shark *Sphyrna zygaena:* Long et al., 1968), whereas one study was extended also to the squalomorph shark *Squalus acanthias* (Smeets and Nieuwenhuys, 1976). The immunohistochemical investigations of Wasowicz et al. (1999) on GFAP in a galeomorph shark (*Scyliorhinus canicula*) found radial ependymoglia to be the predominant element, with scarce astrocyte-like cells, mainly around the vessels. Immunohistochemistry was also applied previously by Chiba (2000, *Scyliorhinus torazame* and *Mustelus manazo,* S-100 protein). Kálmán and Gould (2001) investigated a squalomorph shark (*Squalus acanthias*), in which the immunohistochemical reaction to GFAP revealed only radial ependymoglia. Even in medium-sized sharks (*Ginglymostoma, Galeocerdo, Negaprion*), aforementioned impregnation studies described radial ependymoglia as the predominant element, and astrocyte-like (or at least non-ependymal) cells were scarce, most of them in perivascular position. These cells are attached to the vessels by their bodies, extending their 'vasculofugal' processes into the surrounding brain substance (Horstmann, 1954; Klatzo, 1967; Long et al., 1968; Wasowicz et al., 1999). Apovascular round perikarya with single long processes were also found, similar cells were described in quail (*Cothurnix cothurnix japonica*, Cameron-Curry et al., 1991) as 'unipolar astrocytes'.

6.1.2. Previous studies on the astroglial structure on batoids

Former investigations on the astroglial structure of batoids occurred mainly in *Torpedo* and *Raja* (*T. marmorata, T. ocellata,* and *Raja clavata* silver impregnation Horstmann, 1954; *T. marmorata,* GFAP immunohistochemistry Wasowicz et al., 1999). In the ray *Torpedo marmorata* they also found astrocytes, but only in a low number.

The cited study was confined to the telencephalon, mesencephalon, and spinal cord, i.e. it did not cover the rhombencephalon and cerebellum. Since in Torpediniformes the lateral ventricles are rather obliterated, radial ependymoglia here could not be described. Bundgaard and Cserr (1991, *Raja erinacea*) found that perivascular and submeningeal glia were formed by cell bodies. In the skate *Raja erinacea* (Kálmán and Gould, 2001) astrocytes were found, but they were rather scarce, almost confined to the vessels and the surface of the telencephalon and mesencephalon. The rhombencephalon contained bundles and septa formed by glial processes between the axon fascicles. The cerebellar Bergmann-fibers were not visualized. These authors mentioned the attachment of cell bodies to the vascular and meningeal surfaces, in contrast to that found in mammals. In birds, however, the astrocytes have similar positions (quail, *Cothurnix cothurnix japonica* Cameron-Curry et al., 1991; chicken, *Gallus domesticus*, Kálmán et al., 1993).

6.2. Differences in immunoreactivities

On the whole, immunostaining to S-100, and mainly to glutamine synthetase revealed more astroglial elements, than did immunostaining to GFAP. Since S-100 also occurs in the oligodendrocyte lineage (Hachem et al., 2005), S-100 immunopositive structures were considered astroglia only if their shape or the presence of other astroglial markers supported their astroglial character. Whereas radial ependymoglia always proved to be immunopositive to GFAP, like in former studies (Dahl and Bignami, 1973; Wasowicz et al, 1999; Kálmán and Gould, 2001), a contingent of astrocytes, mainly apovascular ones, in batoids, *Squalus acanthias* and *Callorhinchus milii* and the batoid Bergmann-glia could be visualized only on the basis of immunoreactivity to S-100 protein or glutamine synthetase. Similar features were observed in birds and mammals formerly (see introduction 2.6.2-2.6.3). The Bergmann-glia also proved to be GFAP-immunonegative in birds (chicken, *Gallus domesticus*: Dahl and Bignami, 1973; Dahl et al., 1985; Roeling and Feirabend, 1988; Kálmán et al., 1993; quail, *Cothurnix cothurnix japonica:* Cameron-Curry et al., 1991).

Therefore, like in Amniotes, also in skates and rays the prepoderance of astrocytes was accompanied by an increasing number of GFAP-immunonegative astrocytes, and areas poor in or devoid of GFAP immunoreactivity (Kálmán, 2002). It seems that not the appearance, but the preponderance of astrocytes correlates with the enlargement of the brain. However, despite the glutamine synthetase immunostaining, the

rhombencephala and spinal cords of skates and rays proved to be dominated by ependymoglia, like in the previous study confined to GFAP (Kálmán and Gould, 2001).

6.3. Astrocytes is sharks

The studies on sharks presented in this paper, applying glutamine synthetase and S-100 immunohistochemistry, demonstrated the structures found by the previous investigations (Wasowicz et al., 1999; Kálmán and Gould, 2001), but astrocytes, including the 'unipolar astrocytes' were found in *Squalus*, in both peri- and apovascular positions. The presence of more numerous, GFAP-immunoreactive, apovascular, and multi-processed cells in the telencephalon of *Pristiophorus* seems to be an apomorphic feature as compared to *Squalus*. Notably, the status of the phylogenetic placement of Pristiophoriformes is highly controversial (see introduction), the numerous telencephalic astrocytes in *Pristiophorus* may be regarded as a feature pointing toward batoids. However, the large ventricles and the preponderant radial glia are typical selachian features. Density of astrocytes in galeomorph sharks were in midposition between that of *Pristiophorus* and *Squalus*.

6.4. Astroglial system of Myliobatiformes

The astroglial system of a representative of Myliobatiformes has not been described as yet. Among batoids, Myliobatiformes have the highest brain weight/body weight ratios (Jerison, 1973; Northcutt, 1978, 1981; Smeets et al., 1983), a very complex cerebellum (fig. 6o), etc., whereas skates (Rajiformes) represent a more simple type. From the three Myliobatiformes genera represented in this investigation, *Mobula* seems to have the highest degree of cerebralization, telencephalization, and cerebellar evolution (fig. 6j,o). This is reflected in the following differences in the astroglial structure. Only in *Mobula* could a considerable astrocyte population be found in every brain part, even with GFAP immunostaining. Perivascular glia contacting blood vessels only with their processes were found only in *Mobula*, a situation commonly found in mammals. In Myliobatiformes, including *Mobula* no radial glia was found in the impar telencephalic ventricle, in contrast to skates. However, ependymal processes, although short ones, were present in the remnant of mesencephalic ventricle, and in the rhombencephalic ventricle.

6.5. Astroglial architecture of a holocephalan species

I also present the first study on the glial architecture of a representative species, *Callorhinchus milii,* of the Holocephali. All immunohistochemical approaches used in the present work revealed similar radial glial structures, although most of the structures were revealed by using glutamine synthetase immunostaining with DAB reaction. Especially astrocyte-like elements were observed only with immunostaining against glutamine synthetase or S-100, but not with GFAP immunostaining. Typical astrocyte-rich territories were not found in *C. milii*, only scarce astrocyte-like elements, mainly in the telencephalon.

The brains of chimaeras were classified as laminar type like that of *Squalus* by Northcutt (1977, 1978) and Butler and Hodos (2005), therefore, the present observations are compared first with the glial architecture of a representative squalomorph shark, *S. acanthias*.

6.5.1. Astroglial structures similar in *Squalus* and *Callorhinchus*

In general, the glial architecture of *C. milii* was similar to that of *S. acanthias*. The predominant elements were radially oriented ependymoglia (Horstmann, 1954: tanycytes). Occasionally curved 'radial' glial processes were seen in *C. milii* like in *Squalus* and other animals (turtle: Kálmán et al., 1994, 1997; caiman: Kálmán and Pritz, 2001), which is the result of morphogenetic processes. However, in the ventral segment of the telencephalic hemispheres of *C. milii*, glial processes crossed each other close to the meningeal surface, which is unusual for radial glia.

In the cerebellum the glial structures of the granular and molecular layers were distinct, with parallel glial processes perpendicular to the meningeal surface in the latter (Bergman fibers). In *C. milii*, as well as in *Squalus* (Kálmán and Gould, 2001), however, these processes were less regular than in Amniotes (either reptiles, or birds, or mammals).

The radial glial pattern revealed tectal layers in *C. milii,* as in *S. acanthias* (Kálmán and Gould, 2001), and in representatives of some other vertebrate groups (carp, *Cyprinus carpio*, Teleostei, Kálmán, 1998; lizard, *Gallotia galloti*, Monzón-Mayor et al., 1990; turtle, *Pseudemys scripta elegans*, Kálmán et al., 1994; caiman, *Caiman crocodylus*, Kálmán and Pritz, 2001). On the basis of differences in

immunoreactivity I distinguished five layers in the tectum mesencephali (Smeets also distinguished five layers in *Hydrolagus*), while in Elasmobranchs six different layers were described (Smeets, 1983). The gray matter and the white matter were similar to those found in *Squalus* and in all other vertebrates having a radial ependymoglial system. In the reticular formation a similar pattern was seen like in *Squalus acanthias* (Kálmán and Gould, 2001), and in a crocodilian (*Caiman crocodilus*, Kálmán and Pritz, 2001), but not in turtles (*Pseudemys scripta elegans*, Kálmán et al., 1994, *Mauremys leprosa*, Kálmán et al., 1997; *Trionyx sinensis*, Lazzari and Franceschini, 2006).

6.5.2. Astroglial structures different in *Squalus* and *Callorhinchus*

A continuation of the sulcus limitans lateralis, a ’pony-tail’ like bundle of glial processes completed the separation between pallial and subpallial areas in the telencephalon. No similar structure was found in *Squalus* (Kálmán and Gould, 2001) but such formation does occur in caiman (*Caiman crocodilus*, Kálmán and Pritz, 2001) and in the domestic chicken (Kálmán et al., 1993).

On the meningeal surface, radial glial processes were seen to form endfeet-like structures, which appeared similar to the glia limitans in *Squalus* and other vertebrates having radial ependymoglia (teleosts, reptiles). However, further examination of their structure and size, using HE staining in some areas, mainly in the telencephalon, suggested that they were cell bodies inserted between the endfeet, extending processes into the brain substance. In *Squalus* similar cells were not observed (Kálmán and Gould, 2001). Previous studies based on silver impregnation techniques, however, revealed cells of a similar type in *Negaprion brevirostris* (Klatzo, 1967), in *Sphyrna zygaena, Galeocerdo cuvieri, and Ginglymostoma cirratum* (Long et al., 1968), all galeomorph sharks. These cells are probably derived from cross-divisions of radial cells, and may represent a step in the evolutionary process forming ependyma-independent glial elements.

Despite the fact that chimaeras are considered an ancient basal group of cartilaginous fishes (Northcutt, 1977, 1978), the glial architecture found did not reflect this statement.

6.6. Dystroglycan complex and associated proteins in the brain of Chondrichtyes

This study is the first one to demonstrate the occurrence of the components of the DGC in the cerebral vessels of Chondrichthyes, including both Elasmobranchii and Holocephali. DG displayed a rather intense immunoreactivity. Immunostaining against DG visualized the whole brain vascular system, even the characteristics of interspecific and regional differences. Other components of the complex (dystrophin, utrophin, α-dystrobrevin, α-syntrophin) proved to be less immunoreactive. Double-labeling studies, however, showed their colocalization with DG.

It was formerly suggested (Khurana et al., 1992), that DGC plays a general role in the organization of the blood-brain barrier in vertebrates, including Elasmobranchii, despite the fact that the structure of the barrier is different in the latter group (Bundgaard and Cserr, 1981, see also 2.8). In accordance with the role of DGC in the muscular system, the organization of the neuromuscular synapse, and the pathogenesis of the Duchenne-type myopathia (DMD, for reviews see Emery, 1989; Anderson et al., 2002; Montanaro and Carbonetto, 2003) the complex has been widely investigated in the electric organ of electric rays (different *Torpedo* species, e.g. *marmorata*, *ocellata*, *radiata*), because this organ consists of modified musculature. Bowe et al. (1994) and Deyst et al. (1995) found DG there, and proved it to be immunologically related to mammalian DG. According to the review of Marchand et al. (2001) α-syntrophin and utrophin were also described in the electric organ of *Torpedo*. Dystrobrevin was actually discovered in *Torpedo* (Sadoulet-Puccio et al., 1996; Balasumbramyan et al., 1998), and Cartaud et al. (1992) detected dystrophin in the electric organ of the electric ray (*Torpedo marmorata*).

In mammalian brains, there are several dystrophins, as shorter, amino-terminally truncated products of the same gene (by intragene promoter usage, Gorecki et al., 1992). These dystrophin isomorphs are designated as Dp260, Dp140, Dp116 and Dp71 according to their molecular weights (Lidov et al., 1993). The antibody (Dys2, Novocastra) applied by us, however, recognizes the C-terminals, which are uniform in the isoforms.

My results documented the presence of DGC components in the vessels of different Chondrichthyes, without differences regarding either the cerebralization, the preponderant type of astroglia, or the structure of the blood-brain barrier (see also 6.10).

6.7. Aquaporins in Chondrichthyes brain

The presence of aquaporins has been studied mainly in mammals (Hasegawa et al., 1994; Jung et al., 1994; Frigeri et al., 1995). AQP4 proved to be identical with the 'orthogonal array of particles' (OAP, Wolburg, 1995) of the astrocytic cell membrane, described two decades earlier by the freeze-fracture method (Verbavatz et al., 1997; Rash et al., 1998; Nico et al., 2001; Furman et al., 2003). These particles, however, are not ubiquitous in vertebrates. They are missing in toads, frogs and newts (Korte and Rosenbluth, 1981, *Bufo bufo*; Wujek and Reier, 1984, *Xenopus laevis, Triturus viridescens;* Kästner, 1987, *Rana esculenta*), and in fishes (*Carassius auratus*: Wolburg et al., 1983; Kästner, 1987). In lizards (*Anolis chlorocyanus*) and turtles (*Terrapene carolina triunguis*) Kästner (1987) reported their occurrence, contradicting to the results of Wujek and Reier (1984). Their presence is commonly accepted in birds (pigeons and *Gallus domesticus*, Kästner, 1987). In a former study, the occurrence of AQP4 has been described in the chicken (*Gallus domesticus*, Goren et al., 2006). In the ray *(Dasyatis akajei*) and the shark (*Triakis scyllia*), Gotow and Hashimoto (1984) have found intramembranous particles, although not in 'orthogonal array'. The absence of the 'orthogonal array', however, may not rule out the presence of AQP4, since Furman et al. (2003) published that only the M23 isoform of AQP4 forms orthogonal arrays, whereas the M1 isoform does not. The present study, however, failed to detect aquaporins in chondrichthyans by immunostaining to either type 4, which is predominant in mammals (Hasegawa et al., 1994; Jung et al., 1994; Frigeri et al., 1995), or type 9, which marks 'tanycytes' in mammals (Elkjaer et al., 2000), i.e. similar glial elements to those prevailing in sharks and holocephalans.

6.8. Evolution of radial ependymoglia

There are two hypotheses to explain the replacement of radial ependymoglia with astrocytes during evolution. One of them attributed it to the thickening of the brain wall and reduction of the ventricular system. These result in the elongation of the radial glial processes, which involves the increase of surface/volume ratio of the cell, and renders the trans-membrane ionic balance vulnerable (Reichenbach et al., 1987; Reichenbach, 1989). The solution is replacement by astrocytes. The other opinion is that the increasing complexity of vascular network required the appearance of astrocytes, because the radial glia was already incapable of perivascular glia formation (see e.g.

Wicht et al., 1994). Both phenomena occur in skates, as immunohistochemical studies on DG demonstrated, the complexity of vascular network in parallel with the astrocyte predominance and the reduction of radial glial system. Nevertheless, the fact that astrocytes also occur in the thin-walled telencephalon of sharks, but only a part of them contribute to the formation of perivascular glia contradicts the opinion that either the thickening of the brain or the growing complexity of the vascular system would induce the appearance of astrocytes, although they might have promoted the preponderance of astrocytes, once present. Formerly, the study on the evolution of astroglial system in Amniotes resulted in a similar conclusion (Kálmán and Pritz, 2001). It is noteworthy that astrocytes appear always as complementary elements, forming mixed populations with the radial glia (also in Amniotes, in reptiles, see Monzon-Mayor et al., 1990; Yanes et al., 1990; Lazzari and Franceschini, 2001; Kálmán and Pritz, 2001). Also, this seems to deny the suggestion that the apperance of astrocytes is caused by an 'incapability' and 'extinction' of radial glia. A probable explanation could be that astrocytes, having smaller territories than long radial glial cells, may provide a more adaptable environment to the neurons.

6.9. Correlation between cerebralization and glial pattern

There was no specific astroglial structure to distinguish the brains of galeomorph and squalomorph sharks. Among the predominant radial glia, astrocyte-like structures were also found in all the four shark species investigated (either galeomorphs or squalomorphs), almost exclusively in the telencephalon. Note that the macroscopic structures are similar in these species: thin brain wall, large ventricles (fig. 6a-e,k,m). The astroglial structure did not seem to reflect that the galeomorph sharks have brains of 'elaborated' type, in contrast to the 'laminar' brains of squalomorph sharks. However, it should be taken into consideration that some galeomorph sharks, especially the small-sized species, like *Scyliorhinus* and *Cephaloscyllium*, do not express fully the features of elaborated brains. Unfortunately, for us it was impossible obtaining brains to conduct such study on the most typical large-sized Galeomorphii (*Sphryna, Isurus)*, which express the highest brain weight/body weight ratio among sharks (Jerison, 1973; Northcutt, 1978, 1981). Former silver impregnation studies in large- and medium-sized sharks, as nurse shark, (*Ginglymostoma cirratum:* Long et al., 1968; Schroeder and Ebbesson, 1975), lemon shark (*Negaprion brevirostris:* Klatzo, 1967), tiger shark and

hammerhead shark (*Galeocerdo cuvieri, Sphyrna zygaena:* Long et al., 1968) revealed a preponderance of radial glia, intermingled with scarce astrocytes. Immunhistochemical studies on these species have not been conducted as yet.

Therefore, it seems that the astroglial structures correspond to the macroscopic structure of brain, rather than the laminar/elaborated categories. In different species with 'elaborated' brains either radial ependymoglia ('tanycytes'), or astrocytes may be predominant. The same is found in Amniotes, comparing the 'tanycytic' brains of reptiles, with only scarce astrocytes (if at all), to the 'astrocytic' brains of birds and mammals (Kálmán and Hajós, 1989; Hajós and Kálmán, 1989; Monzon-Mayor et al., 1990; Yanes et al., 1990; Lazzari and Franceschini, 2001; Kálmán and Pritz, 2001). Among the ray-finned fishes (Actinopterygii) Teleostei have 'elaborated' brains (Butler and Hodos, 2005), but they have only a few astrocyte-like elements, confined to some areas (Kálmán, 1998).

One principal difference was observed, however, when sharks (any shark) were compared to skates and rays. In skates and rays astrocytes were predominant elements, although radial ependymoglial processes were also found, mainly in skates. The prevalence of astrocytes, however, extended only to the telencephalon and mesencephalon, where the macroscopic differences from the shark brains were conspicuous (fig. 6f-j, 6l). In the brain of skates and rays these parts underwent conspicuous changes of gross anatomy during evolution. In the rhombencephalon, and in the spinal cord, which proved to be rather conservative during evolution (fig. 6p-t, Smeets and Nieuwenhuys, 1976; Nieuwenhuys et al., 1997; Butler and Hodos, 2005), however, there was no principal difference in the astroglial architecture between sharks and batoids. Here the general brain structure remained similar in the different groups of Elamobranchii, and the ependymoglial structure persisted. It is a meaningful difference with the astroglial evolution of Amniotes, in which the astrocytes became predominant in every part of the brain, regardless of its progressive or conservative morphology. In the different groups of Amniotes (reptiles, birds, mammals) the macroscopic structure of rhombencephala is rather similar (fig. 6x-z), actually, they are even similar to those of elasmobranchs, due to the conservative structure (Smeets and Nieuwenhuys, 1976; chapters of Nieuwenhuys et al., 1997; Butler and Hodos, 2005). In birds and mammals, however, astrocytes predominate in the rhombencephalon like in every other part of the

brain (see e.g. Hajós and Kálmán, 1989; Kálmán et al., 1993), whereas in reptiles, the rhombencephalon contains ependymoglia (Kálmán et al., 1994; Kálmán and Pritz, 2001). The macroscopy of the avian tectum is similar to the reptilian tectum (a thin-walled 'shell', fig. 6u,v), yet the birds have here astrocytes, in contrast to the ependymoglia of reptiles (Monzón-Mayor et al., 1990; Kálmán et al., 1993; Kálmán et al., 1994; Kálmán and Pritz, 2001), but similarly to mammals (Hajós and Kálmán, 1989), which have thick-walled tectum with reduced ventricle ('aqueduct', fig. 6w).

6.10. Correlation between the vascular immunostaining and glial pattern

In my results, cerebral vessels were delineated by immunoreactivities to both GFAP, and S-100 protein, and, best of all, glutamine synthetase. This immunoreactivity was observed applying either fluorescent or peroxidase method (see e.g. fig. 13a). No labeling was found, if primary antibody was omitted. In former studies, a similar continuous GFAP immunolabeling was found along the brain vessels in Chondrichthyes: *Squalus acanthias* and, less intensely, in *Raja erinacea* (Kálmán and Gould, 2001), as well as in *Scylliorhinus canicula* and *Torpedo marmorata* (Wasowicz et al., 1999), but not in other vertebrates (rat, *Rattus norvegicus:* Kálmán and Hajós, 1989; Japanese quail, *Coturnix coturnix japonica*: Cameron-Curry et al., 1991; chicken, *Gallus domesticus*: Kálmán et al, 1993; turtle, *Pseudemys scripta elegans* Kálmán et al, 1994*; caiman, Caiman crocodylus:* Kálmán and Pritz, 2001*;* lizards, *Gallotia galloti:* Monzón-Mayor et al., 1990; Yanes et al., 1990; and *Podarcis sicula:* Lazzari and Franceschini, 2006; carp, *Cyprinus carpio:* Kálmán, 1998).

The species studied here represented different chondrichthyan groups with differences in the composition of the blood-brain barrier, degree of cerebralization and the preponderant glial element. In Elasmobranchii the continuous vascular immunolabeling with glial markers might be attributed to the fact that their blood-brain barrier is formed by perivascular glia, rather than by endothelial cells, in contrast to all other vertebrates (Bundgaard, 1982; Bundgaard and Cserr, 1981, 1991; Cserr and Bundgaard, 1984; Abbott, 1995; Bundgaard and mugnaini, 2008). In Holocephali, however, the blood-brain barrier is endothelial, as in the majority of vertebrates, nevertheless, unexpectedly, the immunostaining of vessels with glial markers was similar to that occurring in Elasmobranchii. Despite the differences in the composition

of the barrier, the present immunohistochemical reactions did not reveal any difference in the presence of DGC or its associated proteins either.

On the other hand, although tanycytes are prevalent glial elements in sharks, and the vessels follow their radial course, whereas in skates and rays astrocytes are preponderant and the vessels form a network, no difference was found in the immunhistochemical staining of DG.

6.11. Potential significance of differences in glial architecture, ancient and recent features in chondrichthian evolution

On the basis of the discussion presented above, the presence rather preponderance of astrocytes as opposed to radial ependymoglia seems to be an apomorphic feature in some cartilaginous fishes, similarly to that found in Amniotes. Therefore, groups of Amniotes, such as birds and mammals, and groups of chondrichthians, such as Rajiformes or Myliobatiformes, where the preponderant glial structures are astrocytes, can be considered as more advanced groups, as compared to those where radial ependymoglia predominate. The preponderance of astrocytes seems to be an apomorphic feature as well, when compared to brains with a scarce number of astrocytes.

The astrocyte predominance seems to have evolved in parallel with the increasing number of GFAP immunonegative astrocytes, and areas poor in or devoid of GFAP immunoreactivity, like in Amniotes (Kálmán, 2002). Therefore, the GFAP immunonegativity is regarded as an apomorphic feature.

The orientation of the perivascular astrocytes may have potential significance in astroglial evolution. Glia limitans had been composed by endfeet on the surface of blood vessels and the meningeal surface, which were replaced by cell bodies having long and lately enshortened processes.

7. Appendix: Ecological and ethological perspectives

The relative brain development reflects the dimensionality of the environment, agile prey capture and phylogeny in sharks (Yopak et al., 2007). Among batoids, Myliobatiformes have the highest brain weight/body weight ratios (Jerison, 1973; Northcutt, 1978, 1981; Smeets et al., 1983), a very complex cerebellum (fig. 6o), etc., whereas skates (Rajiformes) represent a more simple type. Of the three Myliobatiformes genera represented in our investigation, *Mobula* seems to have the highest degree of cerebralization, telencephalization, and cerebellar evolution (see fig. 6j,o), therefore the potential ecological significance of enlarged brain parts, especially that of large-brained galeomorph sharks and *Mobula* is discussed below.

7.1. Habitat

The shark species with the largest brains relative to body mass are benthopelagic or pelagic, chiefly found in reef or coastal- oceanic subhabitats (Yopak et al., 2007), where the largest-brained teleosts live as well (Bauchot et al., 1977). It is suggested that the requirements for learning the complex spatial organization of the reef habitat might have influenced the evolution of brain size (Bauchot et al., 1977; Northcutt, 1978, 1989). A possible connection between increased relative brain size and complexity of habitat has also been reported in mammals (Budeau and Verts, 1986). The reef habitat is the most complex and stratified form of habitat in the aquatic environment, and there seems to be a selective advantage if the predators can learn the complex spatial organization, and recognize and pursue prey that is well camouflaged or has complex defence mechanisms (Northcutt, 1978). The brains of pelagic species tend to show specialization rather than generalization in their structural development.

7.2. Social interactions

According to Kotrschal et al. (1998) the increase in relative brain size is related to complex social behaviours. This kind of ’social intelligence’ has been correlated with brain size also in birds and mammals (Striedter, 2005). The cognitive abilities of cartilaginous fishes have been scarcely studied, however, carcharhinid and sphyrnid sharks are considered to be social animals (Springer, 1967; Myrberg and Gruber, 1974; Klimley, 1985) that aggregate or form true schools. This might be related to complex social and reproductive behaviours, such as dominance hierarchies and courtship behaviour. Mobulas also form schools (Coles, 1916; Compagno, 1997), but there is only

a single report describing the complex courtship behaviour of another Mobulid species, *Manta birostris* (Yano, 1999).

7.3. Thermoregulation

Endothermy in birds and mammals underlies their high activity levels, making them more efficient in obtaining food. Among sharks, *Isurus* and *Lamna* are able to maintain body temperatures well above ambient temperature of environment (Carey and Teal, 1969), and among the Mobulid rays, in *Mobula tarapacana* and *Manta birostris*, a brain warming counter-current heat exchanger has been described around their brain (Alexander, 1995, 1996; Schweitzer, 1986). Interestingly, the same families are also characterized as large-brained elasmobranchs.

7.4. Reproduction

Relative brain size also appears to be related to the mode of reproduction. Mobulas have gestation periods as long as two years (Wourms, 1977) and species in the families of carcharhiniforms, sphyrnids, dasyatids and myliobatids have evolved yolk sac placentae or placental analogs (trophonemata), increasing energy flow to the embryos by 800 to 5000 % (Wourms, 1977). The same families have the most complex neural organization and the highest brain mass/body mass ratios known for elasmobranches (Northcutt, 1978).

7.5. Telencephalic features in relation to behaviour

Shark species have been categorized (Yopak et al., 2007) by their habitat in association with the relative development of different brain areas. Thus, the relative size of the brain or each of its component structures can be envisaged as a consequence of phylogenetic grouping, locomotor behaviour, habitat, and lifestyle.

Sphyrnid sharks with a brain complexity very similar to the *Mobula*'s are active hunters that live in a 3-dimensional environment (pelagic) and show potential for social behaviour. These sharks with the highest level of neural development clearly show greatly hypertrophied telencephalons and cerebella. The *Sphyrna mokarran* has evolved a particularly large telencephalon that accounts for almost 67% of its brain. *Sphyrna* live in reef habitats, and an increase in the relative size of the telencephalon is believed to be associated with complex environment in this shark species, like in many other vertebrates (Riddell and Corl, 1977; Barton et al., 1995; Huber et al., 1997; Striedter,

2005). Interestingly, both *Mobulas* and Sphyrnid sharks have an extremely broad head, which might help increase the efficiency of different sensation modalities and their complex integration.

7.6. Cerebellar features in relation to behaviour

It is suggested that the cerebellum modulates motor tasks (Paul and Roberts, 1979; New, 2001) and error correction (Gluck et al., 2001; Montgomery et al., 2002). Others think that it is involved in the coordination of target tracking and the analysis of the consequences of organisms' own movements, rather than the control of these movements themselves (Paulin, 1993).

Sharks with the most highly foliated cerebella are all wide-ranging, migratory species (Yopak et al., 2007), which would arise the question whether *Mobulas* might travel long distances, however there are no data available on the migratory behaviour of Mobulids as yet.

The brains of *Alopias* species are characterized by a large and heavily foliated cerebellum, which thought to be related also to the evolution of the method of prey capture, which involves the use of the extremely elongated upper lobe of the caudal fin to stun and capture prey (Compagno, 1984; Last and Stevens, 1994; Lisney and Collin, 2006). In the case of Mobulids, which feed on planktonic crustaceans, it might be related to the complex motor control required for hovering at the cleaning stations or somersaulting in the water column to collect shrimps in a more efficient way. Other large-bodied plankton feeders (basking shark, *Cetorhinus maximus*), with locomotor patterns requiring less complex coordination, also have relatively large cerebella, however without asymmetry and with less foliation than it was found in *Mobula*.

Generally speaking, cerebellar foliation appears to be related to both locomotor abilities and sensory-motor integration (New, 2001), rather than prey capturing itself (Paulin, 1993). This is particularly evident in the case of *Mobula*. New (2001) suggested that those species with larger cerebella use sensory information to perform more multifaceted motor tasks than their close relatives lacking cerebellar hypertrophy. In sharks it is likely that there is a relationship between the level of cerebellar foliation and both swimming speed and mode of locomotion. Sharks with higher degrees of foliation display subcarangiform or thunniform swimming, whereas those with low degrees of

foliation (slow moving sharks) are characterized by anguilliform swimming and axial undulation of the body. *Sphyrna* and *Carcharhinus falciformes* are pelagic sharks using a subcarangiform swimming mode and capable of long-distance swimming with high maneuverability (Donley and Shadwick, 2003; Wilga and Lauder, 2004), *Mobulas* use undulation of the pectoral fins. Holocephalans swim by undulation of the pectoral fins (Wilga and Lauder, 2004) as well, and they have relatively large cerebella - compared to their telencephalon- , although not highly foliated. Thus, the structure of the cerebellum might be related to the dexterity of the pectoral fins and enhanced motor capabilities.

Very little is known about the behavioural and learning capacities of the large-brained elasmobranchs, especially Mobulids, since these are very difficult to study in their natural environment. More research would be needed in order to clarify the capacities of the large-brained chondrichtians connected to the specific morphological characteristics of their brain.

8. Conclusions

1) On the whole, immunostaining to S-100, and mainly to glutamine synthetase revealed more astroglial elements, than immunostaining to GFAP, especially astrocytes in *Squalus acanthias* (Squalomorphii), and *Callorhinchus milii* (Holocephali), and in batoids apovascular astrocytes in the telencephalon and the Bergmann glia.

2) It was the first immunohistochemical study on the astroglia of representatives of Myliobatiformes order. It revealed advanced features to other batoids, e.g. lack of radial glia in the telencephalon, true astrocytes in the granular layer of cerebellum, in the rhombencephalon, and in the spinal cord. GFAP immunopositive astrocytes were found in each brain region of *Mobula japanica* and only in *Mobula* was found perivascular glia contacting the vessel only by its processes, a situation commonly found in mammals. Most of advanced features were found in the *Mobula japanica*.

It was the first mapping of astroglia on a representative of Holocephali, *Callorhinchus milii*. Its astroglial architecture proved to be similar to the brain of *Squalus acanthias*, a squalomorph shark of a less advanced brain type, since neither of them had GFAP-immunopositive astrocytes. *C. milii* however, had some advanced features: some telencephalic territories could be recognized on the basis of their glial pattern, and on the meningeal surface glial cells are inserted between the endfeet of radial glia.

3) The difference in astroglial architecture between sharks (radial ependymoglia predominate) versus skates and rays (astrocytes predominate) was confined only to the prosencephalon and mesencephalon. Even applying immunohistochemical reaction against glutamine syntethase, astrocytes did not prevail in conservative brain regions, such as rhombencephalon, as they did in the progressive brain regions.

4) Applying immunohistochemical reaction against glutamate syntethase and S-100 protein supported the former results obtained by immunostaining of GFAP that in Chondrichthyes vessels are labeled with glial markers. Immunostaining against DG visualized the whole vascular system in cartilaginous fishes, even the characteristics of interspecific and regional differences. DGC and its associated proteins could be found throughout the vessels of the chondrichthyan species studied, similarly to mammals, while AQP4 and AQP9 are possibly absent, similarly to other vertebrates, excluding birds and mammals.

5) There was no specific astroglial structure to distinguish the brains of galeomorph and squalomorph sharks. Even applying immunohistochemical reaction against glutamine syntethase, astrocytes proved to be minor component of astroglial system in galeomorphs investigated in this studies, in contrast to batoids. On the other hand, scarce astrocytes also occurred in squalomorphs, despite the thin brain wall. It seems that in Chondrichthyes the astroglial structures correspond to the local macroscopic structure of brain, rather than to its general features: the grade of cerebralization, and the laminar/elaborated categories. Neither the differences in their blood-brain barrier, nor the differences in their cerebralization were reflected in any differences of immunoreactivity to DG. However, in the telencephalon, the vascular network could be associated, to some extent, to differences in astroglial architecture.

6) Although, the evolutionary changes of astroglia had some similarities in Elasmobranchii and Amniota, there was one meaningful difference: in Elasmobranchii astrocytes did not prevail in conservative brain regions as they did in the progressive brain regions.

In appendix:

7) The large brain size in some elasmobranch families could be connected to habitat, special thermoregulation abilities and/or increased energy flow to the embryos. The enlargement of telencephalon is present in chondrichthyes that live in a 3-dimensional environment (pelagic) and this enlargement is probably related to complex social behaviours. The large, heavily foliated and asymmetric cerebellum might be associated to wide-ranging, migratory behaviour, and appears to be related to locomotor abilities and sensorymotor integration.

9. Summary

Chondrichthyes display a wide range of cerebralization, differences in the glial architecture and in the composition of the blood-brain barrier. The present study supplements the former glial impregnation studies and GFAP immunohistochemistry with the immunohistochemical detections of glutamine synthetase and S-100 protein. The examination was extended to representatives of important groups of Chondrichthyes (myliobatiform rays, Holocephali), also to brain parts (rhombencephalon), on which no glial study has been done as yet. To reveal some characteristic features of the blood-brain barrier of cartilaginous fishes the dystroglycan complex (DG) and some of its associated proteins were also investigated, as well as aquaporin-4 and aquaporin-9.

Immunostaining to S-100, and mainly to glutamine synthetase revealed more astroglial elements, than did immunostaining to GFAP. By using glutamine synthetase astrocytes could be revealed in *Squalus acanthias* (Squalomorphii) and *Callorhinchus milii* (Holocephali), and GFAP immunonegative astrocytes and Bergmann glia were visualized in batoids. Myliobatiform rays, especially *Mobula japanica,* the representative of Mobulidae family, manifested advanced features to other batoids, e.g. appearance of astrocytes in cerebellum, lower brain stem, and spinal cord. The glial architecture of *C. milii,* a representative of Holocephali, proved to be similar to that of *S. acanthias*, but showed some advanced features: some telencephalic territories had individual glial pattern, and in the meningeal surface glial cells were inserted between the endfeet of radial glia. Immunostaining against DG and its associated proteins, but not aquaporins were detected in the vessels of every species investigated. Interspecific differences of blood-brain barrier, cerebralization, or astroglial architecture were not reflected in any differences of immunoreactivity.

There was no specific astroglial structure to distinguish the brains of galeomorph and squalomorph sharks. There was only difference between sharks and batoids (preponderance of astrocytes in latters), which confined to the prosencephalon and mesencephalon. It seems that the astroglial structures correspond to the local macroscopic structure of brain, rather than to the general cerebralization, and the laminar/elaborated categories. Astrocytes did not prevail in conservative brain regions as they did in the progressive brain regions in Elasmobranchii, in contrast to Amniota.

10. Összefoglalás

A porcos halakban a cerebralizációnak, az astroglia architektúrának, és a vér-agy gát összetételének különböző formáit találjuk. A jelen tanulmány kiegészíti a korábbi glia-impregnációs és GFAP immunhisztokémiai vizsgálatokat a glutamin szintetáz és S-100 protein immunhisztokémiai kimutatásával. A vizsgálatokat kiterjesztettem eddig nem vizsgált porcos hal csoportokra (myliobatiform ráják, tömörfejűek), illetve agyterületekre is (rhombencephalon), amelyek glia szerkezetéről nincs, vagy alig van adat. A vér-agy gát jobb megismerése céljából a disztroglikánt (DG) és néhány kapcsolt proteinjét is vizsgáltam, valamint az aquaporin 4–et és 9-et.

Általánosságban, az S-100 protein, de főleg a glutamin szintetáz több asztroglia elemet jelölt, mint a GFAP immunfestés. A glutamin szintetáz immunfestése asztrocitákat tett láthatóvá *Squalus acanthias*-ban (Squalomorphii), *Callorinchus milii*–ben (Holocephali), illetve GFAP-negatív asztrocitákat és Bergmann-gliát batoidokban. A Myliobatiformes rendbe tartozó ráják, főleg a *Mobula japanica*, a Mobulidae család képviselője, előrehaladott tulajdonságokat mutatott más rájákhoz képest, pl. asztrociták megjelenését a kisagyban, a nyúltvelőben, és a gerincvelőben. A *Callorhinchus milii*, a tömörfejűek reprezentánsa leginkább a *Squalus acanthias*-éhoz hasonló gliaszerkezetet mutatott, némely előrehaladottabb sajátsággal: sajátos gliaszerkezetű telencephalon-területek, gliasejtek beépülése a meningeális felszínen a radiális glia végtalpai közé. A DG ill. a köré épült komplexbe tartozó fehérjék kimutathatóak voltak a porcoshalak ereiben, de aquaporinok nem. Bár az egyes fajok, ill. csoportok között jelentősek a különbségek a vér-agy gát szerkezetében, a cerebralizációban, ill. a gliaszerkezetben, ezek egyike sem tükröződött immunhisztokémiai eltérésekben.

Nem volt olyan specifikus asztroglia struktúra, amely különböző lett volna a galeomorf és a squalomorf cápákban, csak a cápák és a ráják között volt különbség (asztrociták túlsúlya az utóbbiakban). Ez a különbség is a prosencephalonra és a mesencephalonra korlátozódott. Úgy tűnik, hogy az asztroglia struktúra inkább az agy helyi makroszkópos struktúrájával függ össze, mint a cerebralizáció általános fokával, ill. a lamináris/elaborált csoportosítással. A magzatburkosaktól eltérően a porcoshalakban az asztrociták nem váltak uralkodó struktúrává a konzervatív agyterületeken, csupán a progresszív agyterületeken.

10. Acknowledgements

Most of the fresh specimens were provided by Tasmanian fishermen. I am grateful to Barry Bruce, Alastair Graham, John Stevens and Michelle Treloar at the CSIRO Marine Research Laboratories (Hobart, Tasmania, Australia), Institute of Marine Biology (Kotor, Montenegro), Tropicarium Budapest (Hungary), Glenn Northcutt at the Scripps Institution of Oceanography (San Diego, USA), John O'Sullivan at the Monterey Bay Aquarium (USA), Oscar Sosa Nishizaki at CICESE (Mexico), João Pedro Correia at Oceanario de Lisboa (Portugal), Ellen Freund and Heidi Dewar for their help in providing fresh specimens. I wish to thank Maria Bako and Erzsebet Oszwald for their help in tissue processing. The study was supported by OTKA 60930 grant (to M. Kalman) and Semmelweis University School of Doctoral Studies. I also thank Prof. Andras Csillag for critically reading the thesis and for helpful suggestions concerning the style and composition of text.

I am grateful to my family and good friends who worked hard to keep my soul healthy in the long and difficult time to accomplish this work.

12. References

Abbott NJ. (1995) Morphology of non-mammalian glial cells: functional implications. In: Neuroglia. Kettenmann H, Ransom BR, editors, Oxford University Press, New York, Oxford, pp: 97-116.

Abd-el-Basset EM, Ahmed I, Fedoroff S. (1990) Actin and actin-binding proteins in differentiating astroglia in tissue culture. J Neurosci Res 30: 1-17.

Agre P, King LS, Yasui M, Guggino WB, Ottersen OP, Fujiyoshi Y, Engel A, Nielsen S. (2002) Aquaporin water channels from atomic structure to clinical medicine. J Physiol 542:3-16.

Agre P, Kozono D. (2003) Aquaporin water channels: molecular mechanisms for human diseases. FEBS Lett 555:72-78.

Alexander RL. (1995) Evidence of counter-current heat exchanger in the ray, *Mobula tarapacana* (Chondrichthyes: Elasmobranchii: Batoidea: Myliobatiformes). J Zool (Lend) 237:377-384.

Alexander RL. (1996) Evidence of brain-warming in the mobulid rays, Mobula tarapacana and *Manta birostris* (Chondrichthyes: Elasmobranchii: Batoidea: Myliobatiformes). Zool J Linn Soc, 118:151-164.

Amiry-Moghaddam M, Ottersen OP. (2003a) The molecular basis of water transport in the brain. Nature Rev Neurosci 4:991-1001.

Amiry-Moghaddam M, Otsuka T, Hurn PD, Traystman RJ, Haug F-M, Froehner SC, Adams ME, Neely JD, Agre P, Ottersen OP, Bhardwaj A. (2003b) An α-syntrophin-

dependent pool of AQP4 in astroglial end-feet confers bidirectional water flow between blood and brain. Proc Natl Acad Sci USA 100:2106-2111.

Amiry-Moghaddam M, Frydenlund DS, Ottersen OP. (2004) Anchoring of aquaporin-4 in brain: molecular mechanisms and implications for the physiology and pathophysiology of water transport. Neuroscience 129: 999-1010.

Anderson JL, Head SI, Rae C, Morley JW. (2002) Brain function in Duchenne muscular dystrophy. Brain 125: 4-13.

Ariëns-Kappers CU. (1906) The structure of the teleostean and selachian brain, J Comp Neurol, 16: 1-112.

Arregui CO, Carbonetto S, McKerracher L. (1994) Characterization of neural cell adhesion sites: point contacts are the sites of interaction between integrins and the cytoskeleton in PC12 cells. J Neurosci. 14: 6967-6977.

Arnason U, Gullberg A, Janke A. (2001) Molecular phylogenetics of gnathostomous (jawed) fishes: old bones, new cartilage. Zool Scr, 30: (4) 249-255.

Balasumbramyan S, Fung ET, Huganir RL. (1998) Characterization of the tyrosine phosphorylation and distribution of dystrobrevin isoforms. FEBS Lett, 432:133-40.

Barton RA, Purvis A, Harvey PH. (1995) Evolutionary radiation of visual and olfactory brain systems in primates, bats and insectivores. Phil Trans Res Soc London Bull, 348: 381-392.

Bauchot R, Bauchot ML, Platel R, Ridet J.M. (1977) The brains of Hawaiian tropical fishes: Brain size and evolution. Copeia, 1:42-46.

Bowe MA, Deyst KA, Leszyk JD, Fallon JR. (1994) Identification and purification of an agrin receptor from *Torpedo* postsynaptic membranes: a heteromeric complex related to the dystroglycans. Neuron, 12:1173-80.

Budeau DA, Verts BJ. (1986) Relative brain size and structural complexity of habitats of chipmunks. Journal Mammal, 67: 579-581.

Bullock TH, Moore JK, Fields RD (1984) Evolution of myelin sheaths: both lamprey and hagfish lack myelin. Neurosci Lett, 48:145-148.

Bundgaard M, Cserr HF. (1981) A glial blood-brain barrier in Elasmobranchs. Brain Res, 226:61-73.

Bundgaard M, Abbott NJ. (2008) All vertebrates started out with a glial blood-brain barrier 4-500 million years ago. Glia, 56(7):699-708.

Bundgaard M. (1982) The ultrastructure the cerebral blood capillaries in the ratfish *Chimaera monstrosa.* Cell Tiss Res, 226:145-154.

Bundgaard M, Cserr HF. (1991) Barrier membranes at the outer surface of the brain of an Elasmobranch, *Raia erinacea*. Cell Tiss Res, 265:113-120.

Butler AB, Hodos W. (1996) Vertebrate neuroanatomy, Evolution and adaptation. John Wiley and Sons, Inc. New York, Chichester, Brisbane, Toronto, Singapore.

Butler AB, Hodos W. (2005) Vertebrate neuroanatomy, Evolution and adaptation. 2nd ed. John Wiley and Sons, Inc. New York, Chichester, Brisbane, Toronto, Singapore. pp 84-89.

Cameron-Curry P, Aste N, Viglietti-Panzica C, Panzica GC. (1991) Immunocytochemical distribution of glial fibrillary acidic protein in the central nervous system of the Japanese quail (*Coturnix coturnix japonica).* Anat Embryol, 184:571-581.

Carey FG, Teal JM. (1969) Mako and porbeagle: warmbodied sharks. Comp Biochem Phys, 28:199-204.

Carroll RL. (1988) Vertebrate Paleontology and Evolution. New York: W.H. Freeman and Co.

Cartaud A, Ludosky MA, Tome FM, Collin H, Stetzkowski-Marden F, Khurana TS, Kunkel LM, Fardeau M, Changeux JP, Cartaud J. (1992) Localization of dystrophin, and dystrophin-related protein at the electromotor synapse and neuromuscular junction in *Torpedo marmorata.* Neurosci, 48:995-1003.

de Carvalho MR. (1996) Higher-level elasmobranch phylogeny, basal squaleans, and paraphyly. In: Stiassny, M.L.J., Parenti, L.R., Johnson, G.D. (Eds.), Interrelationships of Fishes. Academic Press, San Diego, pp.35-62.

Cserr HF, Bundgaard M. (1984) Blood-brain interfaces in vertebrates: a comparative approach. Am J Physiol, 246: 277-88.

Chamberlain J. (1999) The dynamics of dystroglycan. Nat Genet, 23: 256-8

Chiba A. (2000) S-100 protein-immunoreactive structures in the brains of the elasmobranchs *Scyliorhinus torazame* and *Mustelus manazo*, Neurosci Lett, 179: (1) 65-68.

Coles RJ. (1916) Natural history notes on the devil-fish, *Manta birostris* (Walbaum) and *Mobula olfersi* (Müller), Bull Am Mus Nat Hist, 28:337-348.

Collins P. (1999) Embryology and development. In: Gray's Anatomy, Ed:Williams Pl, 38. Churchill Livingstone, Edinbourgh, London, New York, Philadelphia, Sidney, Toronto

Compagno LJV. (1973) Interrelationships of living elasmobranchs. Interrelationships of fishes, Academic Press, London , pp.15-61.

Compagno LJV. (1977) Phyletic relationships of living sharks and rays. Am Zool, 17:303-322.

Compagno LJV. (1997) Mobulidae. Devil rays. In K.E. Carpenter and V. Niem (eds.) FAO Identification Guide for Fishery Purposes. The Western Central Pacific.

Compagno LJV. (1984) FAO Species Catalogue. Sharks of the World. An annotated and illustrated catalogue of shark species known to date. I. Hexanchiformes to Lamniformes. Vol 4. Rome: FAO Fisheries Synopsis.

Culligan K, Glover L, Dowling P, Ohlendieck K. (2001) Brain dystrophin-glycoprotein complex: Persistent expression of β-dystroglycan, impaired oligomerization of Dp71 and up-regulation of utrophins in animal models muscular dystrophy. Cell Biol, 2: 2.

Dahl D, Bignami A. (1973) Immunohistochemical and immunofluorescence studies of the glial fibrillary acidic protein in vertebrates. Brain Res, 61:279-283.

Dahl D, Crosby CJ, Sethi JS, Bignami A. (1985) Glial fibrillary acidic (GFA) protein in vertebrates: Immunofluorescence and immunoblotting study with monoclonal and polyclonal antibodies, J Comp Neurol, 239: (1) 75-88.

Dawson MR, Levine JM, Reynolds R. (2000) NG2-expressing cells in the central nervous system: are they oligodendroglial progenitors? J Neurosci Res, 61: (5) 471-479.

Deyst KA, Bowe MA, Leszyk JD, Fallon JR. (1995) The alpha-dystroglycan-beta dystroglycan complex. Membrane organization and relationship to an agrin receptor. J Biol Chem, 270:25956-9.

Donley JM, Shadwick RE. (2003) Steady swimming muscle dynamics in the leopard shark *Triakis semifasciata*. J Exp Biol, 206: 1117-1126.

Douady CJ, Dosay M, Shivji MS, Stanhope MJ. (2003) Molecular phylogenetic evidence refuting the hypothesis of Batoidea (rays and skates) as derived sharks, Mol Phylogenet Evol, 26:215–221.

Doucette JR. (1984) The glial cells in the nerve fiber layer of the rat olfactory bulb. Anat Rec, 210:385-391.

Durbeej M, Henry MD, Ferletta M, Campbell KP, Ekblom P. (1988) Distribution of dystroglycan in normal adult mouse tissues. J Histochem Cytochem, 46:449-457.

Ehmsen J, Poon E, Davies K. (2002) The dystrophin-associated protein complex. J Cell Sci, 115:2801-2803.

Elkjaer M-L, Vajda Z, Nejsum LN, Kwon T-H, Jensen UB, Amiry-Moghaddam M, Frøkiaer J, Nielsen S. (2000) Immunolocalization of AQP9 in liver, epididymis, testis, spleen, and brain. Biochem Biophys Res Comm, 276:1118–1128.

Emery AE. (1989) Clinical and molecular studies in Duchenne muscular dystrophy. Prog Clin Biol Res, 306:15-28.

Frigeri A, Gropper MA, Umenishi F, Kawashima M, Brown D. (1995) Localization of MIWC and GLIP water channel homologs in neuromuscular, epithelial and glandular tissues. J Cell Sci 108:2993-3002.

Furman CS, Gorelick-Feldman DA, Davidson KG, Yasumura T, Neely JD, Agre P, Rash JE. (2003) Aquaporin-4 square array assembly: opposing actions of M1 and M23 isoforms. Proc Natl Acad Sci USA, 100:13609-14.

Gluck MA, Allen MT, Myers CE, Thompson RF. (2001) Cerebellar substrates for error correction in motor conditioning. Neurobiol Learn Mem, 76:314-341.

Gorecki DC, Monaco AP, Derry JMJ, Walker AP, Barnard EA, Barnard PJ. (1992) Expression of four alternative dystrophin transcripts in brain regions regulated by differents promoters. Hum Mol Genet, 1:505-510.

Goren O, Adorján I, Kálmán M. (2006) Heterogeneous occurrence of aquaporin-4 in the circumventricular organs in rat and chicken. Anat Embryol, 211:155-172.

Gotow T, Hashimoto PH. (1984) Plasma membrane organization of astrocytes in elasmobranch with special reference to the brain barrier system. J Neurocytol, 13:727-742.

Gould RM, Fannon AM, Moorman SJ. (1995) Neural cells from dogfish embryod express the same subtype-specific antigens as mammalian neural cells in vivo and in vitro. Glia, 15:401-418.

Hachem S, Aguirre A, Vives V, Marks A, Gallo V, Legraverend C. (2005) Spatial and temporal expression of S100B in cells of oligodendrocyte lineage. Glia, 51:81-97.

Hajós F, Kálmán M. (1989) Distribution of glial fibrillary acidic protein (GFAP)-immunoreactive astrocytes in the rat brain. II. Mesencephalon, rhombencephalon and spinal cord, Exp Brain Res, 78: (1) 164-173.

Hasegawa H, Ma T, Skach W, Matthay MA, Verkman AS. (1994) Molecular cloning of a mercurial- insensitive water channel expressed in selected water-transporting tissues. J Biol Chem, 269:5497-5500.

Hatakeyama S, Yoshida Y, Tani T, Koyama Y, Nihei K, Ohshiro K, Kamiie JI, Yaoita E, Suda T, Hatakeyama K, Yamamoto T. (2001) Cloning of a new aquaporin (AQP10) abundantly expressed in duodenum and jejunum. Biochem Biophys Res Comm, 287:814–819.

Henry MD, Campbell KP. (1999) Dystroglycan inside and out. Curr Opin Cell Biol 11: 602-607.

Henry MD, Satz JS, Brakebusch C, Costell M, Gustafsson E, Fässler R, Campbell KP. (2001) Distinct roles for dystroglycan, ß1integrin, and perlecan in cell surface laminin organization. J Cell Sci, 114:1137-1144.

Horstmann E. (1954) Die Faserglia des Selachegehirns. Z. Zellforsch, 39:588-617.

Hösli E, Hösli L. (1993) Receptors for neurotransmitters on asrocytes in the mammalian central nervous system. Prog Neurobiol, 40:477-506.

Huber R, van Staaden MJ, Kaufman LS, Liem KF. (1997) Microhabitat use, trophic patterns and the evolution of brain sructure in African cichlids. Brain Behav Evol, 50:167-182.

Huxlin KR, Sefton AJ, Furby JH. (1992) The origin and development of retinal astrocytes in the mouse. J Neurocytol, 21:530-544.

Ibraghimov-Beskrovnaya O, Ervasti JM, Leveille CJ, Slaughter CA, Sernett SW, Campbell KP. (1992) Primary structure of dystrophin-associated glycoproteins linking dystrophin to the extracellular matrix. Nature, 355 (6362), 696-702.

Jancsik V, Hajós F. (1999) The demonstration of immunoreactive dystrophin and its developmental expression in perivascular astrocytes. Brain Res, 831:200-205.

Jung JS, Bhat RV, Preston GM, Guggino WB, Baraban JM, Agre P. (1994) Molecular characterization of an aquaporin cDNA from brain: candidate osmoreceptor and regulator of water balance. Proc Natl Acad Sci USA, 91:13052–13056.

Jerison HJ. (1973) Evolution of the brain and intelligence. Academic Press, New York, London, p 482.

Jessen KR, Mirsky R. (1983) Astrocyte like glia in the peripheral nervous system: An immunohistochemical study of enteric glia. Neurosci J, 3:2206-2218 .

Johnston JB. (1911) The telencephalon of ganoids and teleosts, J Comp Neurol, 21:489-591.

Jones LS. (1996) Integrins: possible functions in the adult CNS. Trends Neurosci, 19:68-72.

Kálmán M, Hajós F. (1989) Distribution of glial fibrillary acidic protein (GFAP)-immunoreactive astrocytes in the rat brain. I. Forebrain. Exp Brain Res, 78:147-163.

Kálmán M, Székely A, Csillag A. (1993) Distribution of glial fibrillary acidic protein-immunopositive structures in the brain of the domestic chicken (*Gallus domesticus*). J Comp Neurol, 330:221-237.

Kálmán M, Kiss Á, Majorossy K. (1994) Distribution of glial fibrillary acidic protein-immunopositive structures in the brain of the red-eared freshwater turtle (*Pseudemys scripta elegans*). Anat Embryol, 189:421-434.

Kálmán M, Martin-Partido G, Hidalgo-Sanchez M, Majorossy K. (1997) Distribution of glial fibrillary acidic protein-immunopositive structures in the developing brain of the turtle *Mauremys leprosa*. Anat Embryol, 196:47-65.

Kálmán M. (1998) Astroglial architecture of the carp (*Cyprinus carpio*) brain as revealed by immunohistochemical staining against glial fibrillary acidic protein (GFAP). Anat Embryol, 198:409-433.

Kálmán M, Ari Cs. (2001) Comparative study on astroglial markers, GFAP, glutamine synthetase and S-100 in skate brain. Ann Anat, 183:104.

Kálmán M, Gould RM. (2001) GFAP-immunopositive structures in spiny dogfish, *Squalus acanthias*, and little skate, *Raja erinacea*, brains: differences have evolutionary implications, Anat Embryol, 204: 59-80.

Kálmán M, Pritz MB. (2001) Glial fibrillary acidic protein-immunopositive structures in the brain of a crocodilian, *Caiman crocodilus*, and its bearing on the evolution of astroglia, J Comp Neurol, 431: (4) 460-480.

Kálmán M. (2002) GFAP expression withdraws - a trend of glial evolution? Brain Res Bull, 57:509-511.

Kästner R. (1987) Comparative studies on the astrocytic reaction in the lesioned central nervous system of different vertebrates. J Hirnforsch, 28:221-232.

Kettenmann H, Ransom BR. (2005) The concept of neuroglia: a historical perspective In: Neuroglia, Ed: Kettenmann H, Ransom BR, Oxford University Press.

Khurana TS, Watkins SC, Kunkel LM. (1992) The subcellular distribution of chromosome 6-encoded dystrophin-related protein in the brain. J Cell Biol, 119:357-66.

Kitagawa K, Sinoway MP, Yang C, Gould RM, Colman DR. (1993) A proteolipid protein gene family: expression on sharks and rays and possible evolution from an ancestral gene encoding a pore-forming polypeptide. Neuron, 11:433-448.

Klatzo I. (1967) Cellular morphology of the lemon shark brain. In: Sharks, skates, and rays. Eds: Gilbert PW, Mathewson RF, Rall DP, Johns Hopkins Press, Maryland, pp: 341-359.

Klimley AP. (1985) Schooling in *Sphyrna lewini*, a species with a low risk of predation: a nonegalitarian state. J Comp Ethol, 70: 297-319.

Korte GE, Rosenbluth J. (1981) Ependymal astrocytes in frog cerebellum. Anat Rec, 199:267-279.

Kotrschal K, van Staaden MJ, Huber R. (1998) Fish brains: evolution and environmental relationships. Rev Fish Biol Fish, 8:373-408.

Last PR, Stevens JD. (1994) Sharks and Rays of Australia, CSIRO Publications, Melbourne.

Lazzari M, Franceschini V. (2001) Glial fibrillary acidic protein and vimentin of astroglial cells in the central nervous system of adult *Podarcis sicula* (Squamata, Lacertidae). J Anat, 198:67-75.

Lazzari M, Franceschini V. (2006) Glial cytoarchitecture in the central nervous system of the soft-shell turtle, *Trionyx sinensis*, revealed by intermediate filament immunohistochemistry. Anat Embryol, 211 (5): 497-506.

Lidov HGW, Byers TJ, Kunkel LM. (1993) The distribution of dystrophin in the murine central nervous system: an immunocytochemical study. Neurosci, 54:167-187.

Linnaeus C. (1758) Systema Naturae, Ed. X. (Systema naturae per regna tria naturae, secundum classes, ordines, genera, species, cum characteribus, differentiis, synonymis, locis. Tomus I. Editio decima, reformata.) Holmiae. Systema Nat. ed. 10 v. 1: i-ii + 1-824.

Linser PJ. (1985) Multiple marker analysis in the avian optic tectum reveals three classes of neuroglia and carbonic anhydrase-containing neurons. J Neurosci, 5:2388-2396.

Lisney TJ, Collin SP. (2006) Brain morphology in large pelagic fishes: a comparison between sharks and teleosts. J Fish Biol, 68: 532-554.

Llinás R, Nicholson C, Precht W. (1969) Preferred centripetal conduction of dendritic spikes in alligator Purkinje cells. Science, 10;163(863):184–187.

Long DM, Bodenheimer TS, Hartmann JF, Klatzo J. (1968) Ultrastructural features of the shark brain. Am J Anat, 122:209-236.

Ludwin SK, Kosek JC, Eng LF. (1976) The topographical distribution of S-100 and GFA proteins in the adult rat brain. An immunocytochemical study using horseradish peroxidase labeled antibodies J Comp Neurol, 165:197-208.

Maisey JG. (1984) Higher elasmobranch phylogeny and biostratigraphy. J Linn Soc, 82:33-54.

Martinez-Hernandez A, Bell KP, Norenberg MD. (1977) Glutamine syntethase: glial localization in brain. Science, 195:1356-1358.

McCarthy K, Prime J, Harmon T, Pollenz R. (1985) Receptor-mediated phosphorylation of astroglial intermediate filament proteins in cultured astroglia J Neurochem, 44:723-730.

McEchran JD, Dunn KA, Miyake T. (1996) Interrelationships of the batoid fishes (Chondrichthyes: Batoidea). In: Stiassny MLJ, Parenti LR, Johnson GD (Eds.), Interrelationships of Fishes. Academic Press, San Diego, pp.63-84.

McKay BE, Molineux ML, Turner RW. (2004) Biotin is endogenously expressed in select regions of the rat central nervous system, J Comp Neurol, 473:86-96.

Montanaro F, Carbonetto S. (2003) Targeting dystroglycan in the brain. Neuron, 37:193-196.

Monzon-Mayor M, Yanes C, Tholey G, de Barry J, Gombos G. (1990) Glial fibrillary acidic protein and vimentin immunohistochemistry in the developing and adult midbrain of the lizard *Gallotia galloti*. J Comp Neurol, 295:569-579.

Montgomery J, Carton G, Bodznick D. (2002) Error-driven motor learning in fish. Biol Bull, 203:238-239.

Moukhles H, Carbonetto S. (2001) Dystroglycan contributes to the formation of multiple dystrophin-like complexes in brain. J Neurochem, 78: 824-834.

Mugnaini E. (1986) Cell junctions of astrocytes, ependyma, and related cells in the mammalian central nervous system, with emphasis on the hypothesis of a generalized functional syncytium of supporting cells. In: Astrocytes. Ed: Fedoroff S, Vernadakis A, New York Acad Press, 1:329-371

Myrberg AAJ, Gruber S. (1974) The behavior of the bonnethead shark, *Sphyrna tiburo*. Copeia, 358-374.

Nelson JS. (1994) Fishes of the world. In: John Wiley & Sons, Inc. (Eds.), New York. Chondrichthyes, pp. 37–65.

New JG. (2001) Comparative neurobiology of the elasmobranch cerebellum: theme and variations on a sensorimotor interface. Environ Biol Fish, 60: 93-108.

Nico B, Frigeri A, Nicchia GP, Quondamatteo F, Herken R, Errede M, Ribatti D, Svelto M, Roncali L. (2001) Role of aquaporin-4 water channel in the development and integrity of the blood-brain barrier. J Cell Sci, 114:1297–1307.

Nico B, Frigeri A, Nicchia GP, Corsi P, Ribatti D, Quondamatteo F, Herken R, Girolamo F, Marzullo A, Svelto M, Roncali L. (2003) Severe alterations of endothelial and glial cells in the blood-brain barrier of dystrophic mdx mice. Glia, 42: 235-251.

Nico B, Nicchia GP, Frigeri A, Corsi P, Mangieri D, Ribatti D, Svelto M, Roncali L. (2004) Altered blood-brain barrier development in dystrophic MDX mice. Neurosci, 125:921-35.

Nicchia GP, Nico B, Camassa LM, Mola MG, Loh N, Dermietzel R, Spray DC, Svelto M, Frigeri A. (2004) The role of aquaporin-4 in the blood- brain barrier development and integrity: studies in animal and cellular culture models. Neurosci, 129, 935-45.

Nieuwenhuys R. (1967) Comparative anatomy of the cerebellum. In: Fox CA, Snider RS (eds), Progr Brain Res, vol 25., Elsevier, Amsterdam, pp 1-93.

Nieuwenhuys R, Ten Donkelaar HJ, Nicholson C. (1997) The central nervous system of vertebrates. Springer Verlag Heidelberg.

Norenberg MD. (1979) The distribution of glutamine synthetase in the rat central nervous system. J Histochem Cytochem, 27:756-762.

Norenberg MD. (1983) Immunohistochemistry of glutamine synthetase. In: Glutamine, Glutamate and GABA. Eds: Hertz L, Kvamme E, McGeer EG, Schousboe A, Alan L. Riss, New York, pp: 95-111.

Northcutt RG. (1977) Elasmobranch central nervous system organization and its possible evolutionary significance, Amer Zool, 17:411-429.

Northcutt RG. (1978) Brain organization in the cartilaginous fishes, in: Sensory Biology of Sharks, Skates and Rays (E.S Hodgson and R.F. Mathewson,eds.), U.S. Government Printing Office, Washington, D.C., pp. 117-193

Northcutt RG. (1981) Evolution of the Telencephalon in Nonmammals, Ann. Rev. Neurosci, 4:301-50.

Northcutt RG. (1985) Brain phylogeny. speculations on pattern and cause. *In* M. J. Cohen and F. Strumwasser (eds.), Comparative neurobiology: Modes of communication in the nervous system, pp. 351–378. Wiley, New York.

Northcutt RG. (1989) Brain variation and phylogenetic trends in elasmobranch fishes. J Exp Zool, 2:83-100.

Northcutt RG. (2002) Understanding Vertebrate Brain Evolution, Int Comp Biol, 42:743-756.

Padmanabhan J, Clayton D, Shelanski ML. (1999) Dibutyryl cyclic AMP-induced process formation in astrocytes is associated with a decrease in tyrosine phosphorylation of focal adhesion kinase and paxillin. J Neurobiol, 39:407-422.

Patel AJ, Weir MD, Hunt A, Tahourdin CSM, Thomas DGT. (1985) Distribution of glutamine sysnthetase and glial fibrillary acidic protein and correlation with glutamate decarboxylase in different regions of the rat central nervous system. Brain Res, 331:1-10.

Paul DH, Roberts BL. (1979) The significance of cerebellar function for a reflex movement of the dogfish. J Comp Phys, 134: 69-74.

Paulin MG. (1993) The role of the cerebellum in motor control and perception. Brain Behav Evol, 41: 39-51.

Privat A, Ratabul P. (1986) Fibrous and protoplasmic astrocytes. In: Astrocytes. Ed: Vernadakis A, Fedoroff S Acad Press, Orlando, Florida, pp: 105-129

Privat A, Gimenez-Ribotta M, Ridet J-L. (1995) Morphology of astrocytes. In: Neuroglia. Ed: Kettenmann H, Ransom BR, Oxford University Press, New York, Oxford, pp: 3-22.

Rakic P. (1981) Neuronal-glial interaction during development. TINS, 4:184-87.

Rakic' P. (1995) Radial glial cells: scaffolding for brain construction. In: Neuroglia. Ed: Kettenmann H, Ransom BR, Oxford University Press, New York, Oxford, pp: 746-762.

Ransom BR. (1995) Gap junctions. In:Neuroglia. Ed: Kettenmann H, Ransom BR, Oxford University Press, New York, Oxford, pp:299-318.

Rash JE, Yasumura T, Hudson CS, Agre P, Nielsen S. (1998) Direct immunogold labeling of aquaporin-4 in square arrays of astrocyte and ependymocyte plasma membranes in rat brain and spinal cord. Proc Natl Acad Sci USA, 95:11981–11986.

Redies C, Ast M, Nakagawa S, Takeichi M, Martinez de la Torre M, Puelles L. (2000) Morphologic fate of diencephalic prosomeres and their subdivisions revealed by mapping cadherin expression. J Comp Neurol, 421:481-514.

Reichenbach A, Neumann M, Brückner G. (1987) Cell length to diameter relation of rat fetal radial glia - does impaired K+ transport capacity of loss thin cells cause their parinatal transformation in multipolar astrocytes? Neurosci Lett, 73:95-100.

Reichenbach A, Robinson SR. (1995) Ependymoglia and ependymoglia-like cells. In:Neuroglia. Ed:Kettenmann H, Ransom BR, Oxford University Press, New York, Oxford, pp:58-84.

Reichenbach A. (1989) Glia:neuron index: review and hypothesis to account for different values in various mammals, Glia, 2(2):71-7.

Reiner A. (1991) A comparison of neurotransmitter-specific and neuropeptide-specific neuronal cell types present in the dorsal cortex in turtles with those present in the isocortex in mammals: implications for the evolution of isocortex. Brain Behav Evol, 38: 53-91.

Reynolds WW, Karlotski WJ. (1977) The allometric relationship of skeleton weight to body weight in teleost fishes: a preliminary comparison with birds and mammals. Copeia 1977: 160–163.

Riddell WI, Corl KG. (1977) Comparative investigation and relationship between cerebral indices and learning abilities. Brain Behav Evol, 14: 305-308.

Roeling TAP, Feirabend HKP. (1988) Glial fiber pattern in the developing chicken cerebellum: vimentin and glial fibrillary acidic protein immunostaining. Glia, 1:398-402.

Roots BI. (1986) Phylogenetic development of astrocytes. In: Astrocytes. Eds:Vernadakis A, Fedoroff S, Astrocytes. Acad Press, Orlando, Florida, pp:1-34.

Rosenberg PA, Aizenman E. (1989) Hundred-fold increase in neuronal vulnerability to glutamate toxicity in astrocyte-poor cultures of rat cerebral cortex. Neurosci Lett, 103:162-168.

Royuela M, Hougon G, Rivier F, Fehrentz JA, Martinez J, Paniagua R, Mornet D. (2001) Variations in dystrophin complex in red and white caudal muscle from *Torpedo marmorata*. J Histochem Cytochem, 49:857-65.

Sadoulet-Puccio HM, Khurana TS, Cohen JB, Kunkel LM. (1996) Cloning and characterization of human homologue of a dystrophin related phosphoprotein found at the torpedo electric organ post-synaptic membrane. Hum Mol Gen, 5:489-96.

Sasaki H, Mannen H. (1981) Morphological analysis of astrocytes in the bullfrog (*Rana catesbeiana*) spinal cord with special reference to the site of attachment of their processes. J Comp Neurol, 198.

Schmechel DE, Rakic P. (1979) A Golgi study of radial glial cells in developing monkey telencephalon: morphogenesis and transformation into astrocytes. Anat Embryol, 156: 115-152.

Schroeder DM, Ebbesson SOE. (1975) Cytoarchitecture of the optic tectum in the nurse shark. J Comp Neurol, 160:443-462.

Schweitzer J, Notarbartolo-Di-Sciara G. (1986) The rete mirabile cranica in the genus *Mobula*: A comparative study, J Morph, 188:(2) 167 – 178.

Shirai S. (1992) Squalean Phylogeny: A New Framework of 'Squaloid' Sharks and Related Taxa. Hokkaido University Press, Sapporo.

Shirai S. (1996) Phylogenetic interrelationships of Neoselachians (Chondrichthyes: Euselachii). *In* M. Stiassney, L. Parenti, and D. Johnson (eds.), Interrelationships of fishes. Academic Press, New York.

Smeets WJA, Nieuwenhuys R. (1976) Topographical analysis of the brain stem of the sharks *Squalus acanthias* and *Scyliorhinus canicula*. J Comp Neurol, 165:333-367.

Smeets WJAJ, Nieuwenhuys R, Roberts BL. (1983) The central nervous system of cartilaginous fishes, Springer, Berlin Heidelberg New York, pp. 123-148.

Smeets WJAJ. (1997) Cartilaginous fishes. In: Nieuwenhuys R, Ten Donkelaar HJ, Nicholson C (Eds) The central nervous system of vertebrates. Springer Verlag, Heidelberg.

Stensaas LJ, Stensaas SS. (1968a) Astrocytic neuroglial cells, oligodendrocytes and microgliocytes in the spinal cord of the toad. I Light microscopy. Z Zellforsch Mikrosk

Springer S. (1967) Social organization of shark populations. In: Sharks, Skates and Rays (Gilbert PW, Mathewson RF, Rall DP, eds), pp 149-174. Baltimore, MD: Johns Hopkins Press.

Stensaas LJ, Stensaas SS. (1968b) Astrocytic neuroglial cells, oligodendrocytes and microgliocytes in the spinal cord of the toad. II. Electron microscopy. Z Zellforsch, 86:184-213.

Stewart PA, Coomber BL. (1986) Astrocyte in blood-brain barrier. In: Astrocyte. Ed:Fedoroff S, Vernadakis A, Acad Press, New York, pp:311-323.

Striedter GF. (2005) Principles of brain evolution. Sunderland, MA: Sinauer Associates, Inc.

Szuchet S, Plachetzki DC, Eaton KS. (2001) Oligodendrocyte transmembrane protein: a novel member of the glutamate-binding protein subfamily. Biochem Biophys Res Commun, 283: (4) 900-907.

Tawil N, Wilson P, Carbonetto S. (1993) Integrins in point contacts mediate cell spreading factors that regulate integrin accumulation in point contacts vs. focal contacts. J Cell Biol, 120:261-271.

Tian M, Jacobson C, Gee SH, Campbell KP, Carbonetto S, Jucker M. (1996) Dystroglycan in the cerebellum is a laminin α2-chain binding protein at the glial-vascular interface and is expressed in Purkinje cells. Eur J Neurosci, 8:2739-2747.

Tong S, Bullock TH. (1982) Electroreceptive representation and its dynamics in the cerebellum of the catfish, *Ictalurus nebulosus* (Ictaluridae, Siluriformes), J Comp Physiol, 145,3: 289-298.

Uchino M, Hara A, Mizuno Y, Fujiki M, Nakamura T, Tokunaga M, Hirano T, Yamashita T, Uyama E, Ando Y, Mita S, Ando M. (1996) Distribution of dystrophin and dystrophin-associated protein 43DAG (beta-dystroglycan) in the central nervous system of normal controls and patients with Duchenne muscular dystrophy. Intern Med, 35: 189-94.

Vajda Z, Pedersen M, Füchtbauer E-M, Wertz K, Stødkilde-Jørgensen H, Sulyok E, Dóczi T, Neely JD, Agre P, Frøkiaer J, Nielsen S. (2002) Delayed onset of brain edema and mislocalization of aquaporin-4 in dystrophin-null transgenic mice. Proc Natl Acad Sci USA, 99:13131-13136.

Van Nassauw L, Harrison F, Cras P, Callebaut M. (1987) Immunohistochemicalocalisation of S-100 protein, glial fibrillary acidic protein and neuron-specific enolase in the pars distalis of quail, rat and human hypophyses. Histochem J, 86:353-358.

Venero JL, Vizuete ML, Machado A, Cano J. (2001) Aquaporins in the central nervous system. Prog Neurobiol, 63:321–336.

Verbavatz JM, Ma T, Gobin R, Verkman AS. (1997) Absence of orthogonal arrays in kidney, brain and muscle from transgenic knockout mice lacking water channel aquaporin-4. J Cell Sci, 110:2855–2860.

Waehneldt TV. (1990) Phylogeny of myelin proteins. Ann N Y Acad Sci, 605:15-28.

Waehneldt TV, Matthieu JM, Stoklas S. (1987) Immunological evidence for the presence of myelin-related integral proteins in the CNS of hagfish and lamprey. Neurochem Res, 12:869-873.

Warth A, Mittelbronn M, Wolburg H. (2005) Redistribution of the water channel protein aquaporin-4 and the K+ channel protein Kir4.1 differs in low- and high-grade human brain tumors. Acta Neuropath, 109: 418-26.

Wasowicz M, Ward R, Repérant J. (1999) An investigation of astroglial morphology in *Torpedo* and *Scyliorhinus*. J Neurocytol, 28:639-653.

Westergaard N, Sonnewald U, Schousboe A. (1995) Metabolic trafficking between neurons and astrocytes: The glutamate/glutamine cycle revisited. Dev Neurosci, 17:203-211.

Wicht H, Derouiche A, Korf H-W. (1994) An immunocytochemical investigation of glial morphology in the Pacific hagfish: radial and astrocyte-like glia have the same phylogenetic age. J Neurocytol, 23:565-576.

Wilga CAD, Lauder GV. (2004) Biomechanics of locomotion in sharks, rays, and chimaeras. In: Biology of Sharks and Their Relatives (Carrier JC, Musick JA, Heithaus MR, eds), pp 139-202. London: CRC Press.

Winchell CJ, Martin AP, Mallatt J. (2004) Phylogeny of elasmobranchs based on LSU and SSU ribosomal RNA genes, Mol Phylogenet Evol, 31: 214-224.

Wolburg H, Kastner R, Kurz-Isler G. (1983) Lack of orthogonal particle assemblies and presence of tight junctions in astrocytes of the goldfish (*Carassius auratus*). A freeze fracture study. Cell Tissue Res, 234:389-402.

Wolburg H, Risau W. (1995) Formation of the blood-brain barrier. In:Neuroglia. Ed: Kettenmann H, Ransom BR, Oxford University Press, New York, Oxford, pp: 763-776.

Wolburg H. (1995) Orthogonal arrays of intramembranous particles: a review with special reference to astrocytes. J Hirnforsch, 36:239-258.

Wourms JP. (1977) Reproduction and development in chondrichthyan fishes. Amer Zool, 17: 379-410.

Wujek JR, Reier PJ. (1984) Astrocytic membrane morphology: differences between mammalian and amphibian astrocytes after axotomy. J Comp Neurol, 222:607-619.

YamamotoT, Shibata N, Kanazawa M, Kobayashi M, Komori T, Ikeya K, Kondo E, Saito K, Osawa M. (1997) Localization of laminin subunits in the central nervous system in Fukuyama congenital muscular dystrophy: an immunohisochemical investigation. Acta Neuropath, 94:173-169.

Yanes C, Monzon-Mayor M, Ghandour MS, de Barry J, Gombos G. (1990) Radial glia and astrocytes in the adult and developing telencephalon of the lizard *Gallotia galloti* as revealed by immunohistochemistry with anti-GFAP and anti-vimentin antibodies. J Comp Neurol, 295: 559-68.

Yano K, Sato F, Takahashi T. (1999) Observations of mating behavior of the manta ray, *Manta birostris*, at the Ogasawara Islands, Jap Icht Res, 46(3):289-296.

Yoon MS, Puelles L, Redies C. (2000) Formation of cadherin-expressing brain nuclei in diencephalic alar plate divisions. J Comp Neurol, 421:461-480.

Yopak KE, Lisney TJ, Collin SP, Montgomery JC. (2007) Variation in brain organization and cerebellar foliation in chondrichthyans: sharks and holocephalans. Brain Behav Evol, 69(4):280-300.

Zaccaria ML, Di Tommaso F, Brancaccio A, Paggi P, Petrucci TC. (2001) Dystroglycan distribution in adult mouse brain: a light and electron microscopy study. Neurosci, 104:311-24.

13. Publications related to the thesis

Mihály Kálmán, Csilla Ari (2002) Distribution of GFAP immunoreactive structures in the rhombencephalon of sterlet (*Acipenser ruthenus*) and its evolutionary implication; Journal of Experimental Zoology, 293: 395-406.
IF: 1,548

Csilla Ari, Mihály Kálmán (2008) Evolutionary changes of astroglia in Elasmobranchii comparing to Amniotes: a study based on three immunohistochemical markers (GFAP, S-100, and glutamine synthetase) Brain Behav Evol, 71:305-324.
IF: 2,195

Csilla Ari, Mihály Kálmán (2008) Glial architecture of the ghost shark (*Callorhinchus milii*, Holocephali, Chondrichthyes) as revealed by different immunohistochemical markers, Journal of Experimental Zoology (in press)
IF: 2,756

14. Publications not related to the thesis

Gál János, Vincze Zoltán, Jakab Csaba, Ari Csilla, Lefler Kinga Katalin (2005) Multiplex nyeles fibroma homoki tigriscápa (*Carcharias (Odontaspis) taurus*) állkapcsán; Hungarian Veterinary Journal, 127.242-245.
IF: 0,114

Csilla Ari, João P. Correia (2008) Role of sensory cues on food searching behavior of a captive *Manta birostris* (Chondrichtyes, Mobulidae), Zoo Biology (in press)
IF: 0,779

Submitted manuscripts

Csilla Ari (2008) The brain of *Mobula japanica* (spinetail devilray, *Myliobatiformes, Elasmobranchii*) in gross morphological and ecological perspectives, Journal of Fish Biology (submitted)

Csilla Ari, Mihály Kálmán (2008) Immunohistochemical detection of dystroglycan, and some of its associated proteins in the brain of chondrichthyes, Journal of Comparative Biochemistry and Physiology (submitted)

Presented posters

Csilla Ari, Mihály Kálmán, 2001: Search for astroglia in the GFAP-free areas of the brains of cartilagineous and bony fishes applying immunohistochemical staining of glutamine syntethase and S-100 protein; Conference of the Hungarian Neurobiology Society,Szeged

Mihály Kálmán, Csilla Ari, 2001: Comparative study of astroglial markers, GFAP, glutamine syntethase and S-100 in skate brain; 96. Versammlung in Münster, Germany

Csilla Ari, Mihály Kálmán, 2003: Supposed sexual dimorphism on the cerebellum of the ray *Mobula japanica* (order Myliobatiformes); Joint Meeting of Ichthyologists and Herpetologists and the American Elasmobranch Society, Manaus, Brazil

Mihály Kálmán, Csilla Ari, Robert M. Gould, 2003: Similar tendencies in the evolution of astroglia in elasmobranchs and amniotes. Joint Meeting of Ichthyologists and Herpetologists and the American Elasmobranch Society, Manaus, Brazil

Csilla Ari, Mihály Kálmán, 2003: Morphometrical studies on the cerebellum of a ray species (*Mobula japanica*) of the order Myliobatiformes- sexual dimorphism? ; Conference of the Hungarian Neurobiology Society, Balatonfüred

Csilla Ari, István Stuber, 2004: Three-dimensional movements of captive Mobulids (*Manta birostris* and *Mobula mobular*); European Elasmobranch Society meeting, London,England

Csilla Ari, Mihály Kálmán, João P. Correia, István Stuber, 2004: Analysis of movements by computerised tridimensional video reconstruction; Neuroscience Meeting, San Diego, USA

Csilla Ari, João P. Correia, 2005: A study on the sensory and learning capabilities of a captive *Manta birostris* (Mobulidae); Joint Meeting of Ichthyologists and Herpetologists and the American Elasmobranch Society Meeting, Tampa, USA

Mihály Kálmán, Csilla Ari, 2007: Evolutionary correlations of brain structure and glial architecture in Chondrichthyes: forebrain and hindbrain. 5th European Conference of Comparative Neurobiology, Paris, France

Published abstracts

Csilla Ari, Mihály Kálmán, 2001: Search for astroglia in the GFAP-free areas of the brains of cartilagineous and bony fishes applying immunohistochemical staining of glutamine syntethase and S-100 protein; Neurobiology

Mihály Kálmán, Csilla Ari, 2001: Comparative study of astroglial markers, GFAP, glutamine syntethase and S-100 in skate brain; Anat Supl, 183: 104.

Csilla Ari, Mihály Kálmán, 2003: Morphometrical studies on the cerebellum of a ray species (*Mobula japanica*) of the order Myliobatiformes- sexual dimorphism?; Clinical Neuroscience,56:5.